THE REACTIONS OF METHYLENE WITH ISOBUTANE AND CYCLOPROPANE
SAUNDERS, BARBARA BREIDENBACH
ProQuest Dissertations and Theses; 1972; ProQuest Dissertations & Theses Global

INFORMATION TO USERS

This dissertation was produced from a microfilm copy of the original document. While the most advanced technological means to photograph and reproduce this document have been used, the quality is heavily dependent upon the quality of the original submitted.

The following explanation of techniques is provided to help you understand markings or patterns which may appear on this reproduction.

1. The sign or "target" for pages apparently lacking from the document photographed is "Missing Page(s)". If it was possible to obtain the missing page(s) or section, they are spliced into the film along with adjacent pages. This may have necessitated cutting thru an image and duplicating adjacent pages to insure you complete continuity.

2. When an image on the film is obliterated with a large round black mark, it is an indication that the photographer suspected that the copy may have moved during exposure and thus cause a blurred image. You will find a good image of the page in the adjacent frame.

3. When a map, drawing or chart, etc., was part of the material being photographed the photographer followed a definite method in "sectioning" the material. It is customary to begin photoing at the upper left hand corner of a large sheet and to continue photoing from left to right in equal sections with a small overlap. If necessary, sectioning is continued again — beginning below the first row and continuing on until complete.

4. The majority of users indicate that the textual content is of greatest value, however, a somewhat higher quality reproduction could be made from "photographs" if essential to the understanding of the dissertation. Silver prints of "photographs" may be ordered at additional charge by writing the Order Department, giving the catalog number, title, author and specific pages you wish reproduced.

University Microfilms

300 North Zeeb Road
Ann Arbor, Michigan 48106

A Xerox Education Company

Reproduced with permission of the copyright owner. Further reproduction prohibited without permission.

72-24,653

SAUNDERS, Barbara Breidenbach, 1945-
THE REACTIONS OF METHYLENE WITH ISOBUTANE
AND CYCLOPROPANE.

Harvard University, Ph.D., 1972
Chemistry, general

University Microfilms, A XEROX Company, Ann Arbor, Michigan

THIS DISSERTATION HAS BEEN MICROFILMED EXACTLY AS RECEIVED

Reproduced with permission of the copyright owner. Further reproduction prohibited without permission.

The Reactions of Methylene with Isobutane and Cyclopropane

A thesis presented

by

Barbara Breidenbach Saunders

to

The Chemistry Department in partial fulfillment of the requirements for the degree of Doctor of Philosophy in the subject of Chemistry

Harvard University

Cambridge, Massachusetts

February 1972

Reproduced with permission of the copyright owner. Further reproduction prohibited without permission.

PLEASE NOTE:

Some pages may have

indistinct print.

Filmed as received.

University Microfilms, A Xerox Education Company

Reproduced with permission of the copyright owner. Further reproduction prohibited without permission.

The Reactions of Methylene with Isobutane and Cyclopropane

SUMMARY

Research Director: Barbara Breidenbach Saunders
George B. Kistiakowsky February 1972

Ketene was photolyzed at several wavelengths in the presence of large amounts of either isobutane or cyclopropane.

The ketene-isobutane mixture was photolyzed at 214 nm, 277 nm, 313 nm, 322 nm, and 330 nm and the variations in the percentages of methylene in the triplet and singlet states, as reflected in the distribution of products, were studied. Additional photolyses in the presence of varying amounts of CO or O_2 were able to clarify the mechanism of $CH_2(^3B_1)$ production. The absorption of light at the longest wavelengths (330nm and beyond) is primarily the result of the $^3A_2 \leftarrow\!\!- {}^1A_1$ transition in ketene. At 330nm, 75% of the CH_2 resulting from the photodecomposition of ketene($^3A_2$) was in the $^3B_1$ state. At 277 nm, all of the absorption is attributed to the $^1A_2 \leftarrow\!\!- {}^1A_1$ transition and, hence, all of the CH_2 produced from the ketene decomposition is in the $^1A_1$ state. At all wavelengths, the bimolecular crossing from $CH_2(^1A_1)$ to $CH_2(^3B_1)$ competes with the reaction of $CH_2(^1A_1)$ with isobutane and almost 50% of the $CH_2(^1A_1)$ is converted by the isobutane to $CH_2(^3B_1)$. The photolysis of ketene at the intermediate wavelengths is characterized by a mixture of the three processes. Absorption of radiation at 214 nm excites ketene to its second excited singlet state, $^1A_1$, and there is some evidence that the CH_2 produced from the decomposition of this state is $CH_2(^1B_1)$.

The ketene-cyclopropane mixture was photolyzed in the presence of 5% O_2 at 214 nm, 277nm, 313 nm, and 330 nm in order to study the unimolecular decomposition of methylcyclopropane (formed by the reaction of $CH_2(^1A_1)$ and cyclopropane) containing different amounts of energy. The rate of decomposition was largest when 214 nm radiation was used and decreased as the photolyzing energy decreased. The RRKM theory was used to estimate the amount of energy in the excited methylcyclopropane molecule. The difference in decomposition rates was used to estimate the fraction of the photolysis energy that $CH_2(^1A_1)$ carried to the cyclopropane.

Reproduced with permission of the copyright owner. Further reproduction prohibited without permission.

To the men I love, especially my husband, Kim.

Reproduced with permission of the copyright owner. Further reproduction prohibited without permission.

I would like to thank my research director, Prof. George B. Kistiakowsky, for the help and support he has given me. Dr. Jerry Bell kindly lent me a copy of C. J. Mitschele's Thesis, and his discussuions with me were very helpful.

I would like to acknowledge the Woodrow Wilson Foundation and the National Air Pollution Control Administration for their financial support.

I am indebted to my colleagues at Harvard whose friendship and encouragement kept me working when the laboratory seemed against me; a very special thanks to Michael J. Berger, William P. Haugen, Thomas Izod, Lynn Melton, and John and Elizabeth Marlow.

I especially thank my husband, Kim, for his love, understanding, and patience, and, also, my dog, Schnapps, for her affection.

Reproduced with permission of the copyright owner. Further reproduction prohibited without permission.

CONTENTS

1.	Introduction	1
	The Structure of Methylene	1
	The Reactions of Methylene	3
	Intersystem Crossing in Methylene	7
	Chemical Activation and Unimolecular Reactions	9
	The Present Work	16
2.	Apparatus and Techniques	19
	Preparation of Ketene	19
	Spectral Regions and Lamps Used for Photolysis	21
	The Optical Arrangement for Photolysis	25
	Beer's Law Studies and Measurements of Light Intensities	31
	The Purity of the Gases Used in the Photolyses	36
	Product Analysis	38
	Part 1: The Product Analysis of the Isobutane System	40
	Part 2: The Product Analysis of the Cyclopropane System	48
	The Procedure for a Typical Experiment	52
	Differences Between the Light Intensity Measurements at 214 nm and the Longer Wavelengths	55
3.	Results of the Photolysis of the Ketene-Isobutane System	58
	General Trends	58
	The Ketene-Isobutane Photolysis System	73
	The Ketene-Isobutane-O_2 Photolysis System	78
	The Reaction of O_2 with $^1CH_2$	79
	The Determination of the Percent of $^3CH_2$ Present in the Ketene-Isobutane System	80
	The Ketene-Isobutane-CO Photolysis System	82
	The Ketene-Isobutane-Xenon Photolysis System	85

Reproduced with permission of the copyright owner. Further reproduction prohibited without permission.

4. Discussion of the Isobutane Results 87
General Introductory Summary 87
I A Review of Three Possible Mechanisms for the Formation of $^3CH_2$ 89
II The Mechanism of Intersystem Crossing in Methylene 93
A The Intramolecular or Spontaneous Mechanism 94
B The Bimolecular (Intermolecular) Mechanism 98
C The Evidence Against the Intramolecular Mechanism 99
D The Effect of the Nature of the Collision Partner in the Bimolecular Intersystem Crossing of Methylene 101
E The Effect of an Unreactive Gas in a Methylene System 102
F The Effect of a Reactive Gas in a Methylene System 103
G The Percent of $^3CH_2$ Formed from $^1CH_2$ During the Photolysis of Ketene-Alkane Mixtures at Short Wavelengths 105
III The Reactions of Ketene with $^1CH_2$ and $^3CH_2$ 110
A $^1CH_2$ and Ketene 111
B $^3CH_2$ and Ketene 112
IV The Second Source of $^3CH_2$ 115
A Introduction and Evidence 115
B The Absorption of Ketene 117
C The Excited States of Ketene 120
V Discussion of the CO Experiments and the Measurement of ϕ_s 124
A Determination of ϕ_s from the CO Experiments 124
B The Fraction of $^3CH_2$ Determined from ϕ_s 125

Reproduced with permission of the copyright owner. Further reproduction prohibited without permission.

C The Variation of the Quantum Yield Production of Methylene at Different Wavelengths 129
VI Changes in the Rate of Intersystem Crossing with the Energy of $^1CH_2$ 130
A Experimental Results of Other Workers 134
B Summary of Arguments for Energy Dependence in the Rate of Intersystem Crossing 136
VII The Photolysis of Ketene at 214 nm 137
A The Reaction of $CH_2(^1B_1)$ with O_2 139
B The Reaction of $CH_2(^1B_1)$ with Isobutane 140
C The Reaction of $CH_2(^1B_1)$ with CO 141
D Other Possibilities 143
VII Summary of Conclusions 146
5. Results and Discussion of the Cyclopropane Experiments 148
Results 148
An Introduction to Previous Work on the Decomposition of Methylcyclopropane 153
The Applicability of the Strong Collision Assumption 157
An Estimate of the Rate of Reaction of $^1CH_2$ with Cyclopropane 158
Modifications of Dorer and Rabinovitch's Models 166
New Models 173
The Best Model 174
A Comparison of the Results of the RRKM Theory with Those of Other Theories 176
The Partitioning of Energy During the Photolysis of Ketene 179
Distribution of Isomers 182
Appendix I I-1
Appendix II II-1

Reproduced with permission of the copyright owner. Further reproduction prohibited without permission.

Index to Figures

2-1	Ketene Preparation System	20
2-2	The Spectral Distributions for each Monochromator Setting Used	22
2-3	The Absorption Spectrum of Ketene from 200 nm to 400 nm	24
2-4	Spectral Output of the Phillips Zinc Lamp	26
2-5	Characteristics of the Baird Atomic Line Filter	28
2-6	Typical Optical Arrangement	30
2-7	Schematic of the Gas Handling Line at the Photolysis Cell	32
2-8	Gas Chromatographic Sample Inlet System	39
2-9a	Porasil C Column	42
2-9b	Column E	43
2-10	The Calibration of the Response of the Flame Ionization Detector with Propane	44
2-11	Porapak Q and QS Column	51
3-1	Variations in $^3CH_2$ with Wavelength	63
3-2	Neopentane/Isopentane vs. $^3CH_2$ & O_2	64
3-3	Neopentane vs. Pressure of CO	69
3-4	Isopentane vs. Pressure of CO	70
3-5	Total Pentane Yiled vs. Pressure of CO	71
4-1	Two Possible Mechanisms for the Production of $^3CH_2$	92
4-2a	The Qualitative Potential Energy Surface for Ketene Decomposition	95
4-2b	A Qualitiative Jablonski Diagram Showing the Different States of Ketene and Methylene	96
4-3	$k_{isc}(M)/(k_1+k_2)$ vs. Polarizability	109
5-1	Butenes/methylcyclopropane vs. Total Pressure	151
5-2	"Thermal Fall-Off" curves at 720.1°K	171
5-3	"Thermal Fall-Off" curves at 763.8°K	172

Reproduced with permission of the copyright owner. Further reproduction prohibited without permission.

Index to Tables

1-I	The Structure of the Different States of Methylene	18
2-I	The Spectral Distributions from the Monochromator	23
2-II	Spectral Output of the Phillips Zinc Lamp	27
2-III	The Molar Response of the Hydrocarbons with a Flame Ionization Detector	46
3-I	Comparisons of Product Yields and Total Quantum Yields at Different Wavelengths	65
3-II	The Variation in Pentane Yields in the CO Experiments	66
3-III	The Effect of Varying the Composition of the Reaction Mixture at 313 nm	68
3-IV	Some of the Major Reactions in the Ketene-Isobutane Photolysis System	72
4-I	The Polarizabilities of Different Gases Used in Methylene Systems	104
4-II	Comparison of Calculated and Measured Fractions of $^3CH_2$	128
5-I	Results of the Ketene-Cyclopropane Photolyses	152
5-II	Frequency Assignments for Methylcyclopropane Ring Vibrations	159
5-III	Models	161
5-IV	Results of RRKM Calculations	163
5-V	Ketene Photolysis Systems, Rate Constants, and Thermochemistry	165
5-VI	The Results of the Theories of Kassel and Slater	178
5-VII	An Estimate of the Partitioning of Energy During the Photolysis of Ketene	181
5-VIII	Heats of Formation	184
5-IX	A Summary of the Thermochemical Data for the Methylcyclopropane System	185

Reproduced with permission of the copyright owner. Further reproduction prohibited without permission.

1 Introduction

The Structure of Methylene

The biradical methylene, CH_2, is easily produced by the pyrolysis[1] or photolysis of diazomethane,[3] the photolysis of ketene,[3] the photolysis of diazirine,[4] and by the vacuum ultraviolet photolysis of propane.[5] Although its existence had been suspected since 1933, methylene eluded spectroscopic observation until 1959 when the careful and patient work of Herzberg and Shoosmith identified methylene in the ultraviolet flash photolysis of diazomethane in the presence of a large amount of nitrogen.[6]

---

1. Rabinovitch, B. S. and Setser, D. W., J. Am. Chem. Soc. 83, 750 (1969); Setser, D. W. and Rabinovitch, B. S., Can. J. Chem. 40, 1425 (1962).

2. Norrish, R. G. W. and Kirkbride, F.W., J. Chem. Soc. 1933, 119.

3. Norrish, R. G. W., Crone, H. C., Saltmarsh, O., J. Chem. Soc. 1933, 1533; Ross, W. F. and Kistiakowsky, G. B., J. Am. Chem. Soc. 56, 1112 (1934).

4. Frey, H. M. and Stevens, I. D. R., Proc. Chem. Soc. 254, 79 (1962).

5. Koob, R. D., J. Phys. Chem. 73, 3168 (1969); Dhingra, A. K. and Koob, R. D., ibid 74, 4490 (1970); Dhingra, A. K., Vorachek, J. H., and Koob, R. D., Chem. Phys. Letters 9, 17 (1971).

6. Herzberg, G., and Shoosmith, J., Nature 183, 1801 (1959); Herzberg, G., Proc. Roy. Soc. A262, 291 (1961); Herzberg, G. and Johns, J. W. C., ibid. A295, 107 (1966)

Reproduced with permission of the copyright owner. Further reproduction prohibited without permission.

Herzberg identified several different electronic states of methylene. The lowest energy or ground state is a triplet electronic state and appeared to be linear, a $^3\Sigma_g$ state. In 1970, the electron spin resonance spectrum of the triplet state of methylene[7] as well as the latest theoretical calculations[8] indicated that it was actually bent. This $^3B_1$ ground state was confirmed by Herzberg and Johns.[9] The second electronic stato is a bent singlet state, $^1A_1$, and the third electronic state is another singlet state which lies about 30 kcal/mole above the $^1A_1$ state, the $^1B_1$ state. The geometries of all three states are very similar and except for the spin, the $^1B_1$ and $^3B_1$ states are described by the same configuration. In most chemical systems, there is not enough energy available to form the $^1B_1$ state and usually only two states are present, the $^1A_1$ and the $^3B_1$ states which are referred to as $^1CH_2$ and $^3CH_2$. Table 1-I summarizes the properties of the three states of methylene.

---

7. Bernheim, R. A., Bernard, H. W., Wang, P. S., Wood, L. S., and Skell, P. S., J. Chem. Phys. 53, 1280 (1970); Wasserman, E., Yager, W. A., and Kuck, V. J., Chem. Phys. Letters 7, 409 (1970).

8. Harrison, J. F. and Allen, L. C., J. Am. Chem. Soc. 91, 807 (1969); Bender, C. F. and Schaefer, H. F., III, ibid. 92, 4984 (1970).

9. Herzberg, G. and Johns, J. W. C., J. Chem. Phys. 54, 2276 (1971).

Reproduced with permission of the copyright owner. Further reproduction prohibited without permission.

The Reactions of Methylene

Several excellent reviews[10] have appeared which summarize and describe the reaction of methylene and the reader is referred to these for a more complete discussion of the reactions. Only those reactions pertinent to the studies in this thesis will be mentioned here.

Since at least two different electronic states of methylene exist, there is the possibilty of at least two types of reactions every time methylene reacts with a molecule. Both methylenes, $^1CH_2$ and $^3CH_2$, react with the C-C double bond in ketene and diazomethane, the C-H bonds in hydrocarbons,[10] oxygen to form CO, CO_2, H_2; H_2O and other oxidation products,[11] and CO to form ketene.[12]

The $^3B_1$ state of methylene, $^3CH_2$, reacts more slowly with C-H

---

10. Frey, H. M., Prog. React. Kinet., 2, 131 (1964); Bell, J. A., Prog. Phys. Org. Chem., 2, 1 (1964); DeMore, W. B. and Benson, S. W., Adv. Photochem., 2, 219 (1964).

11. Russell, R. L. and Rowland, F. S., J. Am. Chem. Soc. 90, 1671 (1968).

12. a) Bremer-Wilson, T. and Kistiakowsky, G. B., J. Am. Chem. Soc. 80, 2934 (1958)
b) DeGraff, B. A. and Kistiakowsky, G. B., J.Phys. Chem. 71, 1553, 3984 (1967)

Reproduced with permission of the copyright owner. Further reproduction prohibited without permission.

bonds than does the $^1A_1$ state of methylene, $^1CH_2$.[13,14] $^3CH_2$ effectively inserts into the C-H bonds of hydrocarbons in two steps, by abstracting an H atom from the hydrocarbon, RH, to form the methyl radical and an alkyl radical, R, which then recombine to finally form R-CH_2-H.[10] Because of the recombination reactions, the reactions of $^3CH_2$ with a hydrocarbon also result in the formation of recombination products other than just those of the methyl radical recombining with the alkyl radical, e.g., R-R, CH_4, and olefins corresponding to RH-H_2 and C_2H_6. The reaction of $^1CH_2$ with C-H bonds involves a concerted insertion of the $^1CH_2$ between the C and H atoms. This reaction results in no products other than R-CH_2-H.[10]

The reaction of $^3CH_2$ with O_2 occurs faster than does the reaction of $^1CH_2$ with O_2.[11,15] Since the addition of only a few percent of O_2 eliminates $^3CH_2$ as a reactant, the reactions of $^1CH_2$ can be studied. However, there is another method of determining the $^1CH_2$ reaction channels which makes use of more discriminating reactants than O_2. In methylene-hydrocarbon reaction systems,

---

13. Braun, W., Bass, A. M., and Pilling, M., J. Chem. Phys. 52, 5131 (1970)

14. Frey, H. M. and Walsh,R., J. Chem. Soc. (A) 1970, 2115

15. In a methylene-hydrocarbon system, the presence of O_2 can also eliminate the products of $^3CH_2$ reactions by reacting with the radicals formed after the abstraction reaction. There is an additional complication when ketene is photolyzed by wavelengths longer than about 320 nm. The photolysis of ketene in this region involves an excited triplet state of ketene which may react with O_2.

Reproduced with permission of the copyright owner. Further reproduction prohibited without permission.

since the reaction of $^3CH_2$ with a C-H bond is slow, the presence of gases which are more reactive towards $^3CH_2$ than a hydrocarbon will prevent the reaction of $^3CH_2$ and the hydrocarbon. This technique has been used by DeGraff and Kistiakowsky[12b] and Cox and Cventanovic[16] to isolate $^1CH_2$ reactions by including relatively large amounts of CO in their ketene and ketene-hydrocarbon systems. Unlike O_2, CO will not react with alkyl radicals and so some of the potential complications are absent.

Bell[17] has shown that the reaction of $^3CH_2$ with diazomethane is so much faster than its reaction with the C-H bonds in propane, that the presence of even relatively small amounts of diazomethane prevent the reaction of $^3CH_2$ and propane. However, there are so many secondary reactions resulting from the reaction of $^3CH_2$ and diazomethane that this relatively fast reaction often makes the methylene-hydrocarbon system more complicated than when the diazomethane reaction is unimportant. The reaction of ketene with $^3CH_2$ is also faster than the reaction of $^3CH_2$ with C-H bonds; however, this reaction is not nearly as fast as that with diazomethane.

---

16. Cox, R. A. and Cventanovic, R. J., J. Phys. Chem. 72, 2236 (1968)
17. Bell, J. A., J. Phys. Chem. 75, 1537 (1971)

Reproduced with permission of the copyright owner. Further reproduction prohibited without permission.

No previous work has been done which describes the reactions of the $^1B_1$ state of methylene, but on the basis of similar electron configurations, the $^1B_1$ state may react in the same way the $^3B_1$ state does.[18] This is expected when the electronic orbital configuration of methylene is the most important factor in deciding the reaction pathway, such as in the reaction of CH_2 with O_2 and C-H bonds. In cases where the energy of the methylene is more important, the $^1B_1$ state should react more as the $^1A_1$ does. This is expected for the reaction of CH_2 and CO where the $^3B_1$ reacts to a greater extent than the $^1A_1$ or $^1B_1$ because of the formation of the metastable $^3A_2$ state of ketene. Upon reaction with CO, both the $^1A_1$ and $^1B_1$ states form excited singlet states of ketene which decompose very quickly. When ketene is photolyzed at 214 nm, enough energy is available to form methylene in the $^1B_1$ state. The results of our experiments with the ketene-isobutane system photolyzed at 214 nm indicate that methylene is present in the $^1B_1$ state and that the $^1B_1$ state reacts as the $^3B_1$ state does with the C-H bonds and O_2.

---

18. Hoffmann, R., J. Am. Chem. Soc. 90, 1475 (1968); Dobson, R. C., Hayes, D. M., and Hoffmann, R., ibid 93, 6188(1971).

Reproduced with permission of the copyright owner. Further reproduction prohibited without permission.

Intersystem Crossing in Methylene

The photolysis of ketene, diazomethane, diazirine, or propane always produces both forms of methylene, $^1CH_2$ and $^3CH_2$. This has been verified spectroscopically[6,13] and by the decrease in quantum yields of products upon the addition of oxygen or large amounts of carbon monoxide.[12,17,19] Studies of the ketene photolysis system have shown that the relative amounts of $^1CH_2$ and $^3CH_2$ vary with photolyzing wavelength[12b, 19, 20,22,10] and the concentration of non-reactive gases.[22,24] Studies of the diazomethane photolysis system have shown that only the concentration of the non-reactive gases affects the relative amounts of $^1CH_2$ and $^3CH_2$; the concentration of the reactive gases does not affect the relative amounts.[21,6,23] In both the ketene and diazomethane systems, direct spectroscopic observations of $^3CH_2$ have shown that the amount of $^3CH_2$ increases as the concentration of a non-reactive gas, e.g., He, increases. This was was a very important discovery, for it meant that somehow a small, triatomic species

---

19. Ho, S. Y. and Noyes, W. A., Jr., J. Am. Chem. Soc. 89, 5091 (1967).
20. Carr, R. W., Jr. and Kistiakowsky, G. B., J. Phys. Chem. 70, 118 (1966).
21. Bader, R. F. W. and Generosa, J. I., Can. J. Chem. 43, 1631 (1965).
22. Eder, T. W. and Carr, R. W., Jr., J. Chem. Phys. 53, 2258 (1970).
23. Taylor, G. W. and Simons, J. W., Can. J. Chem. 48, 1016 (1970).
24. Cox, R. A. and Preston, K. F., ibid 47, 3345 (1969).

Reproduced with permission of the copyright owner. Further reproduction prohibited without permission.

was able to cross-over from a singlet to a triplet electronic state, a process which is forbidden by quantum mechanics. Methylene is not the only small species in which this spin-forbidden process occurs,[25] but it is one of the lightest.

Such spin-forbidden processes are known among atoms, but only among the very heavy atoms, such as Hg, where the orbitals are considered to be so closely spaced that they interfere with the electron spin, or in other words, where the spin-orbit interactions are large, and thus the spin is not a good quantum number or a precise characteristic for the atom. In these cases, spin does not have to be conserved. A transition from a singlet electronic state to a triplet electronic state has long been known to occur in large polyatomic molecules, for example, in benzene, anthracene, and many organic dye molecules. Quantum theories explain such spin-forbidden transitions by assuming that very closely spaced vibronic levels within either the triplet or singlet manifold allow a matching of energy levels. The resultant transition moment can be calculated using Fermi's Golden Rule.[25,26,27] However, such close spacing cannot occur in as small a triatomic species as CH_2.

---

25. Jortner, J., Rice, S. A., and Hochstrasser, R. M., Adv. Photochem. 7, 149 (1969).

26. Anderson, L. G., Parmenter, C. S., Poland, H. M., and Rau, J. D., Chem. Phys. Letters 8, 232 (1971).

27. Robinson,G. W. and Frosch, R. P., J. Chem. Phys. 38, 1187 (1963): Henry,B. R. and Kasha, M., Ann. Rev. Phys. Chem. 19, 161 (1968)

Reproduced with permission of the copyright owner. Further reproduction prohibited without permission.

Further experiments by Cox and Preston,[24] Eder and Carr,[22] and Bell[17] have established the importance of collisions in the intersystem crossing of CH_2. The prevailing view of the intersystem crossing in the methylene system is that collisions are necessary to convert $CH_2(^1A_1)$ to $CH_2(^3B_1)$ and that the rate of this intersystem crossing can be related to the polarizability of the collision partner. Thus, if $CH_2(^1A_1)$ is present in any system which is free from oxygen or any other similar scavenger, $CH_2(^3B_1)$ is also present, and the amount of $^3CH_2$ will depend on the gases present in the reaction system.

Chemical Activation and Unimolecular Reactions

Methylene has often been used to study the unimolecular decomposition of energy rich hydrocarbons.[28] When methylene is used for this purpose, it is desirable to have only the $^1A_1$ state reacting with the hydrocarbon. There are four reasons for eliminating the reactions of the $^3B_1$ state: reactions of the $^3B_1$ state with the hydrocarbon (1) result in an assortment of closely related side products, (2) are slower than the reactions of the $^1A_1$ state and so the $^3B_1$ state will lose more energy

28. See, for example, the reviews by Bell and Frey, ref. 10 and Rabinovitch, B. S. and Flowers, M. C., Quart. Rev. 1964, 122.

Reproduced with permission of the copyright owner. Further reproduction prohibited without permission.

through collisions and thus form a less energetic product, (3) proceed through a two step mechanism rather than a concerted insertion so that the separate radical intermediates may lose energy before recombining, and (4) will form a less energetic product than the $^1A_1$ state because at least some of the $^3B_1$ state is formed by the collisional conversion of the $^1A_1$ state. Thus, the reaction of $^3B_1$ methylene in a chemical activation system will result in an excited hydrocarbon which contains an ill-defined amount of energy.

Singlet methylene can be used to create a hydrocarbon which contains energy far in excess of that created by thermal collision (simple pyrolysis or thermal decomposition) and unlike thermal decompositions, this energy will be limited to a fairly narrow range. As the photolyzing energy used to decompose the ketene or diazomethane is increased, the average energy of the resulting hydrocarbon is also increased.[29,30] The rate of decomposition is determined from the variation of the products' distribution with pressure. The theories which describe unimolecular decompositions can be used to analyze the experimental rate constant to obtain more detailed knowledge about the activated

---

29. Johnson, R. L., Hase, W. L., and Simons, J. W., J. Chem. Phys. 52, 3911 (1970); Taylor, G. W. and Simons, J. W., Int. J. Chem. Kinet. 3, 25 (1971); Hase, W. L. and Simons, J. W., J. Chem. Phys. 54, 1277 (1971).

30. Butler, J. N. and Kistiakowsky, G. B., J. Am. Chem. Soc. 82, 759 (1960).

Reproduced with permission of the copyright owner. Further reproduction prohibited without permission.

complex, the configuration which the excited molecule must pass through just before decomposing, and the specific rate at which the excited molecule passes through this configuration.

There are many excellent discussions of the theories of unimolecular decomposition[31] and only a brief summary of the pertinent points will be presented here for the purposes of definition. The following reaction scheme is consistent with the three major theories of unimolecular reactions. k_E is the specific frequency at which a molecule of energy E changes into the configuration of the activated complex, $A^{\ddagger}$. k_1 is the rate constant for thermal adivation where the excited molecule, A^*, is produced by thermal collisions, and k_{bi} is the rate constant for chemical activation where the excited molecule is produced by chemical reaction.

$$A + A \xrightarrow{k_1} A^* + A$$

$$B + C \xrightarrow{k_{bi}} A^*$$

$$A^* \xrightarrow{k_E} A^{\ddagger} \longrightarrow \text{products}$$

$$A^* + M \xrightarrow{\omega} A + M$$

In the theories of Kassel[32] and Rice and Ramsperger[33], often known as the RRK theory, the excited molecule, A^*, is made up of a number of loosely coupled oscillators, s, (usually taken to be the molecule's normal modes of vibration or the individual

---

31. Laidler, K. J., Theories of Chemical Reaction Rates, 1969, McGraw-Hill, Inc. New York.

32. Kassel, L. S., J. Phys. Chem. 32, 225 (1928).

33. Rice, O. K. and Ramsperger, H. C., J. Am. Chem. Soc., 49, 1616 (1927); 50, 617 (1928).

Reproduced with permission of the copyright owner. Further reproduction prohibited without permission.

vibrating bonds) which are still separate enough to be described as normal modes and which, for convenience, are all assumed to be of the same frequency. Marcus[34] extended the RRK theory so that both the molecule and complex are made up of all the individual vibrations including each zero-point energy. The RRKM theory also includes the rotations of both the molecule and complex. In both theories, the available energy is statistically distributed among the vibrations, and reaction occurs when enough energy from all of the vibrations and participating rotations is concentrated in one vibration or rotation, the reaction coordinate, so that the bond breaks.

Slater[35] assumes that the molecular vibrations are not coupled and so no energy can be exchanged between them. He envisages the point of reaction to have occured when the vibrations of the molecule cause the critical coordinate, for example, a bond length, to be extended to a specific length. A very detailed treatment of the individual vibrations is needed to apply Slater's theory if the decomposition is to be studied over a wide range of conditions.

Studies of several molecules have shown that Slater's treatment predicts rate constants far smaller than either were

---

34. Marcus, R. A., J. Chem. Phys. 20, 359 (1952).

35. Slater, N. B., Proc. Camb. Phil. Soc. 35, 56 (1939) and Theory of Unimolecular Reactions, Cornell University Press, Ithaca, New York, 1959.

Reproduced with permission of the copyright owner. Further reproduction prohibited without permission.

observed or were predicted by the RRKM or RRK theories.[36] Thus, Slater's assumption that there is no energy flow between normal modes is incorrect. Further evidence was provided by Butler and Kistiakowsky[30] who used methylene to form methylcyclopropane by reactions with cyclopropane and propylene. No oxygen was used and so both the $^1A_1$ and $^3B_1$ states of methylene were reacting with the hydrocarbons. The methylcyclopropane formed from propylene will initially have the energy from the methylene concentrated in a different bond than when it is formed from cyclopropane. If there is no energy flow before decomposition, the distribution of butene isomers in the methylene-propylene system should be different from the distribution in the methylene-cyclopropane system. Butler and Kistiakowsky[30] found the same distribution of isomers in both systems which means that the energy was completely distributed before decomposition.

In the "classical limit", Slater's treatment is as good as the RRK treatment and both, although incorrect, can be useful approximations. When the average energy of the molecule, $\langle E \rangle$, is much larger than the critical energy necessary for decomposition, E_o, the molecule and complex, to a good approximation, can be treated classically. In this classical limit, the expressions for

---

36. See for example ref. 31 and also Gill, E. K. and Laidler, K. J., Proc. Roy. Soc. A250, 121 (1959).

Reproduced with permission of the copyright owner. Further reproduction prohibited without permission.

k_E in both the RRK theory and Slater's theory simplify to

$$k_E = k^{\ddagger}\left[\frac{\langle E\rangle - E_o}{\langle E\rangle}\right]^{s-1} \quad . \qquad (1)$$

The high pressure limit of thermal decompsition, k_∞, in both theories is

$$k_\infty = k^{\ddagger} \exp(-E_o/kT) \quad . \qquad (2)$$

Thus, $k^{\ddagger}$ corresponds to the frequency factor in the high pressure limit and can be determined from an Arrhenius plot of the high pressure limit of thermal decomposition at several temperatures.

RRKM Theory

A great deal of work has been done using the RRKM theory.[28,31,37] The expression for k_E has the form

$$k_E = \frac{1}{h}\,\frac{Z_1^{\ddagger}}{Z_1^{*}}\,\frac{\sum P(E_{vr}^{\ddagger})}{N^{*}(E_{vr})} \quad . \qquad (3)$$

$Z_1^{\ddagger}$ and Z_1^{*} are the products of the partition functions of the degrees of freedom which do not contribute to the energy available for decomposition (the adiabatic degrees of freedom) for the activated complex and molecule, respectively. h is Planck's constant and $E^{\ddagger} = E - E_o$, where E is the energy of the molecule. $\sum P(E_{vr}^{\ddagger})$ is

37. For reviews see Rabinovitch, B. S. and Flowers, M. C., Quart. Rev. 1964, 122 and Spicer, L. D. and Rabinovitch, B. S., Ann. Rev. Phys. Chem. 21, 349 (1970).

Reproduced with permission of the copyright owner. Further reproduction prohibited without permission.

the sum of the degeneracies of all the eigenstates of the active degrees of freedom (vibrational and rotational) for the activated complex at energy $E^{\ddagger}$, and $N^{*}(E_{vr})$ is the energy density of the active degrees of freedom for the molecule at energy E. The expressions for $\sum P(E^{\ddagger}_{vr})$ and $N^{*}(E_{vr})$ are:

$$\sum P(E^{\ddagger}_{vr}) = \frac{Z^{\ddagger}_{r}}{(kT)^{r^{\ddagger}/2}\,\Gamma(1 + r^{\ddagger}/2)} \sum_{E^{\ddagger}_{v}=0}^{E^{\ddagger}} P(E^{\ddagger}_{v})(E^{\ddagger}-E^{\ddagger}_{v})^{r^{\ddagger}/2} \; ;$$

$$r^{\ddagger} \neq 0.$$

$$P(E^{\ddagger}_{vr}) = \sum_{E^{\ddagger}_{v}=0}^{E^{\ddagger}} P(E^{\ddagger}_{v}) \; ; \; r^{\ddagger}=0$$

and

$$N^{*}(E_{vr}) = \frac{Z^{*}_{r}}{(kT)^{r^{*}/2}\,\Gamma(r^{*}/2)} \sum_{E_{v}=0}^{E} P^{*}(E_{v})(E-E_{v})^{r^{*}/2 - 1} \; ;$$

$$N^{*}(E_{vr}) = \left[\frac{\partial \sum_{E_{v}=0}^{E} P^{*}(E_{v})}{\partial E}\right]_{E_{v}=E} \quad ; \; r^{*}=0.$$

Z_r is the partition function for r active internal rotations and overall rotational degrees of freedom. $P(E_v)$ is the degeneracy of the vibrational eigenstate E_v. The stars and daggers refer to properties of the molecule and activated complex, respectively.

Reproduced with permission of the copyright owner. Further reproduction prohibited without permission.

Further details of the theory and methods of evaluating the eigenstates are given in the review article by Setser and Rabinovitch.[38] A computer program which evaluates the vibrational eigenstates as described by Whitten and Rabinovitch[39] and which calculates k_E at specified energy intervals when the other parameters are included is available from Professor B. S. Rabinovitch and is described in the review article by Setser and Rabinovitch.[38]

The Present Work

The experiments described in this thesis are in two parts. The first part of the thesis describes the reaction of the $^1A_1$, $^3B_1$, and $^1B_1$ states of methylene with isobutane, the different absorption regions of ketene, and the rate of intersystem crossing in the methylene system. The second part is a study of the reaction of the $^1A_1$ state of methylene, $^1CH_2$, with cyclopropane and the subsequent decomposition of methylcyclopropane into its four butene isomers. The source of methylene was ketene photolyzed at several wavelengths (214 nm, 277 nm, 313 nm, 322 nm, and 330 nm) chosen to represent each of the three absorption

---

38. Setser, D. W. and Rabinovitch, B. S., Adv. Photochem. 3, 1 (1964).

39. Whitten, G. Z. and Rabinovitch, B. S., J. Chem. Phys. 38, 2466 (1963).

Reproduced with permission of the copyright owner. Further reproduction prohibited without permission.

regions in the near ultraviolet absorption spectrum of ketene. Oxygen and carbon monoxide were used to distinguish between the reactions of the different states of methylene in the isobutane experiments. Oxygen was used to eliminate the reactions of the $^3B_1$ and $^1B_1$ states with cyclopropane. Professor B. S. Rabinovitch kindly supplied us with the computer program used in analyzing the decomposition of methylcyclopropane.

Reproduced with permission of the copyright owner. Further reproduction prohibited without permission.

TABLE 1-I *

Methylene and Configuration	r_o(C-H), Å	H-C-H angle	Approximate Energy
$^3B_1$, $(\sigma)^1(p)^1$	1.07_8	136°	0
$^1A_1$, $(\sigma)^2$	1.112	102.4°	1-2 kcal/mole
$^1B_1$, $(\sigma)^1(p)^1$	1.05	140±15°	30 kcal/mole

* From Herzberg's data, references 6 and 9.

Reproduced with permission of the copyright owner. Further reproduction prohibited without permission.

2 Apparatus and Techniques

Preparation of Ketene

Ketene was prepared by the pyrolysis of acetic anhydride at 520°C and was purified by subsequent trap to trap distillations.[1] After degassing, the acetic anhydride was slowly let into a warm flask (180°C) via a dropping funnel (see fig. 1-1). The liquid was vaporized in the flask and the gaseous acetic anhydride went into the quartz pyrolysis tube which was kept at 520°C. The pyrolyzed gas contained ketene, acetic acid, and unreacted acetic anhydride. The ketene passed through the dry ice-isopropanol trap and condensed in the liquid nitrogen trap; the acetic acid and acetic anhydride remained in the dry ice-isopropanol trap. Three trap to trap distillations using dry ice-isopropanol and liquid nitrogen further purified the ketene which was stored under liquid nitrogen to prevent decomposition and polymer formation. The ketene dimer forms fairly rapidly at vapor pressures of ketene above 100 Torr. Ketene prepared in this way contained less than 100 ppm of ethylene, ethane, and acetylene as determined by mass spectrometric analysis.[2] When analyzed on the gas chromatograph, ketene samples which were passed through the columns at temperatures up to 100°C showed no change in the size of the ethylene peak and no ketene. (Ethylene was the major impurity

---

1. Jenkins, A. D., J. Chem. Soc., 2563 (1962).

2. DeGraff, B. A., private communication.

Reproduced with permission of the copyright owner. Further reproduction prohibited without permission.

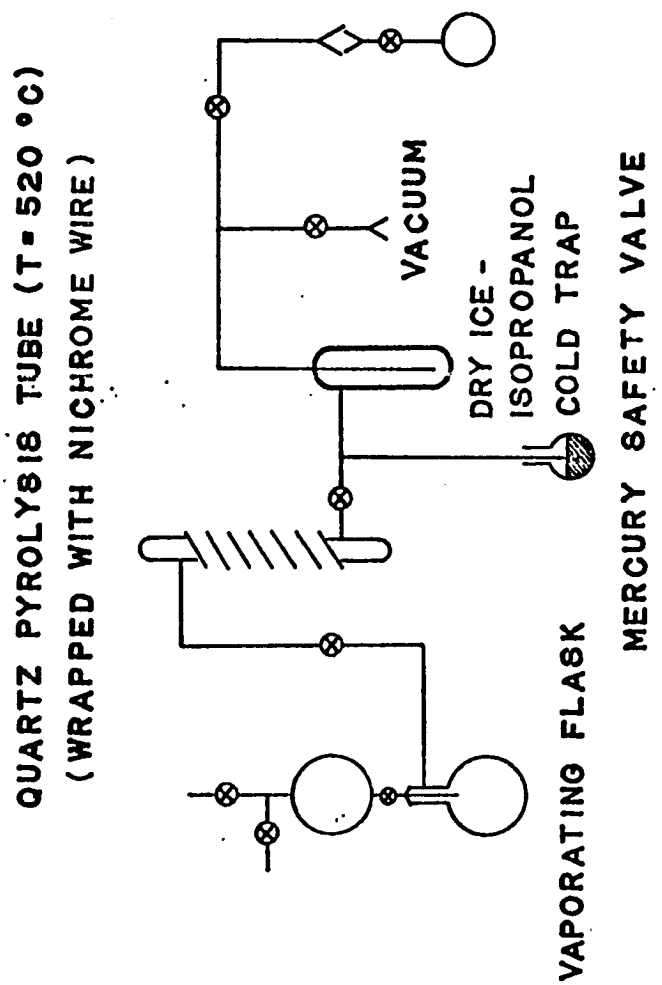

KETENE PREPARATION SYSTEM

Figure 2-1

Reproduced with permission of the copyright owner. Further reproduction prohibited without permission.

in the ketene.) Presumably the ketene sticks to the column and does not decompose to ethylene and CO once it is in the column.

Spectral Regions and Lamps Used for Photolysis

Most of the photolyses were done with an Osram HBO-500 Watt mercury super pressure lamp used in conjunction with a Bausch and Lomb (#33-86-01) grating monochromator. The spectral distributions were determined for specific monochromator settings by use of a (Jarrel-Ash, model 82-000) Ebert spectrometer and RCA-1P28 photomultiplier. The spectral distributions are shown in figure 2-2 and for easy reference, the position of maximum intensity for each setting is listed in Table 2-I. The Ebert spectrometer was calibrated at 313 nm, 334 nm and 366 nm with a mercury lamp. The wavelengths used when describing the experiments are the positions of maximum intensity rather than the monochromator settings. A rough sketch of the spectral output of the Osram HBO-500 Watt lamp in shown in figure 2-3 along with the absorption spectrum of ketene. During the photolyses a Corning filter, number CS 7-54, was placed in front of the photolysis cell to prevent transmission of second order wavelengths from the monochromator and scattered visible light.

Reproduced with permission of the copyright owner. Further reproduction prohibited without permission.

Reproduced with permission of the copyright owner. Further reproduction prohibited without permission.

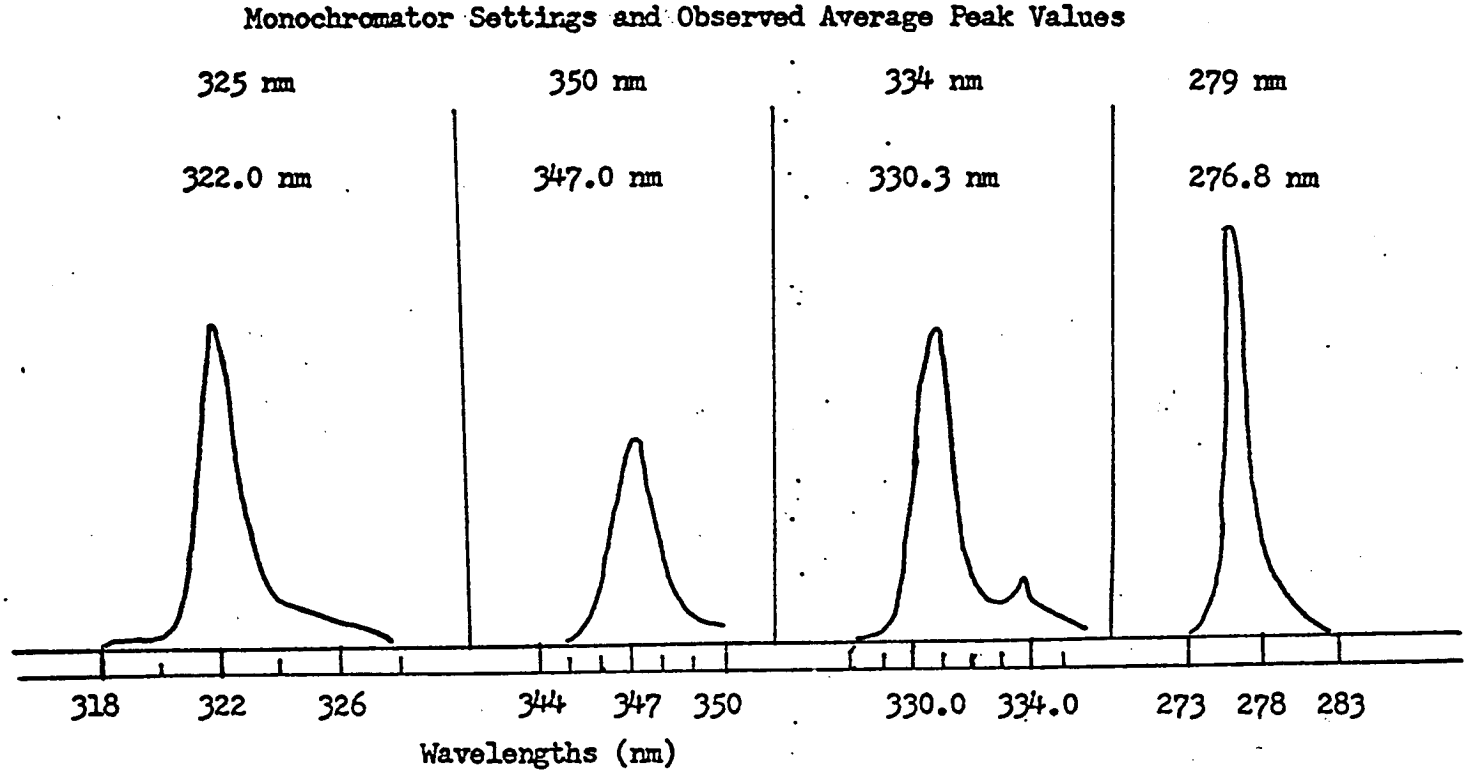

Figure 2-2

The Spectral Distributions for each Monochromator Setting Used.

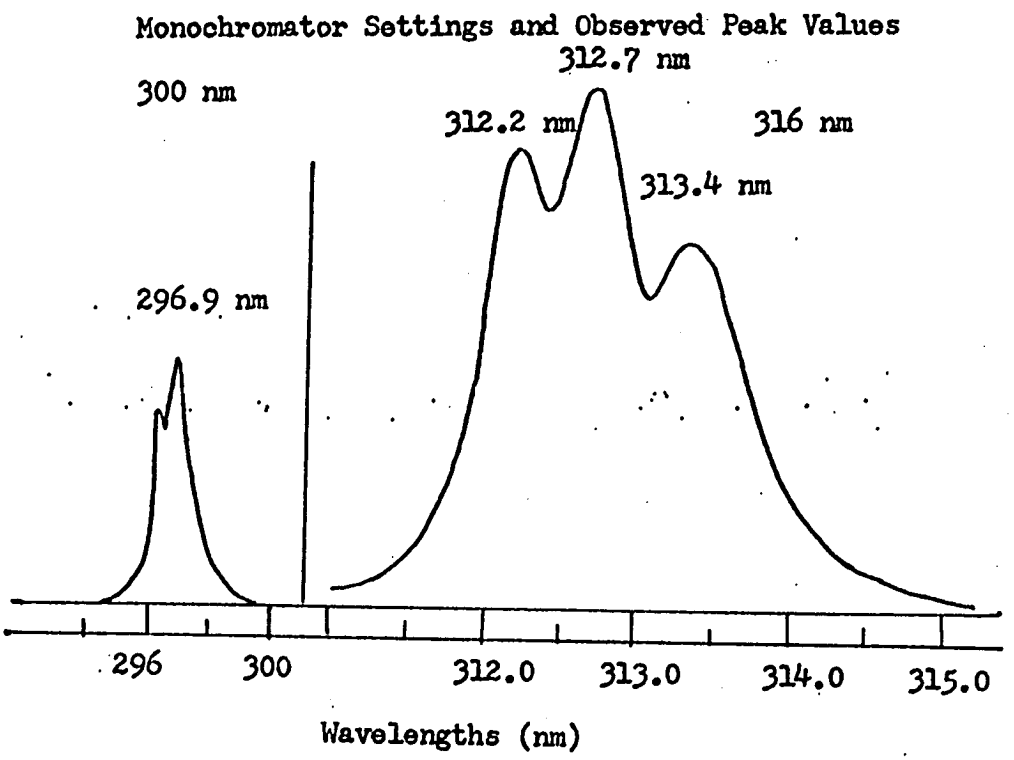

Figure 2-2 continued

Reproduced with permission of the copyright owner. Further reproduction prohibited without permission.

TABLE 2-I

The Spectral Distributions from the Monochromator

Monochromator Setting	Position of Maximum	ϵ $l\text{-mole}^{-1}\text{cm}^{-1}$
279 nm	277 nm	6.9
300 nm	297 nm	10.4
316 nm	313 nm	10.9
325 nm	322 nm	11.5
334 nm	330 nm	12.3
350 nm	347 nm	----

Reproduced with permission of the copyright owner. Further reproduction prohibited without permission.

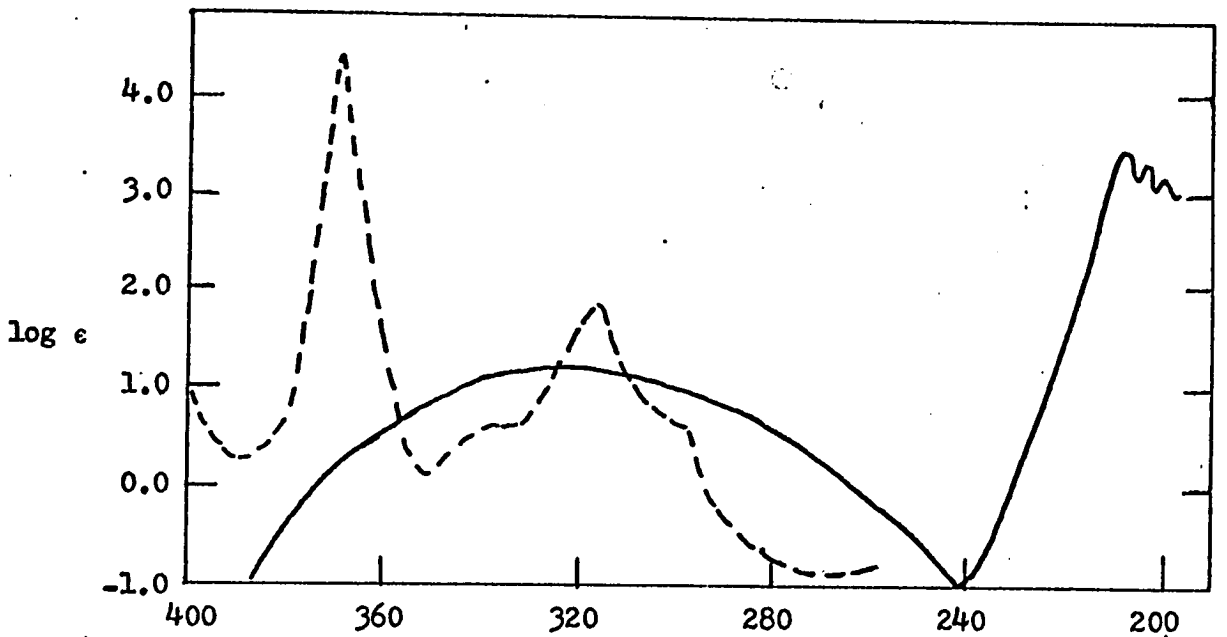

——— ketene absorption, ε= decadic extinction coefficient, liters/mole-cm.

------ output of the Osram HBO-500W mercury lamp, arbitrary units.

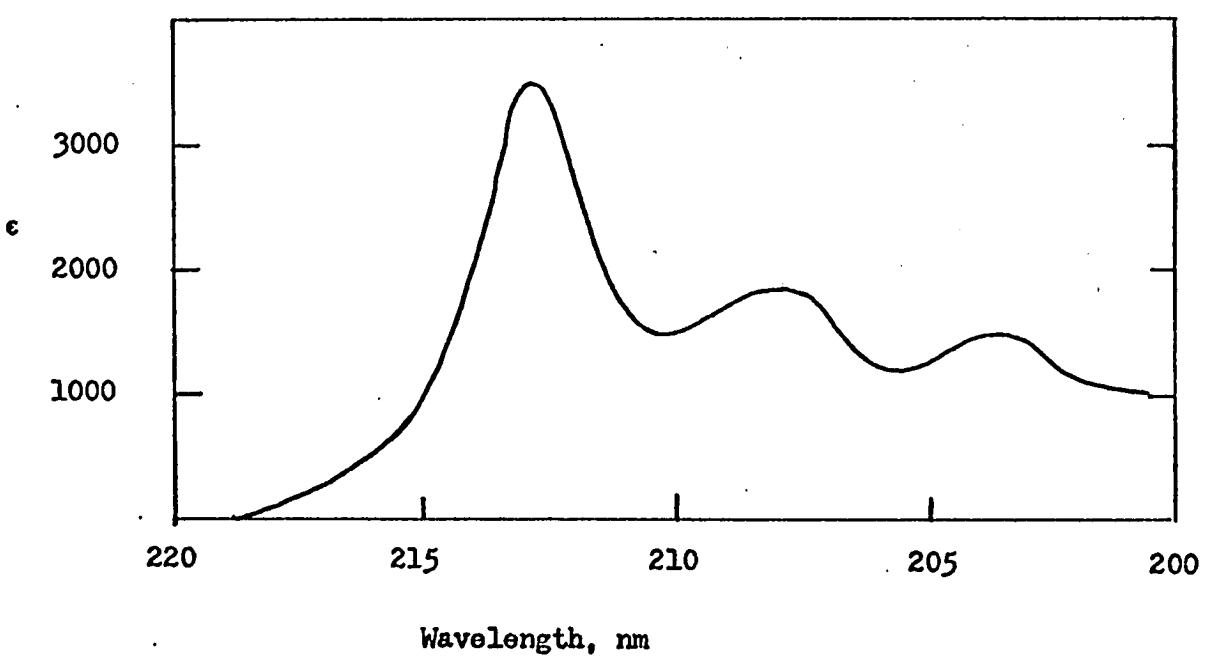

Figure 2-3 The Absorption Spectrum of Ketene from 200 nm to 400 nm (Taken from Sauer, K. H., Ph.D. Thesis (Harvard University, 1957), p.128)

Reproduced with permission of the copyright owner. Further reproduction prohibited without permission.

Photolyses in the 200 nm region were done using light from a Phillips, #93106E, 25 Watt , zinc lamp. The spectral output of the zinc lamp is sketched in figure 2-4 and compared to that found by Yamazaki and Cvetanovic[3] in Table 2-II. A Baird-Atomic standard line filter for 214 nm with a full width of approximately 20 nm(courtesy of Professor W. A. Klemperer and Dr. Lynn Melton) was used to isolate the 214 nm region. Since very little light longer than 230 nm will be absorbed by ketene compared to the light absorbed in the 214 nm region, the filter does not have to have a narrow band pass in order to have a relatively narrow band of effective photolyzing light from the zinc lamp.

The Optical Arrangement for Photolysis

The optical train used with the Osram HBO-500 Watt lamp is shown schematically in figure 2-6. The Osram mercury lamp is virtually a point source lamp. The phototube used to monitor the light was an RCA 935-S5 vacuum diode with a 45 volt battery as the power supply.

The optical train was modified for the 214 nm photolyses. The monochromator and the Corning filter were removed and the Phillips zinc lamp, which is not a point source, was placed as close as possible to the photolysis cell (an asbestos housing

3. Yamazaki, H. and Cventanovic, R. J., J. Chem. Phys. 41, 3703 (1964).

Reproduced with permission of the copyright owner. Further reproduction prohibited without permission.

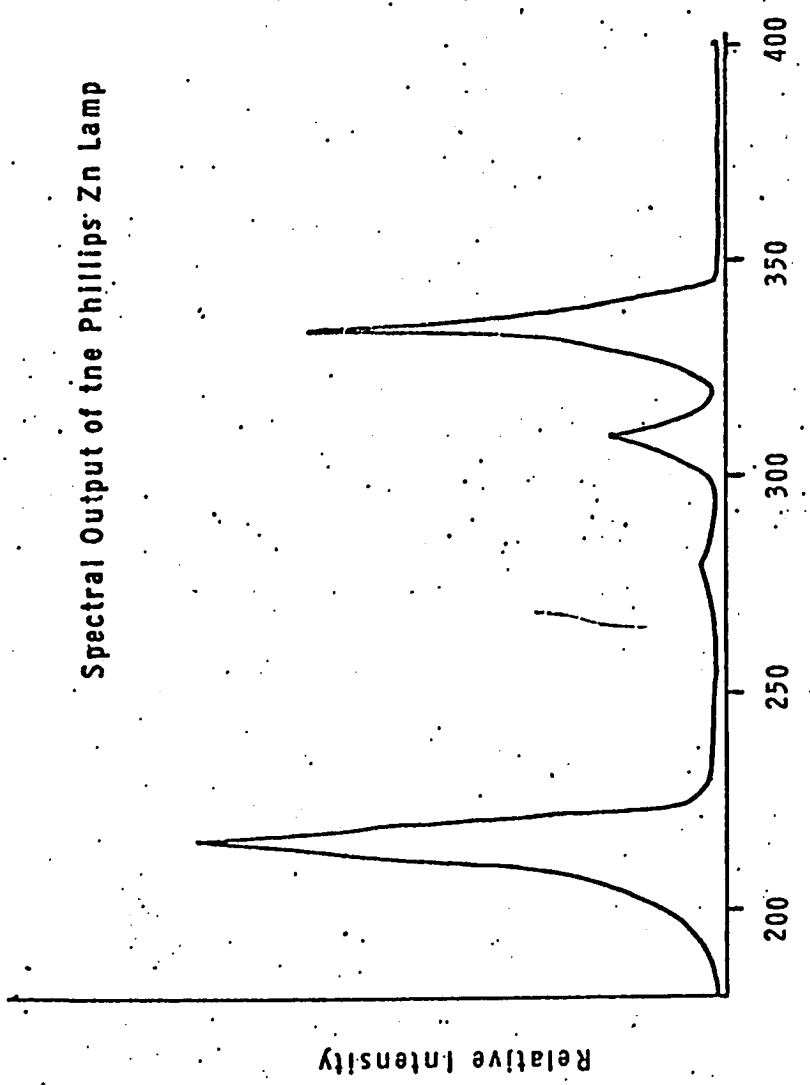

Figure 2.4

Reproduced with permission of the copyright owner. Further reproduction prohibited without permission.

TABLE 2-II

Spectral Output of the Phillips Zinc Lamp (180 nm-400 nm)

Wavelength	This work	Yamazaki and Cventanovic
213.9 nm	50%	51%
280.0 nm	1%	---
309.2 nm	10%	16%
330.3 nm	39%	13%
334.5 nm		15%

Reproduced with permission of the copyright owner. Further reproduction prohibited without permission.

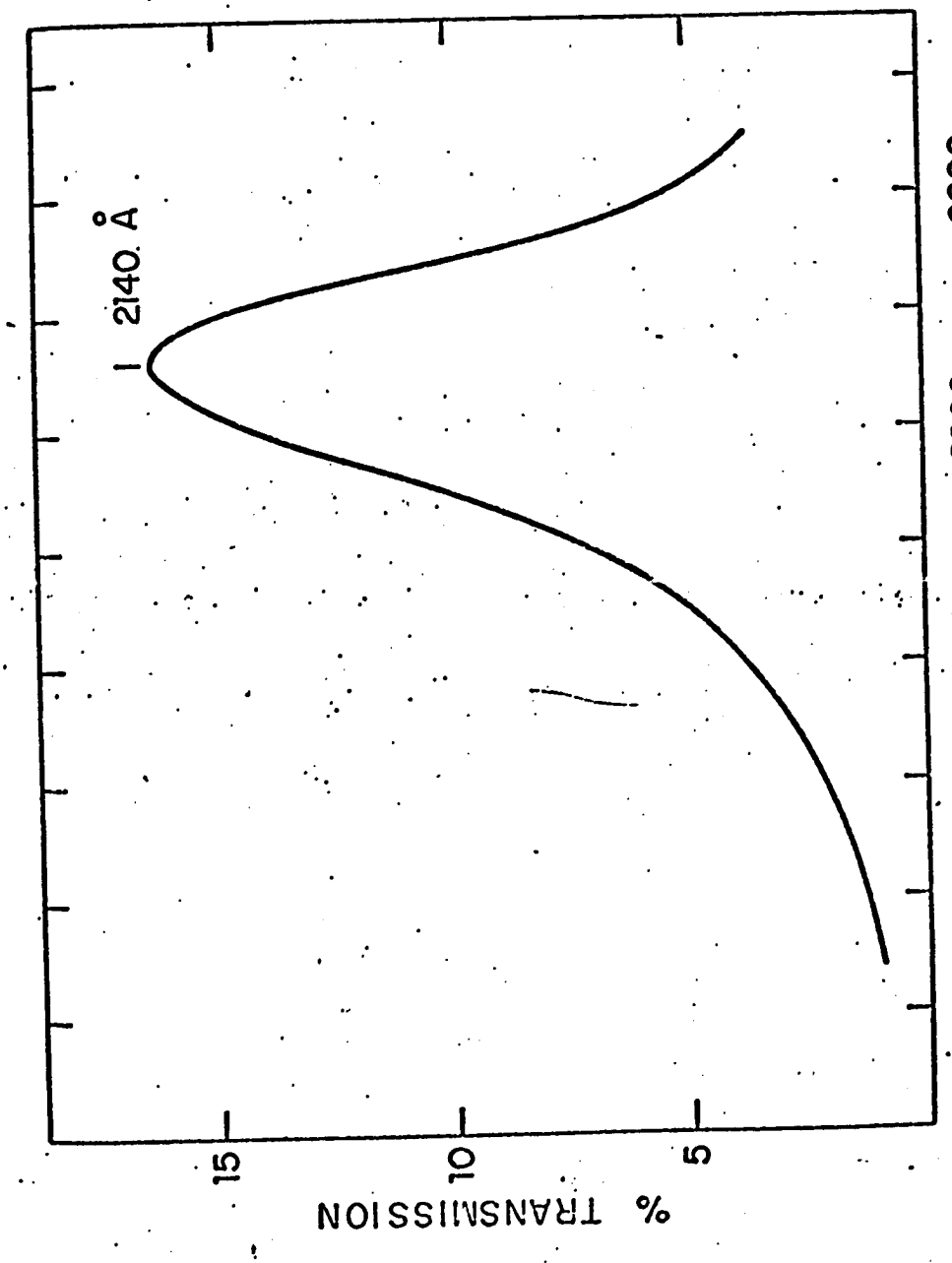

Figure 2-5

Characteristics of the Baird Atomic 214 nm Line Filter (from Walter, T. A., Ph. D. Thesis, Harvard University, 1967, p. 40).

Reproduced with permission of the copyright owner. Further reproduction prohibited without permission.

surrounding the photolysis cell was the limiting factor in positioning the lamp). The short focal length convex lens usually in front of the point source was placed in front of the lamp, and another convex lens replaced the first plano-convex lens and the interference filter was placed just before the cell. The RCA 935 phototube was replaced with a 1-P28 photomultiplier tube with a 300 volt DC power supply. The photomultiplier was connected to a Keithley 601 electrometer and the signal from the electrometer was monitored on the Hewlett-Packard recorder.

A suprasil photolysis cell, 15 cm long and 2 cm in diameter, was connected to a circulating pump which was operated continuously during the photolyses at 214 nm. At this wavelength, the extinction coefficient is so large that 90% of the light is absorbed within 0.65 cm of the front window of the cell. (This calculation assumes that the value of ϵ is 2.64×10^3 l/mole-cm, as given by T. A. Walter.[4]) Stirring is required to ensure that the reactions at 214 nm are not different from the reactions at the longer wavelengths because of local condititions, e.g., depletion of the ketene or extensive reactions of CH_2 with radicals in the volume right behind the front window.

---

4. Walter, T. A., Ph.D. Thesis (Harvard University, 1967)

Reproduced with permission of the copyright owner. Further reproduction prohibited without permission.

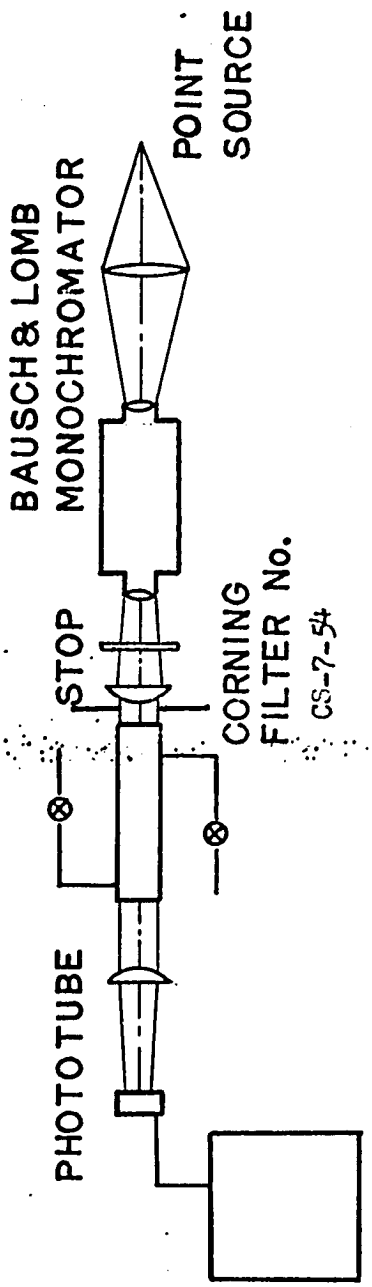

TYPICAL OPTICAL ARRANGEMENT

Figure 2-6

Reproduced with permission of the copyright owner. Further reproduction prohibited without permission.

Pressures in the photolysis cell were measured with a differential Wallace-Tiernan gauge (0-50 Torr) in conjunction with a standard mercury manometer. The polymer deposits on the windows of the photolysis cell were removed periodically with concentrated nitric acid and acetone. After each cleaning, the cell was seasoned by photolyzing ketene and a hydrocarbon (isobutane or cyclopropane) for one to two hours. A schematic of the gas handling line at the photolysis cell is shown in figure 2-7.

Beer's Law Studies and the Measurement of the Light Intensity

A Beer's Law series of absorption measurements in the pressure range of from 5 Torr to 50 Torr was done for each spectral region used. The experimental extinction coefficients and effective wavelengths are listed in Table 2-I. At 214 nm, even with 2.6 Torr of ketene, all of the incident light was absorbed. (Kistiakowsky and Walter[5] Sauer,[6] and Braun, Bass and Pilling[7] all report an extinction coefficient greater than 1000 liters/mole-cm in this wavelength region.)

---

5. Kistiakowsky, G. B. and Walter, T. A., J. Phys. Chem. 72, 3952 (1968).

6. Sauer, K. H., Ph. D. Thesis (Harvard University,1957).

7. Braun, W., Bass, A. M., and Pilling, M., J. Chem. Phys. 52, 5131 (1970).

Reproduced with permission of the copyright owner. Further reproduction prohibited without permission.

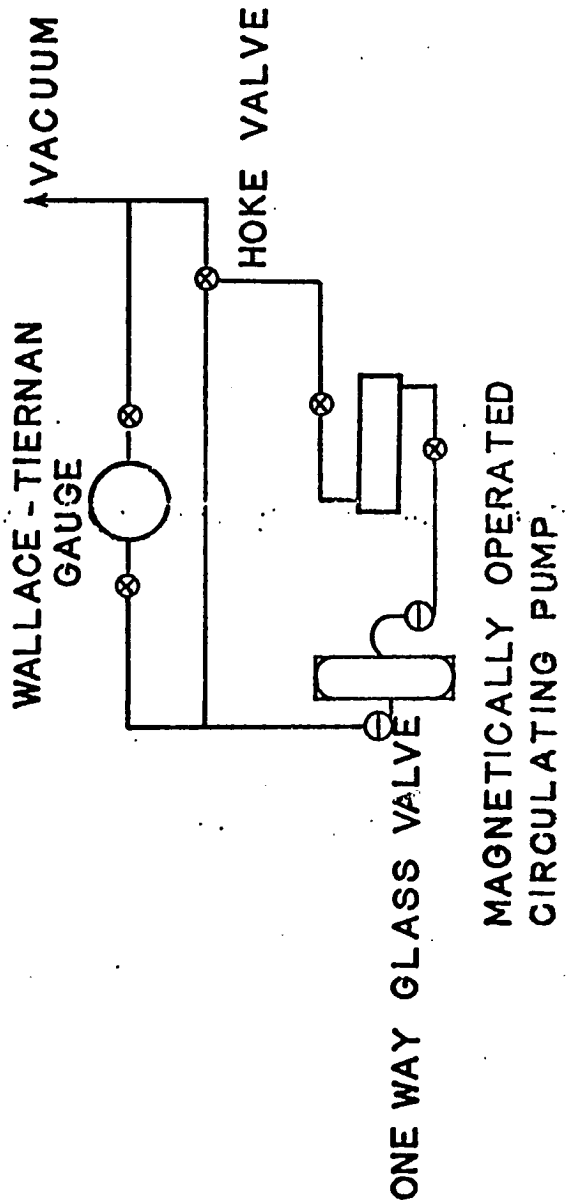

SCHEMATIC OF GAS HANDLING LINE AT THE PHOTOLYSIS CELL

Figure 2-7

Reproduced with permission of the copyright owner. Further reproduction prohibited without permission.

Since absolute yields were to be determined, the amount of light absorbed during each photolysis was needed. The transmitted light was continuously monitored with either the RCA 935 phototube or the 1P-28 photomultiplier and was recorded with the Hewlett-Packard recorder during each photolysis. The power supply for the mercury lamp consisted of ten large lead batteries in the subbasement of the Mallinckrodt Laboratory. Since other members of the department used this power source, the input current of the mercury lamp varied during a typical photolysis and caused the light intensity to fluctuate. For this reason, the lamp's transmitted intensity was averaged over 15 minute intervals for the usual photolysis time of four hours. The amount of ketene decomposed (calculated by both CO yields and hydrocarbon yields) was never larger than 5% (usually 2-3%) so that the variation in the transmitted light was not due to changes in ketene concentration.

The changes in the intensity of the lamp could not be predicted and so the incident intensity during the photolysis was not well known and could not be used to calculate the light absorbed during the photolysis. Instead, the intensity of the light absorbed, I_a, was calculated from the intensity of the transmitted light, I_t, using Beer's Law,

$$I_a = I_t(10^{ecl} - 1.0),$$

Reproduced with permission of the copyright owner. Further reproduction prohibited without permission.

where ϵ is the extinction coefficient in liters/mole-cm,

c is the concentration of ketene in moles/liter,

and l is the length of the photolysis cell, 15.0 cm.

There are two major sources of error in the light measurements: errors of the measurement of the concentration of ketene and errors in the light intensity monitoring system. Generally, the concentration of ketene was known to better than 5%, and for small extinction coefficients, the error in I_a due to errors in the concentration of ketene will be small. In the wavelength region about 277 nm, the extinction coefficient , the intensity of the lamp output and the spectral response of the phototube were all small. Even with amplification, the intensity reading was never more than 20% of the full scale of the recorder. (The intensity readings for most other wavelengths were at least 50% of the full scale.) This small signal meant that the usual deadband error in the recorder (1.5% of the full scale) induced an error of approximately 10% in the light intensity measurements at 277 nm. Since the final product measurements were divided by the intensity of the absorbed light, large errors in the intensity were amplified in the product yields. This can be seen in the results (figures 3-3, 3-4, and 3-5) where the 277 nm yields have the largest random error. Estimating the position of the recorder tracing will result in a larger percentage of uncertainty in the smaller signals.

Reproduced with permission of the copyright owner. Further reproduction prohibited without permission.

Since estimating the position of the recorder tracing depends on the operator's objectivity, there is a chance that the position will be consistently estimated either high or low. The error from the dead band of the recorder will also contribute to a consistently high or low reading.

At 214 nm, the ketene absorbs all of the light entering the photolysis cell. The Keithley electrometer and photomultiplier were used to monitor the transmitted light when no ketene was in the cell.(the incident light intensity) and the light scattered by the components of the optical train.when ketene was in the cell. The transformer for the Phillips zinc lamp was an auto-leak transformer with a 140 Watt rating, and was operated from the line current (115 V, 60 Hz) had an open circuit voltage of 470 V.

Fortunately, the problem of fluctuating light intensity due to the power supply which complicated the experiments using the mercury lamp did not occur with the zinc lamp. The difference in intensity between the incident light and the scattered light (which was measurable and important only at this wavelength) was easily determined. There was very little difference between the incident light measured before and after each photolysis, and this was only a random difference. These two measurements were averaged and used for the incident light intensity.

Reproduced with permission of the copyright owner. Further reproduction prohibited without permission.

The Purity of the Gases used in the Photolyses

The composition of the gas mixtures photolyzed in the isobutane experiments was 100 parts of isobutane, 10 parts of ketene, and 1 part of propane. The composition of the gas mixtures used in the cyclopropane experiments was 10 parts of cyclopropane and 1 part of ketene. Except for cyclopropane, the other hydrocarbons were Phillips Research Grade and were used without further purification. The cyclopropane was C.P. grade and its major impurity (and the only one detected on the gas chromatographic columns used) was 0.3% propylene. The propylene was used as an internal standard for gas chromatographic analysis and was measured before and after each photolysis.

Air Reduction Co. research grade O_2 was used in both the isobutane and cyclopropane experiments, and Air Reduction Co. research grade Xe was used in the isobutane experiments. According to the label, the Xe contained 120 ppm of Kr and less than 2.0 ppm of other impurities.

Matheson research grade CO was used in the isobutane experiments. Matheson lists the impurities as 4 ppm of O_2, 960 ppm of N_2, 15 ppm of Ar, 4 ppm of H_2, and 45 ppm of CO_2. To minimize the formation of $Fe(CO)_5$, a liquid with a measurable

Reproduced with permission of the copyright owner. Further reproduction prohibited without permission.

vapor pressure at room temperature, the Matheson Company stores the research grade CO in a stainless steel tank. They seem to have forgotten that $Ni(CO)_4$, a gas at room temperature, is formed more easily than $Fe(CO)_5$ and the ease of formation is large for impure sources of nickel. The $Ni(CO)_4$ present in the CO absorbed ultraviolet light (300 nm-350 nm) and produced some spurious results in the yields (because of light intensity measurements) until the cause was identified.

With Dr. John H. Marlow's help, the research grade CO from the tank was passed through a piece of pyrex tubing that was gently heated with a Bunsen burner, and a silver mirror, typical of Ni, was deposited at the cooler end of the tube.[8] No metallic plating (or ultraviolet light absorption) was noticed in the C. P. grade CO. C. P. grade CO is stored in a standard steel tank, not in a stainless steel tank. Before use, the research grade CO was passed slowly from the tank through a coil packed with glass helices and immersed in liquid nitrogen and into a storage bulb. The $Ni(CO)_4$, a white crystalline deposit which appeared on the helices just before the liquid nitrogen, was removed by this process. The gas which was stored did not show any absorption in the ultraviolet. No crystalline deposit was seen when C. P. grade

---

8. Walton, H. F., Inorganic Preparations, Prentice-Hall, Inc., (1948), pp. 93-96.

Reproduced with permission of the copyright owner. Further reproduction prohibited without permission.

CO was passed through liquid nitrogen. Only research grade CO which was processed in this manner was used in the experiments. No C. P. grade CO was used.

Product Analysis

A Perkin-Elmer, model 154, Vapor Fractometer and accompanying flame-ionization detector were used to analyze the products. Helium was used as the carrier gas. Hydrogen and Air Zero (air with less than 2 ppm of hydrocarbons - expressed as methane) were used for the flame. A Leeds and Northrup Speedomax W recordor with a disc integrator was used to record the peaks and the integrated areas under the peaks. As will be discussed in the next section, the peak area was not measured solely by the disc integrator.

The sample injector system of the gas chromatograph was modified to allow the introduction of gas samples. A schematic of the injection system is shown in figure 2-8. An Aerograph (Type XA-204), 6-way linear valve with Viton o-rings was used to inject the samples. The samples were measured in the gas burette and then expanded into the coil. (See figure 2-8.) The volumes of the connecting tubing and coil were all known and so the exact fraction of the gas measured in the burette which

Reproduced with permission of the copyright owner. Further reproduction prohibited without permission.

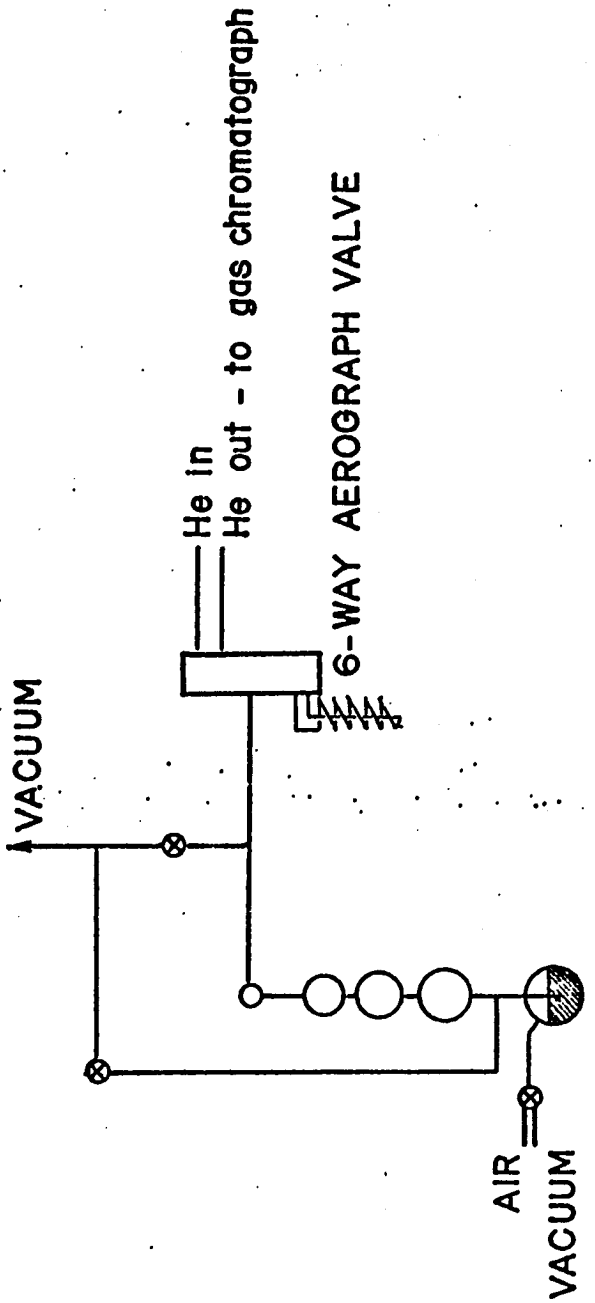

GAS CHROMATOGRAPHIC SAMPLE INLET SYSTEM

Figure 2-8

Reproduced with permission of the copyright owner. Further reproduction prohibited without permission.

passed into the column was also known. One of the valve openings was sealed off so that when the coil was open to the rest of the tubing and the measured gas was let into the coil, the volume of gas not going into the gas chromatograph was a minimum. This dead volume was very small compared to the volume of the coil.

Neither the ketene nor any of the possible oxygen containing compounds (aldehydes, ketones, or alcohols) which might result from the reaction of O_2 and ketene or O_2 and butyl, cyclopropyl, or methyl radicals can be detected with the columns used. Presumably, they are so polar that they are retained on the columns and only gradually bleed off.

Part 1: The Product Analysis of the Isobutane System.

The column finally chosen to analyze the gases expected from the photolysis of the isobutane-ketene-propane mixtures (CH_4, C_2H_4, C_2H_6, C_3H_8, C_4H_8, C_4H_{10}, C_5H_{12}, and C_3H_{18}) was a $\frac{1}{4}$ inch O.D. copper tube 6 m long, packed with 80/100 mesh Porasil C (Waters Associates). The column was crudely temperature programmed in order to elute the octanes before the peaks were too broad to be measurable and within a reasonable analysis time. (At least two analyses were done for each photolysis.) The temperature was set at 70°C until the pentanes were off the column, after which the temperature was reset at 110°C until the octanes

Reproduced with permission of the copyright owner. Further reproduction prohibited without permission.

had eluted. A Perkin-Elmer Column E was used for those experiments in which isobutene was also monitored.

The Porasil C column was chosen because the tailing from the comparatively huge amount of isobutane was small (although as seen from figure 2-9a, the tailing was still significant), the octanes could be measured on the same column with almost all of the major products, and the two largest products (neopentane and isopentane) were well resoved, not too broad, and distinct from the isobutane. Figure 2-9a shows a typical chromatogram (shortened to include the octanes). The isobutene came off within the isobutane tailing on the Porasil C column and was hidden by it, and so for some experiments, the photolyzed gas mixture was also analyzed with a Perkin-Elmer Column E. However, neopentane was only barely distinct from the isobutane on Column E, and as seen in figure 2-9b, the neopentane's base line was much too steep for accurate measurements of the peak area.

The area under a peak is proportional to the amount of gas represented by the peak. Propane was used to calibrate the response of the detector. The calibration is shown in figure 2-10; the peak area increases linearly with an increase in sample size. When detected by flame ionization, the peaks are also proportional to the number of carbons in the hydrocarbon. Ettre[9] has tabulated

---

9. Ettre, L. S., "Relative Molar Response of Hydrocarbons on the Ionization Detectors," in Gas Chromatography, Brenner, N., Callen, J. E., and Weiss, M. D., eds. (Academic Press, New York, 1962).

Reproduced with permission of the copyright owner. Further reproduction prohibited without permission.

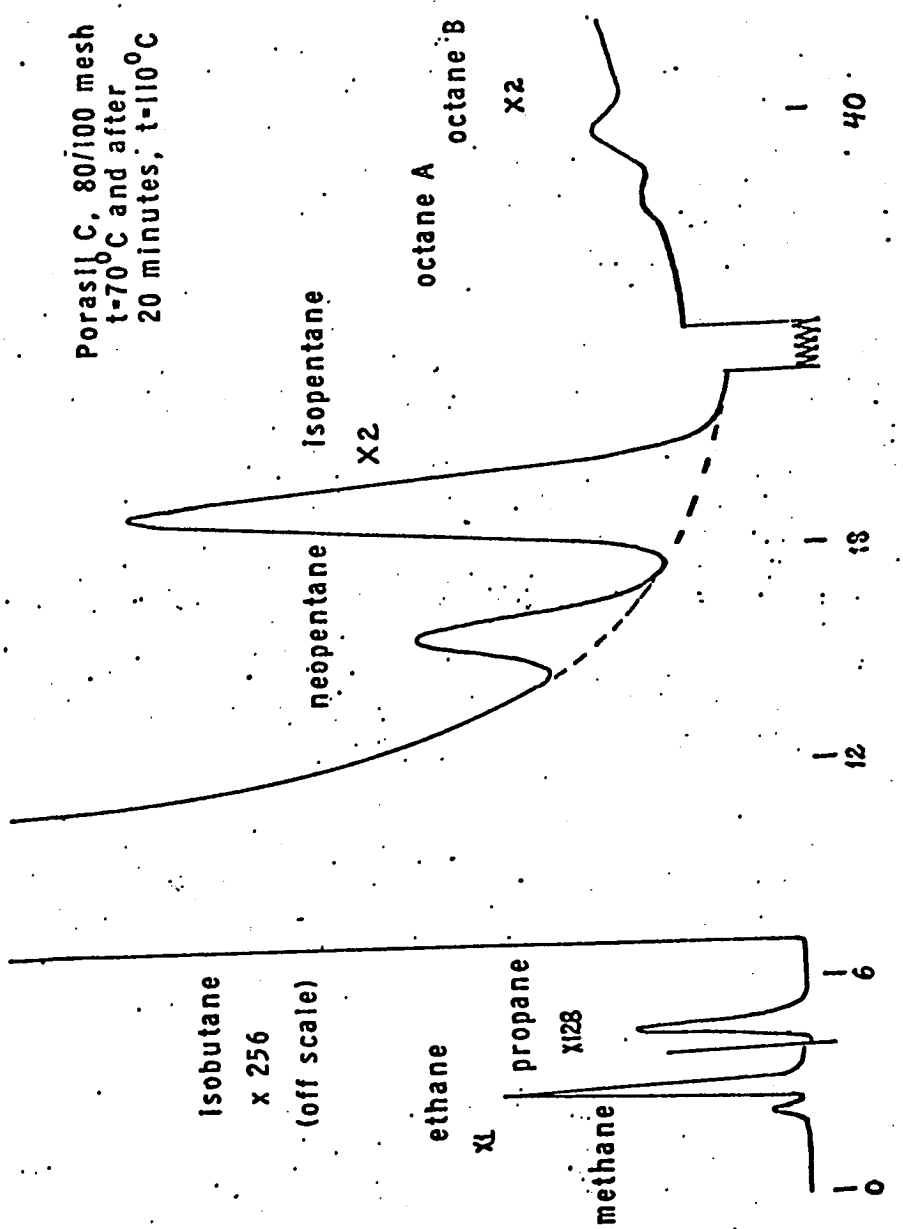

Figure 2-9a

Reproduced with permission of the copyright owner. Further reproduction prohibited without permission.

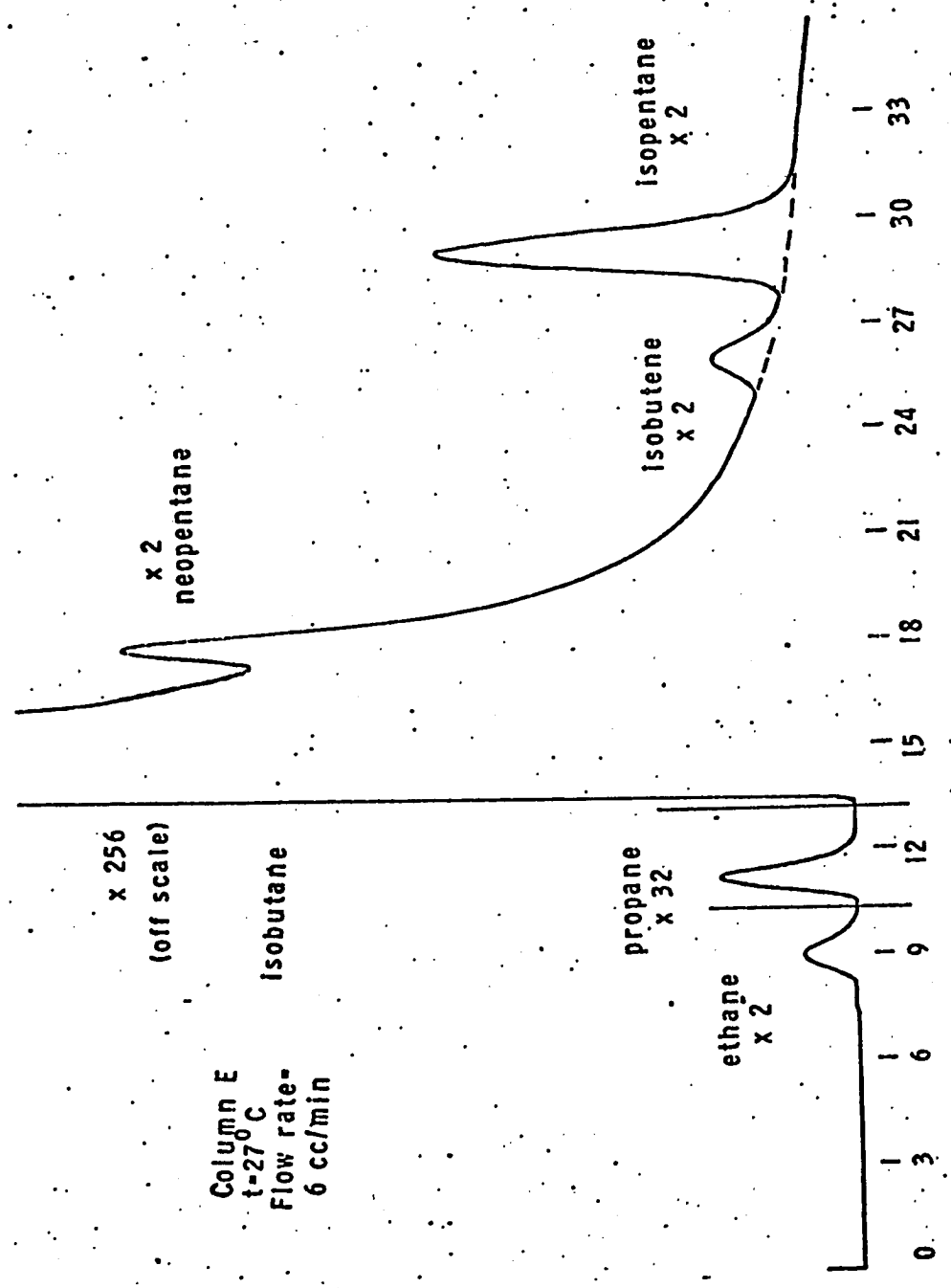

Figure 2-9b

Reproduced with permission of the copyright owner. Further reproduction prohibited without permission.

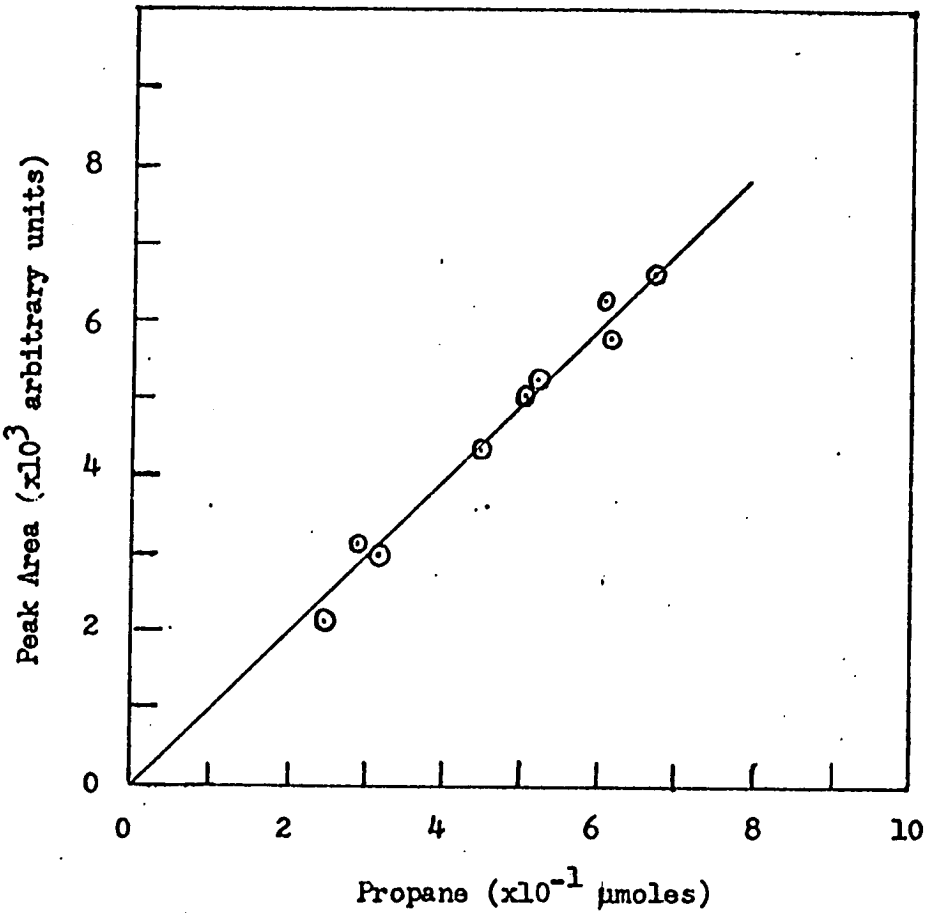

The Calibration of the Response of the Flame Ionization Detector with Propane

Figure 2-10

Reproduced with permission of the copyright owner. Further reproduction prohibited without permission.

the response of various hydrocarbons relative to n-heptane (700). A small portion of his table is repeated in Table 2-III for those alkanes studied in this work. Ettre did not list any olefins and so the olefin responses were estimated to be the same as the corresponding alkane, e.g., isobutene's response was set equal to the isobutane and n-butane response of 378.

Although the detector response increases linearly with increasing sample size, the use of an internal standard is preferred when measuring absolute yields. An internal standard eliminates errors due to errors in measuring the sample size and also serves as a check on the concentration of the hydrocarbons in the unphotolyzed reaction mixture. There was also an additional advantage to using an internal standard with this detector. Each time the detector cap was removed there was a chance that the platinum collecting electrode would be disturbed. Any displacement of the collecting electrode would change the geometry of the electric field and thus the response of the detector. The hydrogen flame was lit manually which required removing and then replacing the detector cap. This was done each day the gas chromatograph was used in order to minimize heat fatigue in the leads within the detector block.

The recorder used with the gas chromatograph was equipped

Reproduced with permission of the copyright owner. Further reproduction prohibited without permission.

TABLE 2-III

The Molar Response of the Hydrocarbons with a Flame Ionization Detector

Hydrocarbon	Ettre's Relative Molar Response	Response Used
Methane	90	90
Ethane	189	189
Propane	284	284
Isobutane	378	378
n-Butane	378	378
Neopentane	---	525
Isopentane	529	525
n-Pentane	524	---
2,5Dimethylhexane	806	800
2,2,4 Trimethylpentane	798	800
2,2,4,4 Tetramethylbutane	---	800

Reproduced with permission of the copyright owner. Further reproduction prohibited without permission.

with a disc integrator. The disc integrator is the most accurate of the methods used to measure peak areas, but only when the base line is straight. The disc integrator was used to measure the earlier peaks, methane, ethane, and propane. The isobutene and pentanes appear on the tail of the isobutane and since the base line has a considerable curvature to it, the disc integration method is not suitable. The base lines were estimated using a French curve (the dotted lines in figure 2-9a). At least two and usually four planimeter tracings were made of each peak. Several different sizes of propane peaks were measured using both methods, disc integration and planimeter tracings. These were used to relate the two methods so that direct comparisons between all the peaks could be made.

A third method of measuring the peak areas was tried. The chromatograms were xeroxed and the peaks were cut out and weighed on a much abused Mettler analytical balance. This method should have been more precise than the planimeter tracings. However, since continuous calibration of the balance would have been necessary to achieve this precision, this method was abandoned in favor of the planimeter method, a much less time consuming method.

The error in measurements from the planimeter method was on

Reproduced with permission of the copyright owner. Further reproduction prohibited without permission.

the order of 2-3% for the larger peaks and as much as 10% for the smaller peaks. (At least four planimeter tracings were made for the smaller peaks.) The error in peak areas as measured by the disc integrator was 2-3%.

Part 2: The Product Analysis of the Cyclopropane System

The products expected from the photolysis of ketene and cyclopropane are methylcyclopropane, isobutene, butene-1, and cis- and trans- butene-2. Ideally, the separation of all five isomers is required. The minimal acceptable separation is the separation of the methylcyclopropane from the butenes and the separation of the butenes from the reactants so that the life-times of the methylcyclopropane can be measured. Several columns were tried and rejected for various reasons.

The first column tried was the Perkin-Elmer Column E (a 30 foot long, 1/8 inch O.D. stainless steel tubing packed with 33% dimethylsulfolane on 60/80 mesh Chromosorb P) operated at 30°C and a flow rate of 6 cm^3/minute. The isobutene and butene-1 peaks were hidden under the very large cyclopropane peak, and the trans-butene-2 was not separated from the methylcyclopropane. The second type of column tried was a silver nitrate-ethylene gylcol (or carbitol) column. Several of these columns were made and tried. The columns had to be operated in an ice bath because

Reproduced with permission of the copyright owner. Further reproduction prohibited without permission.

the Ag-olefin complexes which determine the order of elution are destroyed near room temperature. But even in an ice bath, the columns had an unusually large background noise. The butene-1 came off with the cyclopropane and so could not be measured. The remaining peaks were fairly well resolved, but the noisy background would have prevented any meaningful quantitative analysis.

M. Papic[10] claimed to have separated the C_4's on a Porapak Q column. The column eventually used was a piece of 10 foot long, $\frac{1}{4}$ inch O.D. copper tubing filled with 2 parts of Porapak Q and 1 part of Porapak Q-S (both 50/80 mesh). (The Porapak Q-S is the same as the Porapak Q, but is treated with silane in order to reduce tailing.) The 50/80 mesh Porapak Q separated the products much better than the 80/100 mesh recommended by Papic, and there was no significant peak distortion as claimed by Papic. Although the products (with the exception of the last peak, the cis-butene-2 peak) were not completely resolved from each other, the resolution was the best of the columns tried. The isobutene and butene-1 were not resolved from each other. One of the biggest advantages of this column was that by the time the C_4H_8 products were eluted from the column, there was no tailing from the cyclopropane.

---

10. Papic, M., J. Gas Chromatography 6, 493 (1968).

Reproduced with permission of the copyright owner. Further reproduction prohibited without permission.

A typical chromatogram is shown in figure 2-11. The methane, ethane, ethylene and propylene (unresolved from each other), and cyclopropane are not shown in the figure. Dotted lines show the estimate made for resolution. This lack of resolution introduced the largest error in the yield of methylcyclopropane relative to the olefins for small photolysis pressures where the yield of methylcyclopropane compared to the olefins was smallest. Under these conditions, more than 20% of the methylcyclopropane peak will be under the two side peaks (isobutene and butene-1 and trans-butene-2, figure 2-11).

The error from estimating the shape of the methylcyclopropane when the peaks of the butene isomers were a significant percentage of the products was minimized by comparing the methylcyclopropane peaks with a set of different sized peaks of methylcyclopropane. This set was constructed from the gas chromatographic analysis of 690 Torr of a mixture of 20:1:1, cyclopropane to ketene to oxygen, photolyzed at 313 nm. At this pressure, close to 90% of the total C_4H_8 products was methylcyclopropane. Five different sample sizes of the products were analyzed, and these chromatograms were used as a guide in estimating the shape of the edges of the methylcyclopropane peak in the other photolysis mixtures. At least two planimeter tracings were made for each peak. This method seemed to work fairly well, since the butene to methylcyclopropane ratio for two different sized samples from the same

Reproduced with permission of the copyright owner. Further reproduction prohibited without permission.

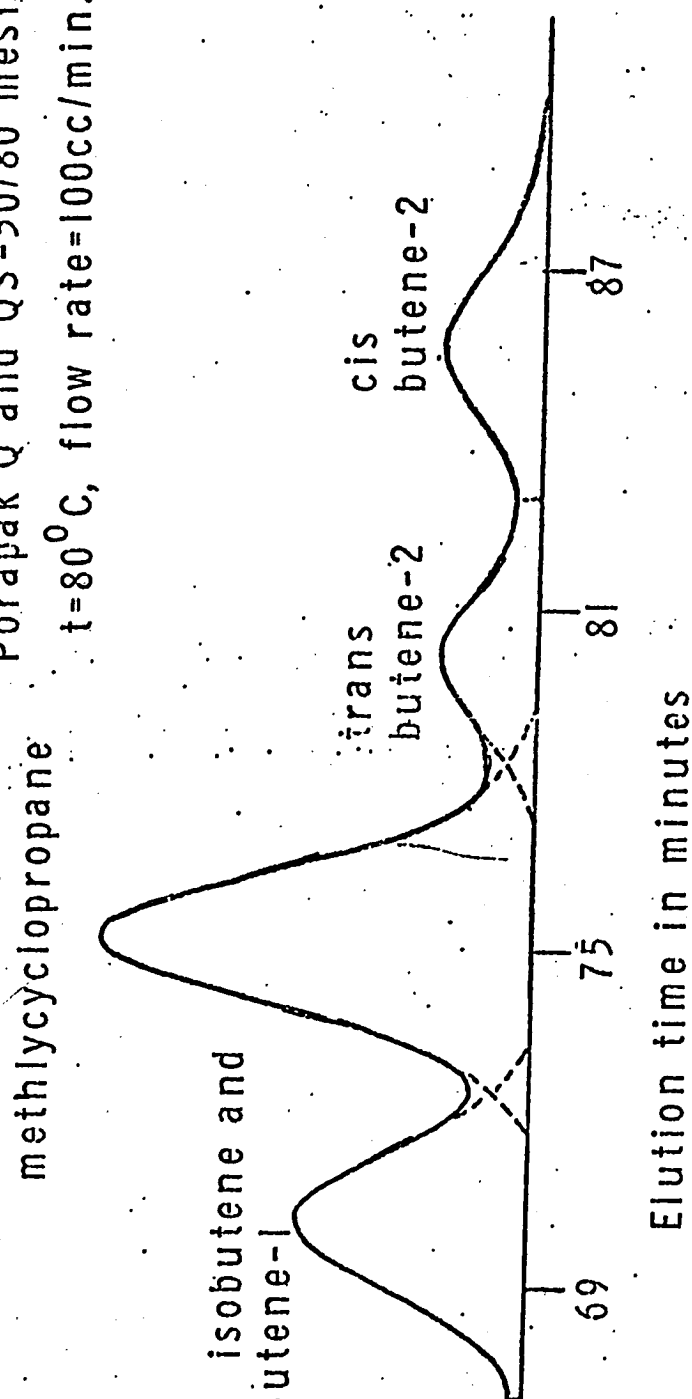

Figure 2-11

Reproduced with permission of the copyright owner. Further reproduction prohibited without permission.

photolyzed mixture generally agreed to within 6%.

The molar responses of all the C_4H_8 isomers was assumed to be the same. Cis- and trans- butene-2 are known to have the same molar response.[11] According to Ettre,[9] both n-butane and isobutane have the same molar response and the response for the two different pentanes differs by less than 1%. In light of these facts, the assumption of equal molar responses for all C_4H_8 isomers is reasonable.

The Procedure for a Typical Experiment

A standard vacuum line with teflon stopcocks or stainless steel valves where the the stopcocks might come in contact with the photolyzed gases was used for handling and measuring the gases. Before each photolysis and before making up any gas mixture, the system was pumped down to 10^{-5} Torr with a mercury diffusion pump, liquid nitrogen trap, and mechanical pump. Each of the stored gases, ketene, isobutane, propane, and cyclopropane, was throughly out-gassed by pumping on the frozen sample during two freeze-thaw cycles before it was used.

The gases were measured with the Wallace-Tiernan gauge and

---

11. Anderson, E. M.,Ph. D. Thesis (Harvard University, 1968).

Reproduced with permission of the copyright owner. Further reproduction prohibited without permission.

mercury manometer and were stored and mixed in a bulb which was taped and painted black in order to prevent any reaction caused by the room lights. The ketene mixture was never used after more than five days of storage because too much of the ketene would have been polymerized and the concentration of ketene in the mixture would have been in error. Periodically, a brown polymer coating on the teflon stirrer and the sides of the flask was removed with acetone. The extent of mixing was checked by light absorption measurements which showed that three hours of mixing was sufficient to completely mix the gases.

If oxygen was to be added to the ketene-isobutane mixture, the oxygen was slowly introduced into the cell and then the mixture was added slowly with the circulating pump on to stir the gases. The entire mixture was mixed in the cell for 1.5 hours before photolysis. In the earlier experiments with oxygen, the ketene-isobutane mixture was added first and then frozen out with liquid nitrogen. The oxygen was added and measured while the mixture was frozen. After the oxygen was added, hot water was used to quickly vaporize and mix the ketene and isobutane with the oxygen. The circulating pump then mixed all of the gases for 1.5 hours before photolysis. This procedure gave spurious results for the oxygen experiments; the yield of isopentane seemed to be larger than in those experiments which had no oxygen. The

Reproduced with permission of the copyright owner. Further reproduction prohibited without permission.

explanation is that the sudden increase in gas pressure forced the oxygen into the dead space connecting the Wallace-Tiernan gauge to the cell. There was no difference if the CO was added before or after the ketene-isobutane mixture (with or without freezing the ketene and hydrocarbons). In the cyclopropane experiments, the oxygen was added to the mixture as it was made up and stored in the flask. In most of the isobutane experiments, the stirring was continued during the photolysis.

The lamp to be used was allowed to warm up and stabilize for 30 to 60 minutes before photolysis. The Phillips zinc lamp neede 30 minutes for the light intensity at 214 nm to stabilize, although visually, 10-15 minutes were enough for the blue and red lights to be stabilized. The Osram mercury lamp needed 45-60 minutes to stabilize.

After photolysis, the product mixture was connected to a trap filled with glass beads and helices and immersed in nitrogen slush for 30 minutes. The nitrogen slush was made by pumping a vacuum on a dewar of liquid nitrogen for at least 30 minutes. Then the non-condensable contents of the cell were Toepler-pumped into a gas burette and storage bulb. If no gases had been added to the ketene-hydrocarbon mixture, the CO yield was measured in the gas burette. Typically this was about 1 μmole of gas. The yield of non-condensables was not measured when CO or O_2 was added.

Reproduced with permission of the copyright owner. Further reproduction prohibited without permission.

because it would have been impossible to see any change, even in the oxygen experiments.

The condensed fraction was transferred to a sampling bulb by heating the trap with hot water and freezing the gases in the sampling bulb. Each sampling bulb had a teflon stopcock and contained 4 glass beads for stirring. In order to ensure a complete transfer of gases, the transferring process was given 30 minutes. After the sample bulb was removed, it was dipped into hot water and stirred vigorously for 5 minutes. The sampling bulb was then attached to the inlet system for the gas chromatograph.

Differences Between the Light Intensity Measurements at 214 nm and the Longer Wavelengths.

The quantum yield for ketene decomposition at 214 nm has been estimated by Walter and Kistiakowsky.[5] They found the CO quantum yield over a pressure range of 2-50 Torr to be between 2.2 and 2.5. Because of the errors involved in making the comparison with the ammonia actinometer, this yield can be rounded off to 2. (A quantum yield of 2.0 means the quantum yield for the decomposition of ketene is 1.0.) The quantum yield of CO at wavelengths shorter than 290 nm has been measured by several

Reproduced with permission of the copyright owner. Further reproduction prohibited without permission.

workers[12] who all agree that it is 2.0±0.2.

Since the optical arrangements at 214 nm were so different from the arrangements at the other wavelengths, it was necessary to relate the light intensity measurements at 214 nm with those at the other wavelengths. At first, 5 Torr of ketene were photolyzed at 214 nm and at 277 nm and both the CO and C_2 hydrocarbon yields were measured. The quantum yield of the CO (or for ketene decomposition) at both wavelengths will be directly proportional to the light absorbed and to the photolysis time. A sample of the ketene used for each photolysis was analyzed on the gas chromatograph and any ethylene measured was subtracted from the product analysis of the photolyzed ketene. In order to be sure the geometry of the electrical field did not change, the flame of the analyzer in the chromatograph was not relit during these experiments. The peak areas per μmole of sample for ethylene, ethane, and acetylene were measured. The comparison between quantum yields of CO at both wavelengths was not very satisfactory because the CO yield was too small to be accurately measured in the gas burette. A conversion factor used to relate the light intensities at the two wavelengths was calculated using the CO yields and

---

12. DeGraff, B. A. and Kistiakowsky, G. B., J. Phys. Chem. 71, 1553, 3984 (1967); Strachan, A. N. and Noyes, W. A.,Jr., J. Am. Chem. Soc. 76, 3258 (1954); Cox, R. A. and Preston, K. F., Can. J. Chem. 47, 3345 (1969).

Reproduced with permission of the copyright owner. Further reproduction prohibited without permission.

also using the C_2 hydrocarbon yields. The conversion factor calculated from these two different product yields differed by more than 50%, and so a new method was tried.

When 50 Torr of isobutane and 5 Torr of ketene were photolyzed at both 313 nm and 277 nm, the quantum yields were equal. (See the chapter of isobutane results, chapter 3.) The measurements of the yields at 313 nm in our system were more accurate than at 277 nm, and so long as the quantum yields are the same at both wavelengths, photolyses at 313 nm are preferred for comparisons with other wavelengths. A comparison of the yields of the photolyses of 50 Torr of isobutane and 5 Torr of ketene at 313 nm and 214 nm gives a conversion factor which relates the two different light intensities and which is very close to the one calculated using the CO yields from the photolyses of ketene at 277 nm and 214 nm discussed above. It has been assumed, of course, that the quantum yields for ketene decomposition are the same at both wavelengths. The decomposition of ketene at 214 nm is pressure independent[5], so the addition of 50 Torr of isobutane should not change the quantum yield for the decomposition of ketene. A comparison of yields is only necessary for the isobutane experiments, and the fact that the quantum yield for ketene decomposition at 214 nm is not known with great certainty is not important as will be discussed in chapter 4.

Reproduced with permission of the copyright owner. Further reproduction prohibited without permission.

3

Results of the Photolysis of the Ketene-Isobutane System

General Trends

Neopentane and isopentane are the major products[1] of the photolysis of a mixture of isobutane, ketene, and propane (in a ratio of 100:10:1). The other significant products are isobutene and the two octanes, 2,2,3,3-tetramethylbutane (octane B) and 2,2,4-trimethylpentane (octane A). The yields of these products are compared for photolyses done at different wavelengths in Table 3-I. Figure 3-1b shows the increase in the ratio of neopentane to isopentane product yields as the photolyzing wavelength increases. In these tables and figures, unless otherwise specified, the yield of a product refers to its yield relative to propane and has been normalized to a standard time and number of photons absorbed.

The photolyzing wavelengths used were 214 nm, 277 nm, 313 nm and 330 nm. Some experiments were tried at 350 nm and 366 nm, but since here the extinction coefficient of ketene is small and the quantum yield decreases to very small values (e.g., 0.01 at 366 nm

---

1. "Products" refers to only the products condensable in liquid nitrogen unless stated otherwise. CO is, of course, a major product, too, but it is not condensable and was not always measured.

Reproduced with permission of the copyright owner. Further reproduction prohibited without permission.

and 50 Torr of ketene),[2,3,4,5] the product yields even after a twenty hour photolysis were too small to be measurable.

In some experiments, oxygen (5-10% of the total pressure) was added to the reaction mixture in order to eliminate the reactions of $^3CH_2$ with isobutane (or ketene). (See Chapter 1, Introduction.) As shown in Tables 3-I, 3-II and 3-III and in figures 3-3, 3-4 and 3-5, the neopentane and isopentane yields were all smaller in those experiments with oxygen than in those without oxygen. The addition of oxygen completely eliminated the isobutene and octanes which are expected when $^3CH_2$ reacts with isobutane. (See page 4 in Chapter 1.) The ratio of neopentane to isopentane in the oxygen experiments was less than in the experiments without oxygen and was between 0.14 and 0.15 regardless of the photolyzing wavelength (see Table 3-II). This agrees well with the results of several other workers.[6,7]

---

2. Taylor, G. H. and Porter, G. B., J. Chem. Phys. 36, 1353 (1962).

3. Connelly, B. T. and Porter, G. B., Can. J. Chem. 36, 1640 (1958).

4. Strachan, A. N. and Noyes, W. A., Jr., J. Am. Chem. Soc. 76, 3258 (1954).

5. Strachan, A. N. and Thornton, D. E., Can. J. Chem. 46, 2353 (1968).

6. Halberstadt, M. L. and McNesby, J. R., J. Am. Chem. Soc. 89, 3417 (1967).

7. Johnson, R. L., Hase, W. L., and Simons, J. W., J. Chem. Phys. 52, 3911 (1970).

Reproduced with permission of the copyright owner. Further reproduction prohibited without permission.

Neopentane and isopentane are products of the reactions of isobutane and both $^1CH_2$ and $^3CH_2$. The reaction of $^1CH_2$ with isobutane is a concerted reaction in which the $^1CH_2$ inserts almost statistically into the C-H bonds of isobutane. Thus, the ratio of neopentane to isopentane expected when only $^1CH_2$ reacts with isobutane is close to 1/9 or 0.11. The reaction of $^3CH_2$ with C-H bonds is a two step reaction. In the first step, $^3CH_2$ abstracts a H from a C-H bond thus forming an alkyl radical and a methyl radical. And in the second step, the alkyl and methyl radicals recombine. $^3CH_2$ abstracts a tertiary H in preference to a secondary H and a secondary H in preference to a primary H. This order of preference is predicted by the order of stability of the resulting alkyl radicals, i.e., the tertiary alkyl radical is the most stable. Thus, the reaction of $^3CH_2$ with isobutane favors the formation of neopentane rather than isopentane, and when $^3CH_2$ reacts with isobutane, the ratio of neopentane to isopentane is expected to be larger than when only $^1CH_2$ reacts with isobutane.[8,9] The addition of oxygen prevents the reaction of $^3CH_2$ with isobutane and the yields of both pentanes and the neopentane / isopentane ratio are expected to be smaller than when no oxygen has been added.

---

8. See the review articles: Frey, H. M., Prog. React. Kinet., 2, 131 (1964); Bell, J. A., Prog. Phys. Org. Chem. 2, 1 (1964); DeMore, W. B. and Benson, S. W., Adv. Photochem. 2, 219 (1964).

9. Dobson, R. C., Hayes, D. M., and Hoffmann, R., J. Am. Chem. Soc. 93, 6188 (1971).

Reproduced with permission of the copyright owner. Further reproduction prohibited without permission.

The ratio of neopentane to isopentane increases as the percentage of $^3CH_2$ increases . Thus, figure 3-1b shows, as expected from other work, that the percentage of $^3CH_2$ increases as the wavelength of the photolyzing light increases.[10,11,12,13]

CO was also added to the photolysis mixture in some experiments. As expected from previous work,[11,14] the addition of CO results in a decrease in the yields of the products from the reactions of both $^1CH_2$ and $^3CH_2$ with isobutane. (See Table 3-II and figures 3-3, 3-4 and 3-5.) When more than 60 Torr of CO has been added to the photolysis mixture, the ratio of neopentane to isopentane is the same as in the oxygen experiments (see Table 3-II) and no isobutene or octanes are present.

In two experiments at 277 nm and 313 nm, xenon was added to the photolysis mixture. In the presence of added "inert" gases.

---

10. See, for example, references 11, 12, 13 and 15.

11. DeGraff, B. A. and Kistiakowsky, G. B., J. Phys. Chem. 71, 1553, 3984 (1967).

12. Ho, S. Y. and Noyes, W. A., Jr., J. Am. Chem. Soc. 89, 5091 (1967).

13. Carr, R. W., Jr. and Kistiakowsky, G. B., J. Phys. Chem. 70, 118 (1966).

14. Cox, R. A. and Cventanovic, R. J., J. Phys. Chem. 72, 2236 (1968).

Reproduced with permission of the copyright owner. Further reproduction prohibited without permission.

the amount of $^3CH_2$ present is expected to increase.[15,16,17,18,19] As anticipated, the yields of the products of the $^3CH_2$ reaction with isobutane (i.e., the neopentane to isopentane ratio, neopentane, isobutene, and the octanes) increased in the xenon experiments as compared to the experiments in which no xenon was added. The yields are shown in Tables 3-I and 3-III.

The details of these experimental results are discussed in more detail in the rest of this chapter and in conjunction with the reactions listed in Table 3-IV which, on the basis of previous work,[12,20] are expected in the ketene-isobutane system.

---

15. Eder, T.W. and Carr, R. W., Jr., J. Chem. Phys. 53, 2258 (1970).

16. Bader, R. F. W. and Generosa, J. I., Can. J. Chem. 43, 1631 (1965); Voisey, M., Trans. Faraday Soc. 64, 3058.

17. Cox, R. A. and Preston, K. F., Can. J. Chem. 47, 3345 (1968).

18. Herzberg, G. and Shoosmith, J., Nature 183, 1801 (1959); Herzberg, G., Proc. Roy. Soc., A262, 291 (1961).

19. Braun, W., Bass, A. M., and Pilling, M., J. Chem. Phys. 52, 5131 (1970).

20. Bell, J. A., J. Phys. Chem. 75, 1537 (1971); Mitschele, C. J., Ph. D. Thesis (University of California, Riverside, 1968).

Reproduced with permission of the copyright owner. Further reproduction prohibited without permission.

FIGURE 3-1

a) The variation in the percent of $^3CH_2$ as measured by the oxygen method(see text) as a function of photolyzing wavelength.

b) The variation of the ratio of neopentane to isopentane yield as a function of the photolyzing wavelength.

c) The variation of the quantum yield of ethylene from ketene photolysis compared to the quantum yield of ethylene from ketene-O_2 photolysis as a function of wavelength. This figure was taken from DeGraff and Kistiakowsky(11) and is a measure of the amount of $^3CH_2$ present in the photolysis mixture. The data are from several workers (See DeGraff and Kistiakowsky).

Reproduced with permission of the copyright owner. Further reproduction prohibited without permission.

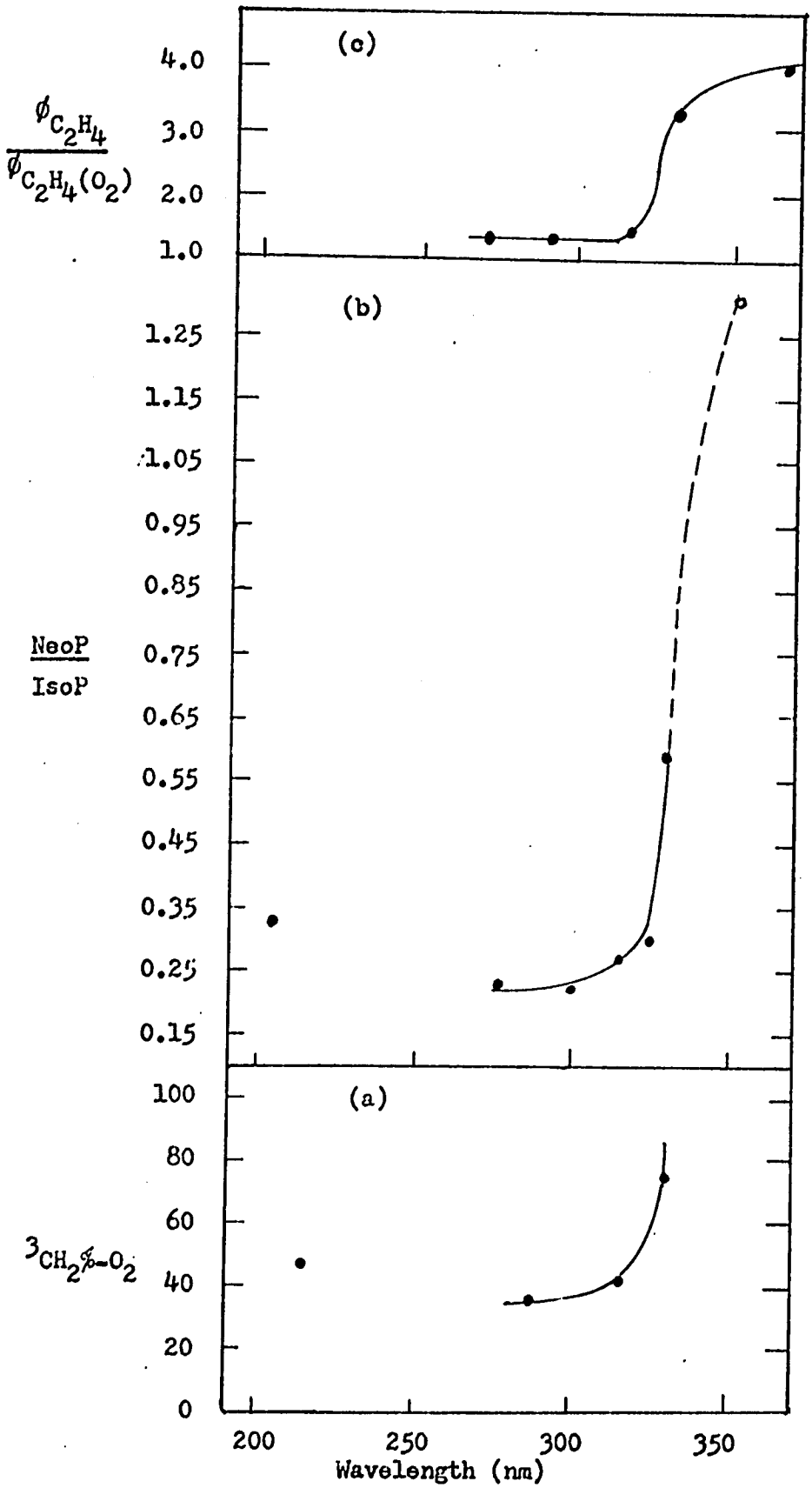

Reproduced with permission of the copyright owner. Further reproduction prohibited without permission.

FIGURE 3-2

$\frac{\text{Neopentane}}{\text{Isopentane}}$ versus $^3CH_2\%\text{-}O_2$ (The percent of methylene present as $^3CH_2$ as determined from the oxygen experiments)

Reproduced with permission of the copyright owner. Further reproduction prohibited without permission.

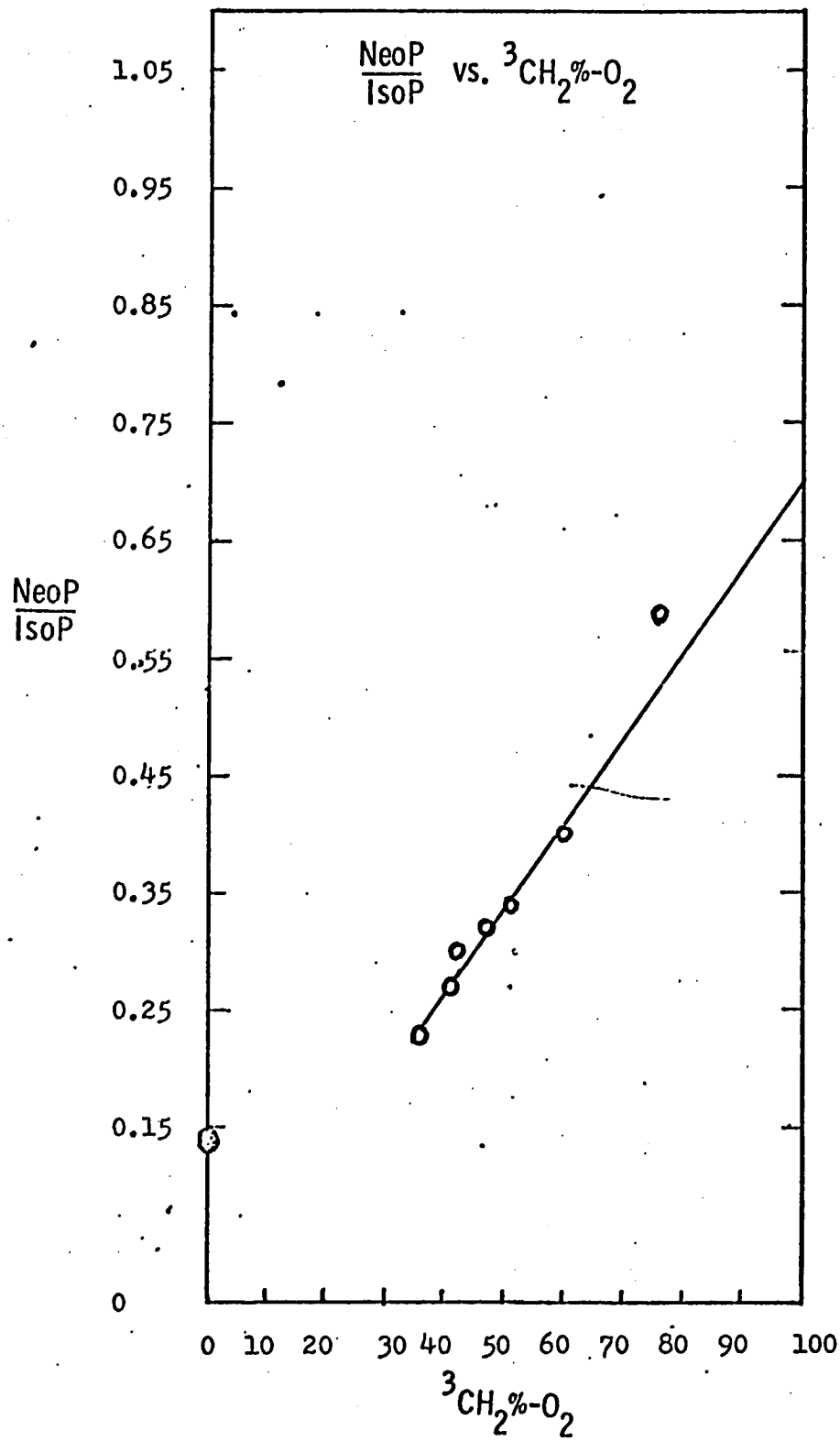

Figure 3-2

Reproduced with permission of the copyright owner. Further reproduction prohibited without permission.

NOTE: In Table 3-I : $R_{Total} = R_{1_{CH_2}} + R_{3_{CH_2}}$ as defined by Eq. 1.

$3^o/1^o$ is the ratio of products of tertiary H abstraction comparded to primary H abstraction from isobutane by $^3CH_2$.

R_{NeoPo_2}/R_{NeoP} and R_{IsoPo_2}/R_{IsoP} are the ratios of product yields in oxygen experiments compared to yields in the absence of oxygen (or other scavenger).

%radical C_5 is the percentage of radicals recombining to form neopentane and isopentane.

Reproduced with permission of the copyright owner. Further reproduction prohibited without permission.

TABLE 3-I

Comparisons of Product Yields and Total Quantum Yields at Different Wavelengths

	313 nm	330 nm	277 nm	277 nm + Xe	214 nm
R_{IsoP}	7.0_7	2.3_2	7.9_8	5.4_6	5.9_5
R_{NeoP}	1.9_1	1.4_2	1.9_6	2.1_8	1.8_4
R_{OctB}	0.3_2	0.3_6	0.2_4	0.4_8	0.3_5
R_{OctA}	0.0_8	0.0_9	0.0_6	0.1_2	0.0_9
$R_{isobutene}$	1.4_1	1.6_5	1.1_1	2.2_1	1.5_9
R_{Total}	12.5_8	7.8_6	12.8_1	13.2_0	12.2_0
$R_{IsoP_{O_2}}/R_{IsoP}$	0.9_2	0.7_4	0.9_3	0.8_5	0.9_0
$R_{NeoP_{O_2}}/R_{NeoP}$	0.5_0	0.1_9	0.5_4	0.3_1	0.4_8
$3°/1°$	61	85	56	69	67
$^3CH_2-O_2$	41%	74%	36%	60%	67%
% radical C_5	30%	28%	30%	30%	27%
$NeoP_3/IsoP_3$	1.6_2	2.4_0	1.6_2	1.6_5	1.6_2

Reproduced with permission of the copyright owner. Further reproduction prohibited without permission.

TABLE 3-II

The Variation in Pentane Yields* in the CO Experiments

CO(Torr)	IsoP	NeoP	TotalP	NeoP/IsoP
	10^{-3}	10^{-3}	10^{-3}	
		214 nm		
0	22.0	7.21	30.8	0.306
82	17.2	3.33	20.5	0.194
98	16.2	2.70	18.9	0.167
187	12.0	2.03	14.0	0.169
O_2	21.4	3.46	24.9	0.162
		277 nm		
0	28.7	6.56	35.3	0.229
80	19.6	2.80	22.4	0.143
157	14.2	2.05	30.2	0.143
O_2	26.7	3.48	30.2	0.143
		313 nm		
0	25.8	6.99	32.8	0.271
13	23.6	5.15	28.2	0.218
14	24.2	5.61	29.8	0.232
30	19.1	3.78	22.9	0.198
35	21.0	3.48	24.5	0.166
65	16.6	2.44	18.4	0.147
75	14.5	2.04	16.5	0.141
80	13.3	1.98	15.3	0.149
93	14.8	2.13	16.9	0.144
115	11.4	1.64	13.0	0.144
150	10.4	1.49	11.9	0.143
200	8.5	1.22	9.7	0.143
264	9.7	1.39	11.1	0.143
275	7.5	1.04	8.5	0.139
305	6.3	0.83	7.1	0.132
O_2	23.8	3.49	27.3	0.146

*These yields are not quantum yields, but are directly proportional to them.

Reproduced with permission of the copyright owner. Further reproduction prohibited without permission.

CO(Torr)	IsoP 10^{-3}	NeoP 10^{-3}	TotalP 10^{-3}	NeoP/IsoP
		322 nm		
0	23.8	7.2	31.0	0.300
14	21.4	4.21	25.6	0.197
66	13.7	2.33	16.0	0.170
154	9.9	1.42	11.3	0.144
244	7.1	0.98	8.1	0.138
O_2	21.4	3.22	24.6	0.150
		330 nm		
0	7.6	4.47	12.1	0.589
5	7.0	2.88	9.9	0.411
14	6.5	2.17	8.7	0.334
20*	6.5	2.35	8.4	0.362
48	4.9	0.83	5.7	0.169
55	4.1	0.93	5.0	0.226
60	4.1	0.58	4.7	0.142
120	2.5	0.34	2.8	0.148
160	1.7	0.24	1.9	0.143
278	2.2	0.31	2.3	0.143
O_2	5.4	0.81	6.2	0.143
350 nm				1.3**
300 nm				0.225

* Average of three experiments

**Isopentane was very small. Both pentane peaks were small and hard to measure, so that this number is very approximate.

Reproduced with permission of the copyright owner. Further reproduction prohibited without permission.

TABLE 3-III

The Effect of Varying the Composition of the Reaction Mixture at 313 nm

	Pressures, Torr						
Isobutane	50	50	50	100	100	100	100
Ketene	5	5	5	10	10	5	5
Xenon	115	-	-	-	-	-	-
Oxygen	-	-	2.5	-	5	-	2.4
	Products ($\times 10^{10}$)						
R_{IsoP}	6.10	6.95	6.34	7.02	6.28	6.86	6.32
R_{NeoP}	2.09	1.89	0.96	1.90	1.00	1.79	0.90
$R_{isobutene}$	1.78	1.40	--	1.16	--	1.49	--
R_{OctB}	0.41	0.32	--	0.28	--	0.33	--
R_{Total}	12.7	12.6	7.34	12.0	7.34	12.4	7.20
R_{CO}	12.6	12.9	--	n.m.	--	12.9	--
NeoP/IsoP	0.33_8	0.27_2	0.15_1	0.27_0	0.15_9	0.26_0	0.14_2

R_{IsoP}, R_{NeoP}, $R_{isobutene}$, R_{OctB}, and R_{CO} are the quantum yields of isopentane, neopentane, isobutene, octane B (2,2,3,3-tetramethylbutane) and carbon monoxide. R_{Total} is the total quantum yield as defined in the text.

Reproduced with permission of the copyright owner. Further reproduction prohibited without permission.

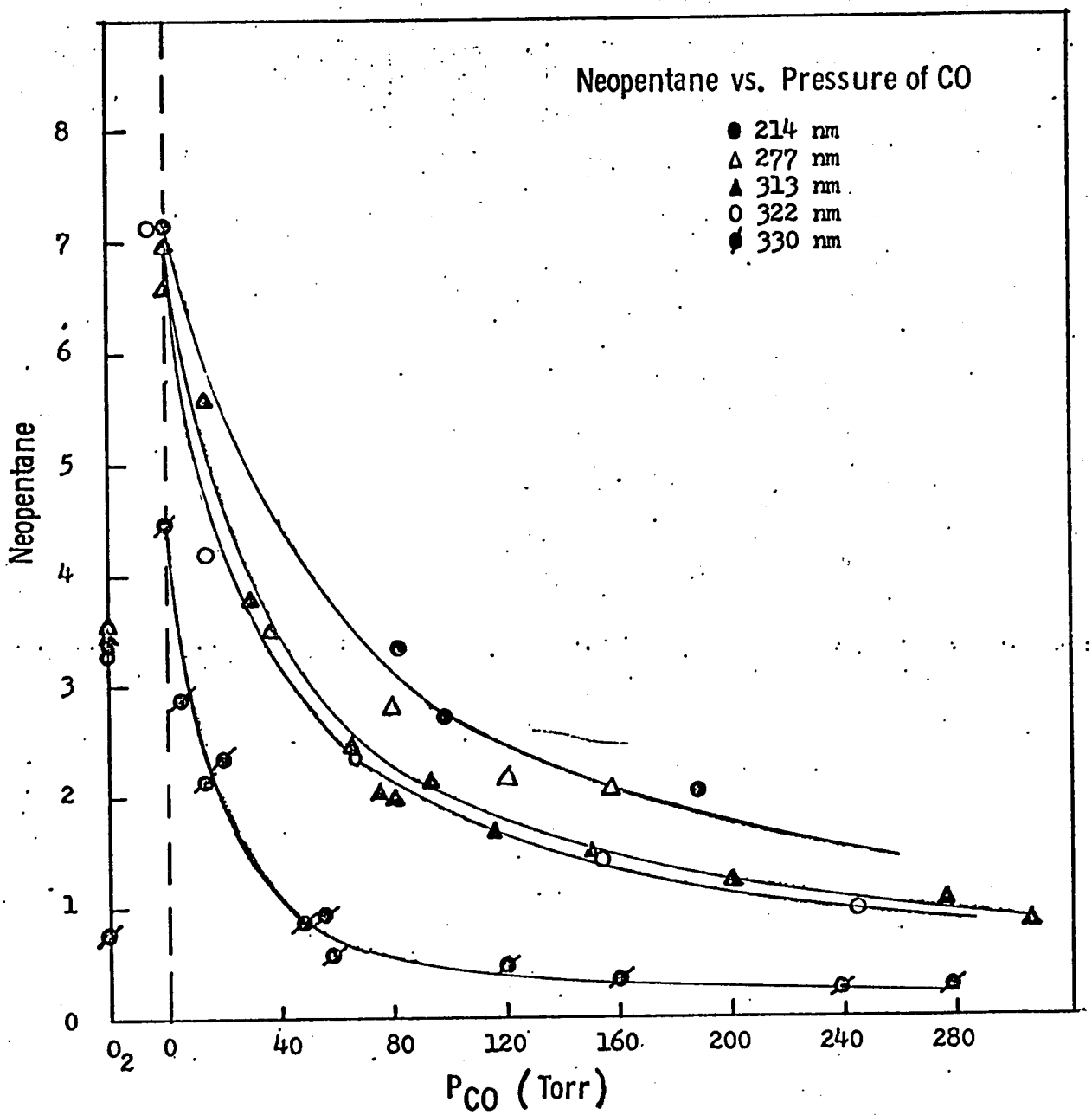

Figure 3-3

Reproduced with permission of the copyright owner. Further reproduction prohibited without permission.

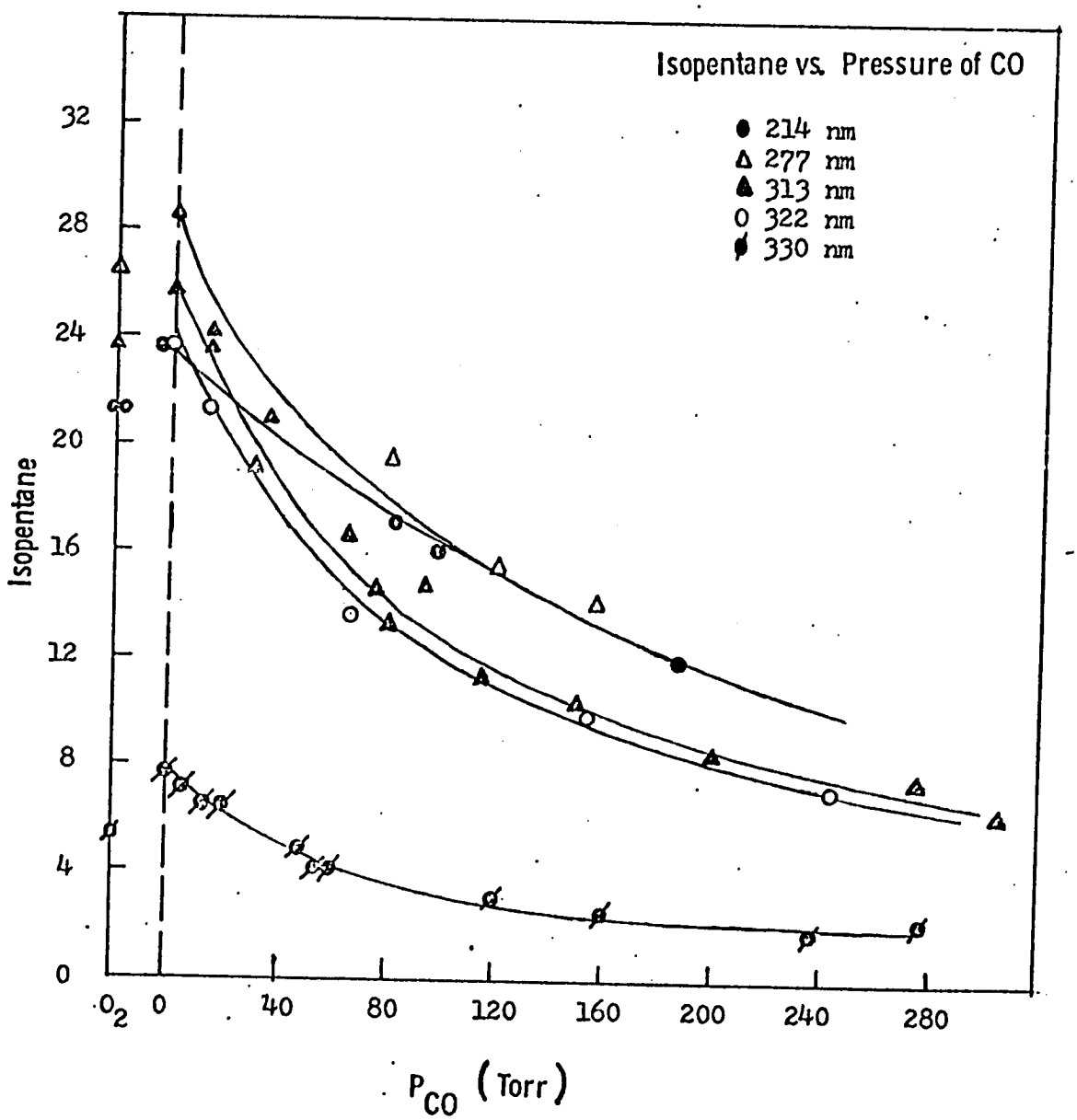

Figure 3-4

Reproduced with permission of the copyright owner. Further reproduction prohibited without permission.

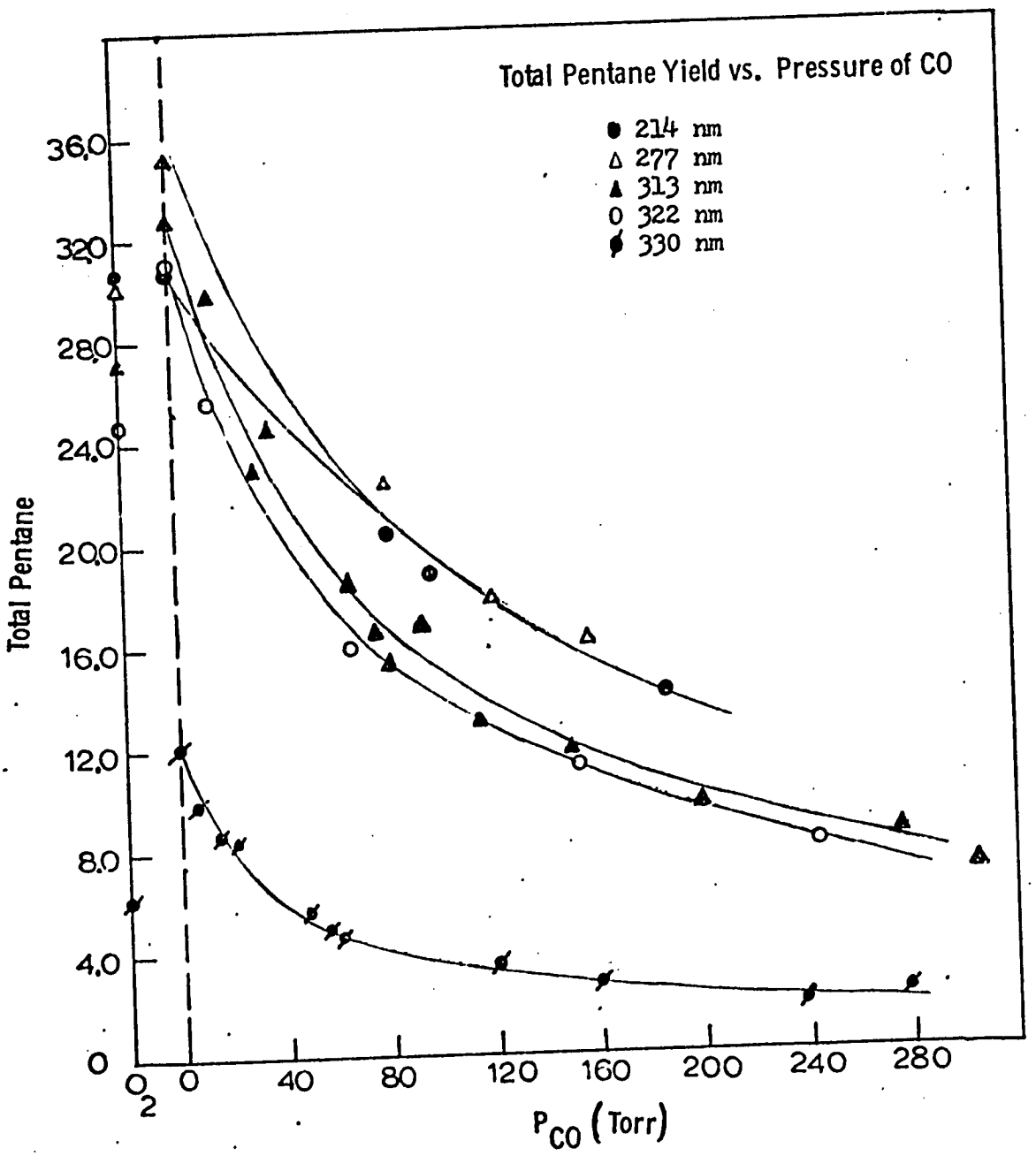

Figure 3-5

Reproduced with permission of the copyright owner. Further reproduction prohibited without permission.

TABLE 3-IV

Some of the Major Reactions in the Ketene-Isobutane Photolysis System

$CH_2CO + h\nu \longrightarrow$	$^1CH_2 + CO$	$\phi_s I_a$	
$CH_2CO + h\nu \longrightarrow$	$^3CH_2 + CO$	$\phi_t I_a$	
$^1CH_2 + IsoB \longrightarrow$	IsoP	k_1	
$^1CH_2 + IsoB \longrightarrow$	NeoP	k_2	
$^1CH_2 + IsoB \longrightarrow$	$^3CH_2 + IsoB$	k_3	
$^3CH_2 + IsoB \longrightarrow$	$t\text{-}C_4H_9\cdot + CH_3\cdot$	k_4	
$^3CH_2 + IsoB \longrightarrow$	$iso\text{-}C_4H_9\cdot + CH_3\cdot$	k_5	
$2t\text{-}C_4H_9\cdot \longrightarrow$	oct-B	k_6	Radical Recombination
$t\text{-}C_4H_9\cdot + iso\text{-}C_4H_9\cdot \longrightarrow$	oct-A	k_7	
$2iso\text{-}C_4H_9\cdot \longrightarrow$	oct-C	k_8	
$2t\text{-}C_4H_9\cdot \longrightarrow$	isobutene + IsoB	k_9	
$t\text{-}C_4H_9\cdot + CH_3 \longrightarrow$	NeoP	k_{10}	
$iso\text{-}C_4H_9\cdot + CH_3 \longrightarrow$	IsoP	k_{11}	
$2CH_3\cdot \longrightarrow$	C_2H_6	k_{12}	
$^1CH_2 + CH_2CO \longrightarrow$	$C_2H_4 + CO$	k_{16}	
$^3CH_2 + CH_2CO \longrightarrow$	$C_2H_4 + CO$	k_{17}	

Notes: Oct-C (2,5 dimethylhexane) was not observed and so reaction k_8 is negligible.
IsoB, IsoP and NeoP refer to isobutane, isopentane and neopentane, respectively.

Reproduced with permission of the copyright owner. Further reproduction prohibited without permission.

The Ketene-Isobutane Photolysis System

In addition to neopentane, isopentane, isobutene and the two octanes, 2,2,3,3-tetramethylbutane and 2,2,4-trimethylpentane, the photolysis of a mixture of ketene and isobutane also results in the formation of methane, ethane, ethylene, a small amount of hexanes, and carbon monoxide. The hexanes, secondary reaction products, are expected from the reactions of methylene with the pentanes. Since only a few percent of the ketene were decomposed during each photolysis, the amount of hexanes formed was too small to be measured. The methane was not monitored closely because it has a measurable vapor pressure, 0.3 Torr at -210°C, the nitrogen slush temperature, and some of it was always pumped by the Toepler pump into the non-condensable fraction along with CO. In all cases, the amount of methane remaining in the condensable fraction was smaller than the ethane yield. Ethylene was eluted from both the Porasil C column and the Perkin-Elmer Column E too close to the propane, which was at least 100 times larger than the ethylene, to be measurable. By comparisons with earlier qualitative experiments performed by Dr. Benjamin DeGraff, the amount of ethylene was estimated to be on the order of 5-8% of the total yield.

Ethane, a $^3CH_2$ product, was measured when neither CO nor O_2 were added. At most wavelengths, ethane was only 5-9% of the

Reproduced with permission of the copyright owner. Further reproduction prohibited without permission.

of the total condensable products. The "total quantum yield", defined on p.76 , is the yield of products from the reactions of both methylenes with isobutane and was used as an estimate of the total amount of CH_2 produced during the photolysis of ketene. Ethane results from the reaction of $^3CH_2$ with both ketene and isobutane[21]. Although the extent of the reaction of $^3CH_2$ with ketene was small (see Chapter 4), the yields of the isobutene and the two octanes were more easily measured, were free from the contribution of the ketene reaction, and were used in preference to the ethane yields. (See, also, Appendix I which estimates some of the steady-state concentrations of the radicals in the ketene-isobutane system).

The neopentane to isopentane ratio increases as the wavelength of the photolyzing light increases which, as mentioned above, indicates that the percent of $^3CH_2$ in the methylene is increasing. There is a sharp rise in the neopentane to isopentane ratio at wavelengths longer than about 320 nm. This sharp increase occurs at the same wavelength that the ratio of the yields of ethylene in a pure ketene system to the ethylene in a ketene-oxygen system sharply increases.[11] Both indicate that at wavelengths longer than 320 nm, the ratio of products from $^3CH_2$ reactions to those from $^1CH_2$ reactions suddenly increases. This correlation is shown in

---

21. See, for example, Frey, H.M. and Walsh, R., J. Chem. Soc. A 1970, 2115 for a discussion of the reactions of $^3CH_2$ with ketene.

Reproduced with permission of the copyright owner. Further reproduction prohibited without permission.

figure 3-1. The reasons for this increase are discussed in Chapter 4.

The ratio of isobutene to octane B is 4.5 for all wavelengths (see Table 3-III). By reactions (6) and (9)

$$\frac{d[OctB]}{dt} = k_6[t\text{-}C_4H_9\cdot]^2 = R_{OctB}$$

and

$$\frac{d[isobutene]}{dt} = k_9[t\text{-}C_4H_9\cdot]^2 = R_{isobutene}$$

so that

$$\frac{[isobutene]}{[OctB]} = \frac{k_9}{k_6} = 4.5.$$ This agrees excellently with the value of 4.59 found by Kraus and Calvert[22] in their work with di-t-butylacetone. Ring and Rabinovitch[23] used a value of 2.20 for the ratio of k_9/k_6. Calculations described in Appendix I confirmed that the reaction

$$t\text{-}C_4H_9\cdot + CH_3\cdot \longrightarrow CH_4 + \text{isobutene} \qquad (k_{18})$$

was a negligible source of isobutene. This was to be expected since CH_4 was such a small part of the products.

In order to compare the yields at various wavelengths, the

---

22. Kraus, J. W. and Calvert, J. G., J. Am. Chem. Soc. 79, 5921 (1957).

23. Ring, D. F. and Rabinovitch, B. S., Can. J. Chem. 46, 2435 (1968).

Reproduced with permission of the copyright owner. Further reproduction prohibited without permission.

rate of formation of the products was needed for each wavelength. The rate of formation of CO was measured at several wavelengths and was normalized to a standard amount of absorbed light. This is referred to in the following pages as the yield of CO. According to the list of reactions given in Table 3-IV, if the reactions of both methylenes with ketene are minor compared to their reactions with isobutane, there is one molecule of CO formed for every CH_2 formed.

Unfortunately, because of the low percentage conversion of ketene, the CO yield was too small to measure accurately in those experiments where the extinction coefficient of ketene was very small. An alternative method for calculating the yields is to equate the yield of the products of the butyl radical reaction and the pentanes with the number of CH_2 radicals formed. Thus,

$$R_{Total} = R_{C_5H_{12}} + 2\,R_{isobutene} + 2\,R_{OctA} + 2\,R_{OctB}$$

$$= R(^1CH_2) + R(^3CH_2). \qquad \text{(Eq. 1)}$$

By reaction (9), one molecule each of isobutene and isobutane is formed from two butyl radicals, but since the amount of isobutane formed cannot be measured, twice the amount of isobutene is used in Eq.1. For those wavelengths where a good measurement of CO was obtained, the yield of CO was, as expected, equal to the total yield (normalized to a standard amount of absorbed light) of C_4, C_5 and C_8 products. (See Table 3-III, where both the CO yield and the total yields are listed for a series of 313 nm

Reproduced with permission of the copyright owner. Further reproduction prohibited without permission.

photolyses.) The total yield of C_4, C_5 and C_8 products will be referred to as the total quantum yield, R_{Total}.

The total quantum yield at 313 nm was found to be equal to that at 277 nm. The total quantum yield at 330 nm is 0.58 of that at 277 nm and 313 nm. Since the quantum yield of CO from the photolysis of ketene at 214 nm was reported as approximately 2.2[24] and the quantum yield of CO at 313 nm and 277 nm is 2.0,[2-5] the total quantum yield at 214 nm was set equal to the yield at 277 nm and 313 nm. This point will be explored in more detail in Chapter 4.

Table 3-III presents the results of a series of experiments, at 313 nm, in which the yields obtained with the standard mixture (50 Torr of isobutane, 5 Torr of ketene, and 0.5 Torr of propane) are compared to the yields resulting from variations in the mixture. The most important observation is that the total quantum yield, R_{Total}, did not change when the isobutane pressure was doubled, when the total pressure of the mixture was doubled, or when xenon was added to the mixture. A second important observation is that the ratio of the neopentane to isopentane yields does not change. when the pressure of isobutane is doubled or when the total pressure of the mixture is doubled. In Chapter 4 we will discuss why these

---

24. Kistiakowsky, G. B. and Walter, T. A., J. Phys. Chem. 72, 3952 (1968).

Reproduced with permission of the copyright owner. Further reproduction prohibited without permission.

two observations justify the assumption that, for these ratios of ketene and isobutane, the reaction of $^3CH_2$ with ketene is minor compared to the reaction with isobutane. The observation that the ratio of neopentane to isopentane does not change when the total pressure is doubled indicates that the intersystem crossing which is responsible for part of the formation of $^3CH_2$ occurs from $^1CH_2$ rather than in ketene. This, too, will be explained in the next chapter.

The Ketene-Isobutane-O_2 Photolysis System

The addition of 2-5 Torr of O_2 to the standard reaction mixture eliminated the products which are usually attributed to radical recombinations, i.e., methane, ethane, isobutene, and the octanes. The remaining products are neopentane and isopentane (and some ehtylene). The yields of both neopentane and isopentane were smaller than in the systems without oxygen.

The ratio of neopentane to isopentane in the presence of O_2 was 0.14-0.15 for all wavelengths and did not vary with the amount of isobutane or with the total pressure. This is in excellent agreement with the values found by other workers using several different sources of methylene,[6,7] but is in striking disagreement with Ring and Rabinovitch.[23] (They found a value of 0.5 in their diazomethane-oxygen system.)

Reproduced with permission of the copyright owner. Further reproduction prohibited without permission.

The Reaction of Oxygen with $^1CH_2$

Since O_2 is known to react very quickly with $^3CH_2$[25] and radicals[26] but not with $^1CH_2$, the addition of O_2 should eliminate the products of the reaction of $^3CH_2$ with isobutane. While Carr[15] finds that $^1CH_2$ does react with O_2 and that this rate constant depends on the photolyzing wavelength of the ketene, the possibilty of the reaction of an excited ketene molecule with oxygen is not excluded in Carr's experiments. Bell also measured the reaction of $^1CH_2$ with O_2,[20] and using his values for the rate, the reaction is slow enough to be negligible when oxygen is only a few percent of the total reactants. Dhingra and Koob also assume the reaction of O_2 with $^1CH_2$ is negligible when oxygen is not present in large amounts.[27] If the ratio of the rate constants for the $^1CH_2$ reaction with O_2 compared to the $^1CH_2$ insertion into isobutane is 0.5, the largest of Carr's ratios, the $^1CH_2$ reaction with O_2 would be 2% of the reaction with isobutane since the ratio of isobutane to oxygen in our experiments was 50 to 2. This point will be more thoroughly explored in Chapter 4.

Two photolyses were done at 313 nm, one with 0.6 Torr of O_2

25. Russell, R. L. and Rowland, F. W., J. Am. Chem. Soc. 90, 1671 (1968).

26. van der Bergh, H. E. and Callear, A. B., Trans. Faraday Soc. 67, 2017 (1971).

27. Dhingra, A. K. and Koob, R. D., J. Phys. Chem. 74, 4490 (1970).

Reproduced with permission of the copyright owner. Further reproduction prohibited without permission.

and one with 4.8 Torr of O_2 added to the standard mixture. There was no difference either in the neopentane to isopentane ratio or in the pentane yields between the two photolyses. Most of the other wavelengths were studied with both 2 Torr and 5 Torr of O_2 added and within experimental error, no difference was observed in the pentane yields. This again demonstrates the unimportance of the reaction of $^1CH_2$ with oxygen in these experiments and only the average values obtained in the O_2 experiments are reported in the final results.

The Determination of the Percent of $^3CH_2$ Present in the Ketene-Isobutane System

The ratio of the total quantum yield of a mixture photolyzed with O_2 to the total quantum yield in the absence of O_2 is a measure of the fraction of methylene present as $^1CH_2$ in the system. Since the total quantum yield is due only to methylene, and on assuming that there are only two forms of methylene, $^1CH_2$ and $^3CH_2$, the percentage of $^3CH_2$ becomes equal to (100- the percentage of $^1CH_2$ as just defined). The percentage of $^3CH_2$ measured by this method is referred to as $^3CH_2\%\text{-}O_2$ to distinguish it from the percentage of $^3CH_2$ measured by other methods. The reaction of $^1CH_2$ with O_2 has thus been ignored. Inclusion of this reaction would only slightly enhance the percentage of $^3CH_2$ measured in the oxygen experiments. The change in $^3CH_2\%\text{-}O_2$ with wavelength

Reproduced with permission of the copyright owner. Further reproduction prohibited without permission.

is shown in figure 3-1a. The variation in $^3CH_2\%-O_2$ parallels the variation in the neopentane to isopentane ratio.

The neopentane to isopentane ratio increases as the percentage of $^3CH_2$ present increases. The relationship between the neopentane to isopentane ratio and the $^3CH_2\%-O_2$ is shown in figure 3-2. A point was added to show the value of the ratio expected when only $^1CH_2$ reacts with isobutane to form the pentanes i.e., when O_2 has been added. The neopentane to isopentane ratio can be expressed as a function of the percent of $^3CH_2$ and of $^1CH_2$,

$$\frac{NeoP}{IsoP} = {}^1CH_2\% \left[\frac{NeoP}{IsoP}\right]_S + {}^3CH_2\% \left[\frac{NeoP}{IsoP}\right]_T \quad . \qquad (Eq.\ 2)$$

$\left[\frac{NeoP}{IsoP}\right]_S$ is the ratio expected when only $^1CH_2$ is present, i.e., the ratio in the presence of oxygen, 0.14-0.15, and $\left[\frac{NeoP}{IsoP}\right]_T$ is the ratio expected when only $^3CH_2$ is present. In Eq. 2, it is assumed that all of the methylene reacts with isobutane to form pentane products, or , in other words, that $^1CH_2\% + {}^3CH_2\% = 100$. As can be seen from Table 3-I, only 30% of the products of the $^3CH_2$ reactions with isobutane are the pentanes. The rest of the products of these reactions are the other radical recombination products, namely isobutene (and isobutane) and octanes. All of the $^1CH_2$ reacts with isobutane to form pentanes. If the neopentane to isopentane ratio is expressed as a function of $^3CH_2$, Eq. 2 becomes

$$\frac{NeoP}{IsoP} = \left[\frac{NeoP}{IsoP}\right]_S + {}^3CH_2\% \left\{0.30 \left[\frac{NeoP}{IsoP}\right]_T - \left[\frac{NeoP}{IsoP}\right]_S\right\} \quad . \qquad (Eq.\ 2a)$$

Reproduced with permission of the copyright owner. Further reproduction prohibited without permission.

Since the intercept of the line in figure 3-2 is not 0.14-0.15, the knowledge of the ratio of neopentane to isopentane when less than 36% of the methylene present is $^3CH_2$ would have been useful. However, when the reaction with isobutane is the main reaction in a methylene system, and no $^3CH_2$ scavengers are present, there will never be less than approximately 36% $^3CH_2$. This last point will be explained in Chapter 4.

Doubling the total pressure of the standard reaction mixture which also contains 4% oxygen does not change either the neopentane to isopentane ratio, the total quantum yield, or the $^3CH_2$%-O_2 at 313 nm (see Table 3-III). Also, doubling the amount of isobutane in the oxygen experiments does not change either the ratio of yields of neopentane to isopentane, or the total quantum yield, or the $^3CH_2$%-O_2 at 313 nm. As will be explained in more detail later, this justifies the assumption that the reaction of $^1CH_2$ with ketene is negligible compared to its reaction with isobutane.

The Ketene-Isobutane-CO Photolysis System

The products attributed to the reactions of $^3CH_2$ are suppressed when CO is added to the standard photolysis mixture. At all wavelengths, the presence of 60 Torr of CO is sufficient to reduce the ratio of neopentane to isopentane to 0.14-0.15, the value observed in the presence of oxygen, and to completely

Reproduced with permission of the copyright owner. Further reproduction prohibited without permission.

suppress the ethane, isobutene, and octanes yields. This is shown in Table 3-II. The decrease in pentane yields at the different wavelengths as the pressure of CO is increased is also shown in this table and in figures 3-3, 3-4 and 3-5.

In some early experiments done at 313 nm, 0.5 Torr of O_2 and 25 to 150 Torr of N_2 were added to the standard ketene-isobutane-propane mixture. Only the pentane products were monitored, and the quantum yields of the pentanes were not determined very accurately, but they were definitely smaller in the presence of O_2 and N_2 than in the presence of only N_2 or in the absence of both N_2 and O_2. Unfortunately, the data are not good enough to determine the extent of the reaction of $^1CH_2$ with N_2. In the presence of N_2 and O_2, the neopentane to isopentane ratio was 0.14-0.15 independent of the pressure of the N_2. These experiments were done to be sure that the ratio of neopentane to isopentane due to only $^1CH_2$ did not change with the addition of large amounts of less reactive, diluent gases, e.g., CO.

In the presence of more than 60 Torr of CO, all of the $^3CH_2$ reacts with CO as judged from the composition of the products. When the ratio of CO to isobutane is larger than 1.2, the reaction of $^3CH_2$ with isobutane is not fast enough to compete with the reaction of $^3CH_2$ with CO. Both $^1CH_2$ and $^3CH_2$ react with CO to form ketene (reactions 13 and 14 below). However, in the concentrations

Reproduced with permission of the copyright owner. Further reproduction prohibited without permission.

of CO used in this study, most of the $^1CH_2$ reacts with isobutane and not with CO. (Thus, for $^1CH_2$, $(k_1 + k_2)$ [IsoB] > k_{13}[CO], but for $^3CH_2$, $(k_4 + k_5)$ [IsoB] < k_{14} [CO].)

$$^1CH_2 + CO \longrightarrow CH_2CO \qquad k_{13}$$

$$^3CH_3 + CO \longrightarrow CH_2CO \qquad k_{14}$$

When the CO concentration is large enough to suppress the reaction of $^3CH_2$ with isobutane, the pentanes are the only products observed (aside from a trace of C_2H_4), and assuming steady state conditions for the radicals, the rate of formation of isopentane is given by

$$\frac{d}{dt}\,IsoP = \frac{k_1[IsoB]\phi_s I_a}{(k_1 + k_2)[IsoB] + k_{13}[CO]} = R_{IsoP} \quad \text{(Eq. 3)}$$

and the rate of formation of neopentane is given by

$$\frac{d}{dt}\,NeoP = \frac{k_2[IsoB]\phi_s I_a}{(k_1 + k_2)[IsoB] + k_{13}[CO]} = R_{NeoP} \quad \text{(Eq. 4)}$$

As mentioned above, the reaction of $^1CH_2$ with ketene is negligible at the ratio of isobutane to ketene used and is omitted.

If we assume that the rate of reaction of $^1CH_2$ with either isobutane or CO does not change very much with a change in wavelength, then the yield of both neopentane and isopentane will be proportional to the quantum yield of $^1CH_2$ produced by photolysis

Reproduced with permission of the copyright owner. Further reproduction prohibited without permission.

at each wavelength. The variations of pentane yields with the pressure of CO are shown in figures 3-3, 3-4, and 3-5.

The Ketene-Isobutane-Xenon Photolysis System

Photolyses of 55.5 Torr of the standard photolysis mixture (100 isobutane: 10 ketene: 1 propane) to which more than 100 Torr of xenon had been added were done at 313 nm and 277 nm. The yields of the products and the exact conditions are summarized in Tables 3-I and 3-III. At each wavelength, the ratio of neopentane to isopentane with xenon present was larger than without xenon, but the total quantum yield was the same. In one extra experiment done at 277 nm, 2.3 Torr of oxygen was added to the xenon mixture, and the $^3CH_2$-O_2 measured for these conditions was 60%. The fraction of $^3CH_2$ present thus increases upon the addition of so-called inert gases as evidenced by the increase in both the neopentane to isopentane ratio and the $^3CH_2$-O_2. This is in agreement with the findings of other workers.[15-20]

A similar experiment with xenon and oxygen to compare the total quantum yield in the presence of O_2 with the total quantum yield in the absence of O_2 and so determine the percent of $^3CH_2$ was not made at 313 nm. Nevertheless, the percent of $^3CH_2$ formed in the presence of xenon at 313 nm can be estimated. As the data in Table 3-I indicate, 30% of the butyl radicals recombine to

Reproduced with permission of the copyright owner. Further reproduction prohibited without permission.

form the pentane products (reactions 10 and 11). The rest of the butyl radicals, 70%, disproportionate and recombine (reactions 6, 7 and 9) to form isobutane and isobutene and the two octanes. The isobutene and the octanes were measured in this xenon experiment at 313 nm and since their yields are 70% of the total yield of butyl radicals, the yield of butyl radicals can be calculated. Since only $^3CH_2$ forms the butyl radicals, the percentage of these divided by the total quantum yield is the percentage of methylene that is $^3CH_2$. This calculation is equivalent to the method used to determine the percent of $^3CH_2$ with the oxygen experiments, $^3CH_2\%\text{-}O_2$. When evaluated as just described, the percent of $^3CH_2$ present in the photolysis of the standard mixture and 115 Torr of Xe at 313 nm was found to be 51%. The observed ratio of neopentane to isopentane for this experiment and for the Xe experiment at 277 nm and of each $^3CH_2\%\text{-}O_2$ have been included in figure 3-2. These data fall right in line with those of experiments in which an "inert" gas was not added.

Reproduced with permission of the copyright owner. Further reproduction prohibited without permission.

4

Discussion of the Isobutane Results

General Introductory Summary

There have been several measurements of the fraction of $^3CH_2$ formed in ketene and diazomethane photolyses. The fractions measured do not always agree and depend on precursor, photolyzing wavelength, added gases, and the method used to determine the amount of $^3CH_2$ present. In this chapter we discuss the variations of the percent of $^3CH_2$ as a function of wavelength in terms of two mechanisms for the formation of $^3CH_2$. We believe that in order to explain the results presented in the previous chapter there must be two sources of $^3CH_2$, one being an intersystem crossing from the $^1CH_2$ to the $^3CH_2$ (a spin forbidden process), the other a direct absorption of the photolyzing light to form the $^3A_2$ excited state of ketene (a spin and symmetry forbidden process) and the subsequent decomposition of the $^3A_2$ state to $^3CH_2$ and CO. The transition from the ground state ($^1A_1$) of ketene to the $^3A_2$ state predominates at longer wavelengths (longer than 320 nm). The intersystom crossing from $^1CH_2$ to $^3CH_2$ is a bimolecular process with the colliding molecule providing a coupling between the singlet and triplet states of methylene and thereby easing the restrictions on spin. This is the major source of $^3CH_2$ at shorter wavelengths. The results of the CO experiments

Reproduced with permission of the copyright owner. Further reproduction prohibited without permission.

provide a method of determining the amounts of $^1CH_2$ and $^3CH_2$ produced directly from the photodecomposition of ketene. This can be used together with the data for the intersystem crossing at shorter wavelengths to determine the amount of $^3CH_2$ formed under different conditions.

The mechanism of the intersystem crossing and its application to the less complicated system at the shorter wavelengths (277 nm) will be discussed first. The evidence for and the description of the mechanism involving triplet ketene will be discussed next, and then the two mechanisms will be combined to describe the photolysis system at intermediate wavelengths. The last section will describe the differences between the 214 nm photolysis system and the photolysis systems at the other wavelengths and will discuss the evidence for a third electronic state of methylene, the $^1B_1$ state, produced at 214 nm.

Reproduced with permission of the copyright owner. Further reproduction prohibited without permission.

I A Review of Three Possible Mechanisms for the Formation of $^3CH_2$

In the twelve years since Herzberg[1,2] first identified the presence of $^3CH_2$ after the photolysis of diazomethane, several mechanisms for the production of $^3CH_2$ during the photolysis of ketene or diazomethane have been proposed.[3] This discussion will be limited to the details of photolysis of ketene.

In the simplest mechanism, the ketene is assumed to be excited by light to either a triplet state (a spin forbidden transition) or a singlet state which then decomposes, with spin conservation, to $^3CH_2$ or $^1CH_2$. (The decomposition of a singlet ketene state to $^3CH_2$ and $CO(^3\pi)$, the first excited state of CO, requires far too much energy to be feasible at the wavelengths studied.) However, this mechanism alone cannot explain the apparent increase in the percent of $^3CH_2$ that occurs when the ketene is photolyzed in the presence of increasing concentrations of

---

1. Herzberg, G. and Shoosmith, J., Nature 183, 1801 (1959); Herzberg, G., Proc. Roy. Soc., A262, 291 (1961).

2. Herzberg, G. and Johns, J. W. C., ibid., A295, 107 (1966).

3. For an introduction see the review articles, Frey, H. M., Prog. React. Kinet., 2, 131 (1964); Bell, J. A., Prog. Phys. Org. Chem. 2, 1 (1964); and DeMore, W. B. and Benson, S. W., Adv. Photochem. 2, 219 (1964).

Reproduced with permission of the copyright owner. Further reproduction prohibited without permission.

supposedly inert gases. At some point, either the methylene or ketene must be involved in a spin forbidden process. Methylene and ketene are both too simple molecules to be expected to undergo an intramolecular (or spontaneous), spin forbidden intersystem crossing.[4] Collisions of the excited ketene or the $^1CH_2$ with other molecules and subsequent intersystem crossing have been suggested to explain the increase in the fraction of $^3CH_2$ with an increase in the pressure of the added gases.[1,2,5-9]

Two of the various mechanisms which can explain a bimolecular intersystem crossing are shown schematically in figure 4-1. Scheme A is a bimolecular intersystem crossing of ketene in the first excited singlet state, $^1CH_2CO^*$ or actually $^1A_2$, to the lowest triplet state of ketene, $^3CH_2CO^*$ or $^3A_2$. According to this mechanism, the decomposition of the excited singlet ketene is slow enough to compete with a bimolecular intersystem crossing to the lowest tripet state of ketene. The $^3A_2$ state then decomposes

---

5. Voisey, M., Trans. Faraday Soc. 64, 3058 (1968).
6. Cox, R. A. and Preston, B. S., Can. J. Chem. 47, 3345 (1969).
7. Ring, D. F. and Rabinovitch, B. S., ibid. 46, 2435 (1968).
8. Eder, T. W. and Carr, R. W., Jr., J. Chem. Phys. 53, 2258 (1970).
9. Bell, J. A., J. Phys. Chem. 75, 1537 (1971).

4. This is discussed in more detail on pages 98-100.

Reproduced with permission of the copyright owner. Further reproduction prohibited without permission.

to $^3CH_2$ and CO. Scheme A requires that the percent of $^3CH_2$ increases as the total pressure of the system increases. Scheme B differs in that the excited singlet state of ketene, $^1CH_2CO^*$, decomposes very quickly to $^1CH_2$ and CO and the bimolecular intersystem crossing is a reaction of the $^1CH_2$ and not of the $^1CH_2CO^*$ or $^1A_2$. state. At first glance, scheme B also seems to predict that the fraction of $^3CH_2$ should increase as the total pressure of the system increases. However, once the $^1CH_2$ is formed, there will be a competition between the intersystem crossing reaction and any other reactions of $^1CH_2$. This competition will limit the percent of $^3CH_2$ formed from $^1CH_2$, so that increasing the total pressure of the system will not increase the percent of $^3CH_2$.

Scheme A has been discounted by the experimental results of numerous workers[5, 10-13] who have studied mixtures of ketene and a reactive gas (e.g., propane, n-butane, and methylethyl-ether) and have found a constant ratio of the products of $^3CH_2$ reaction compared to the products of $^1CH_2$ reactions. In our work, doubling the pressure of the standard ketene-isobutane mixture

---

10. Mitschele, C. J., Ph.D. Thesis (University of California, Riverside, 1968).

11. Ho, S. and Noyes, W. A., Jr., J. Am. Chem. Soc. 89, 5091 (1967).

12. Dees, K. and Setser, D. W., J. Phys. Chem 75, 2240 (1971).

13. Halberstadt, M. L. and McNesby, J. R., J. Am. Chem. Soc. 89, 3417 (1967).

Reproduced with permission of the copyright owner. Further reproduction prohibited without permission.

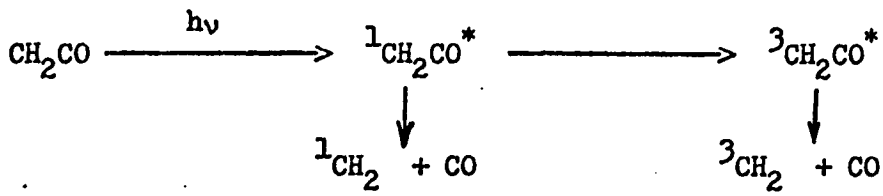

SCHEME A

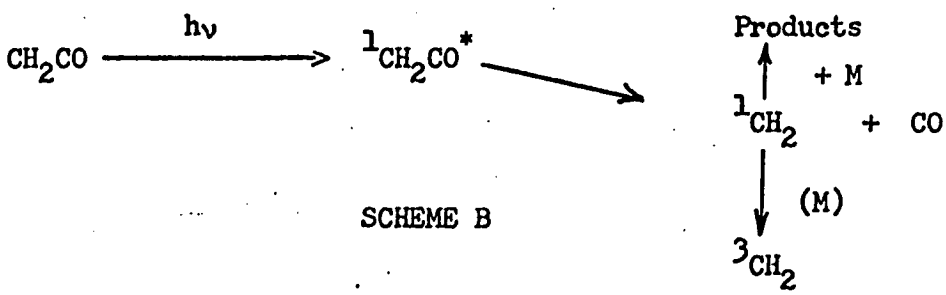

SCHEME B

Figure 4-1

Two possible mechanisms for the production of $^3CH_2$ via a bimolecular intersystem crossing.

Reproduced with permission of the copyright owner. Further reproduction prohibited without permission.

did not change either the neopentane to isopentane ratio or the measured percent of $^3CH_2$, which again discounts scheme A. Only scheme B is left as a description of the production of $^3CH_2$.

According to scheme B, the photolysis of ketene in the presence of an inert gas, such as xenon, will not affect the total amount of methylene produced, but will increase the percent of $^3CH_2$ formed in the system. In our work, the presence of Xe during the photolysis of the ketene-isobutane mixture at 313 nm and 277 nm increased the neopentane to isopentane ratio and the measured percent of $^3CH_2$ ($^3CH_2$%-O_2), but did not change the total quantum yield. (See Tables 3-I and 3-III,) Voisey[5], however, found that adding an inert gas to his ketene-ether system decreased the total quantum yield. As will be explained later, this decrease is probably due to the interfering reaction of $^3CH_2$ with ketene. (See page 114.) Scheme B, a vague and undetailed outline, can explain some of the most prominent features of ketene photolysis, but part of the description is still missing.

II The Mechanism of Intersystem Crossing in Methylene

The details of the mechanism of the intersystem crossing of methylene from the $^1A_1$ state to the $^3B_1$ state have not been specified in scheme B. The collision partner, M, induces the

Reproduced with permission of the copyright owner. Further reproduction prohibited without permission.

intersystem crossing, but the way in which it affects the $^1CH_2$ has not been explained.

When the $^1CH_2$ is produced from the decomposition of the $^1A_2$ state of ketene, it is formed with some excess energy, if the photolyzing light has more energy than is needed to form $^1CH_2$ and CO from ketene. The heat of reaction for the decomposition of ketene is 76.4 kcal/mole (see Table 5-VIII) which is smaller than the energy of the photolyzing light at any wavelength used in this study. The excess energy from the photolysis may appear as vibrational energy in the $^1CH_2$, and this is the assumption made in assigning the relative positions of the methylene and ketene energy levels in figure 4-2b. There are two possible ways for methylene in the $^1A_1$ state to cross over into the $^3B_1$ state, and both require a collision at some instant to effect the transition.

A The Intramolecular or Spontaneous Mechanism

In the first conception, a collision of the vibrationally excited $CH_2(^1A_1)$ state causes the $CH_2(^1A_1)$ to lose some of its vibrational energy to the surrounding molecules. The $CH_2(^1A_1)$ in its lowest vibrational level spontaneously or intramolecularly crosses over to the $^3B_1$ state. This corresponds to pathways a and b of figure 4-2b, a pressure dependent vibrational relaxation of $CH_2(^1A_1)$ followed by a fast pressure independent inter-

Reproduced with permission of the copyright owner. Further reproduction prohibited without permission.

Figure 4-2a

The qualitiative potential energy surfaces for the decomposition of ketene as a function of the C=C bond distance.

This diagram is taken in part from references 12 and 19. T_o is between 40 and 50 kcal/mole. The difference between the $^1A_2$ and $^3A_2$ states is 30-40 kcal/mole.

Reproduced with permission of the copyright owner. Further reproduction prohibited without permission.

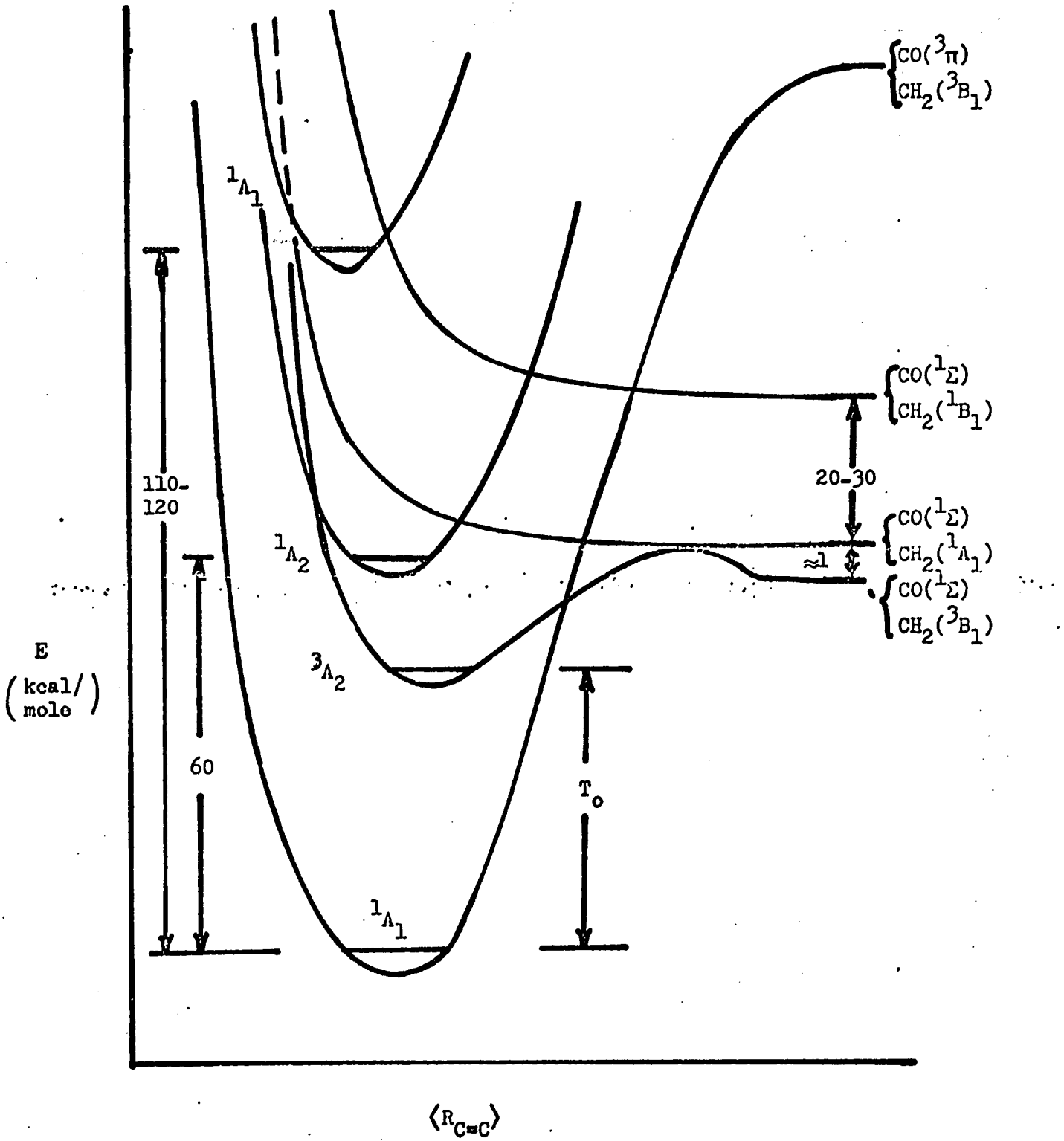

Figure 4-2a

Reproduced with permission of the copyright owner. Further reproduction prohibited without permission.

Figure 4-2b

A qualitative Jablonski diagram showing the different states of ketene and methylene.

The energies of the states of ketene are taken from Laufer and Keller,[21] and the position of the second excited singlet state, $^1A_1$, is estimated from the absorption spectrum of ketene and corresponds to the change in extinction coefficients at 250 nm. The $^1A_1$ abd $^3B_1$ states of methylene are estimated to be about 1.5 kcal/mole apart.[1,2,8,12,13] The position of the $^1B_1$ state of methylene is estimated by Herzberg[1,2] to be 20-30 kcal/mole above the $^1A_1$ state of methylene.

The upward arrows 1, 2, 3, and 4 represent the absorption of 366 nm, 313 nm, 277 nm, and 214 nm light by ketene. The downward arrows represent different amounts of vibrational relaxation. The horizontal arrows, 5 and 6 represent the decomposition of ketene to CH_2 and CO. The horizontal arrow 7 represents an intersystem crossing from the $^1A_2$ state to the $^3A_2$ state in ketene.

Pathways a and b describe vibrational relaxation of $CH_2(^1A_1)$ followed by a crossing from the $^1A_1$ state with very little vibrational energy to the $^3B_1$ state. (See references 14 and 15) Pathways d and e describe a crossing from vibrationally excited $CH_2(^1A_1)$ to $CH_2(^3B_1)$ which subsequently undergoes vibrational relaxation. (See references 5, 6, and 8 and also the theoretical calculations of Chang, T. and Basch, H., Chem. Phys. Letters 5, 147 (1970).)

Reproduced with permission of the copyright owner. Further reproduction prohibited without permission.

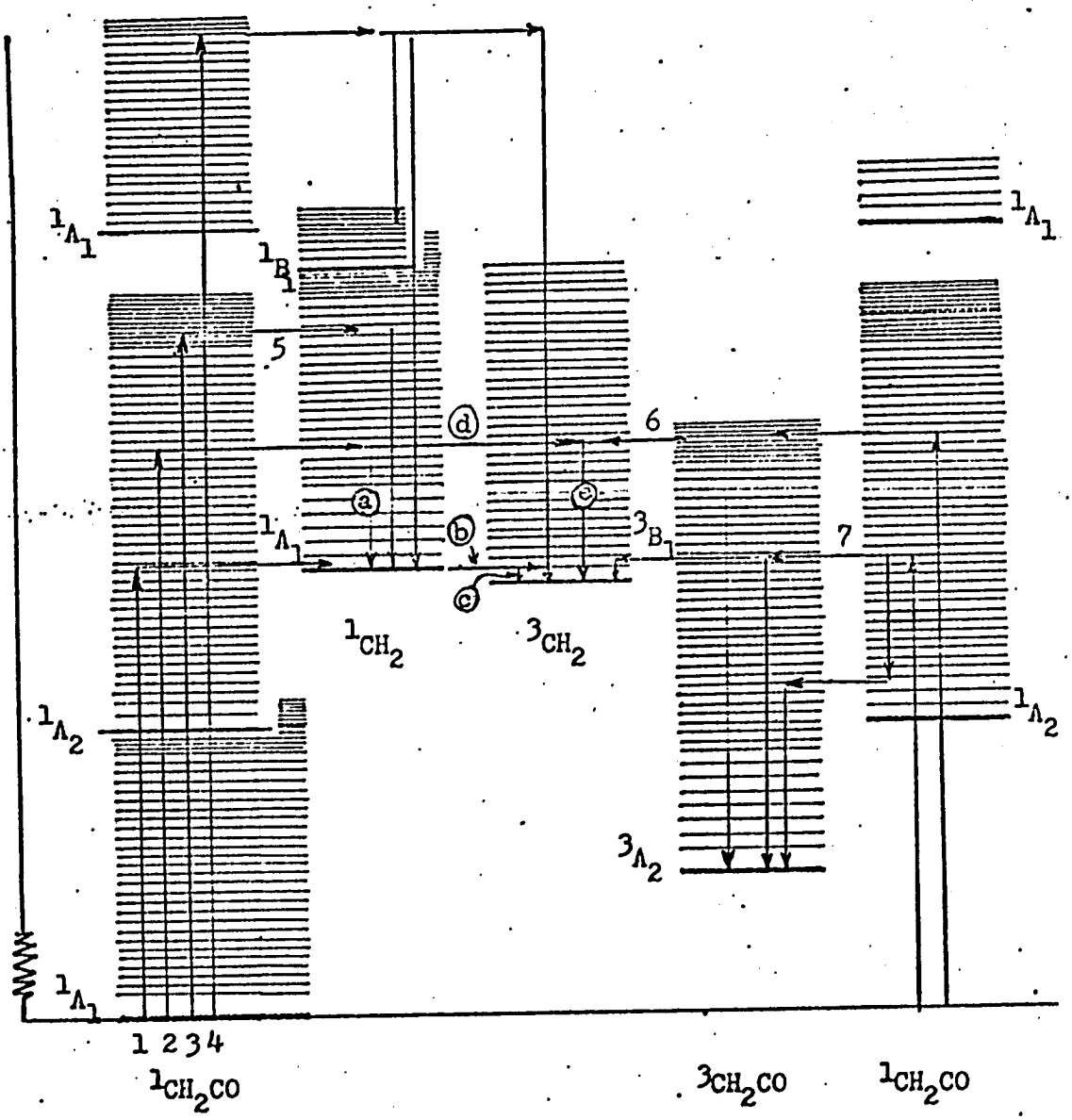

Figure 4-2b

Reproduced with permission of the copyright owner. Further reproduction prohibited without permission.

system crossing to the $CH_2(^3B_1)$.

According to both Bader and Generosa[14] and Matsen and Klein[15], the rate of the intramolecular intersystem crossing of methylene in the $^1A_1$ state will be larger at lower vibrational levels. Bader and Generosa use Zener's formula which relates the rate of crossing to the reciprocal of the difference in steepness of the two potential surfaces (here, $CH_2(^1A_1)$ and $CH_2(^3B_1)$) at their point of intersection and to the reciprocal of the velocity of the nuclei as the molecule approaches the point of intersection. (The velocity of the nuclei will be smallest in the lowest vibrational energies.) Matsen and Klein use Coulson and Zalewski's formula, a more complicated form of Zener's equation, and emphasize that the rate of crossing is proportional to the overlap of the vibrational wavefunctions of the two electronic states. This is a maximum when the nuclear motion is smallest at the point of intersection. In both cases, an acceleration in the vibrational relaxation of the $^1A_1$ state of methylene will mean an increase in the rate of intersystem crossing. Therefore, those systems having the inert gas with the highest efficiency of vibrational energy transfer should have the largest fraction of $^3CH_2$.

---

14. Bader, R. F. W. and Generosa, Can. J. Chem. 43, 1631 (1965).

15. Matsen, F. A. and Klein, D. J., Adv. Photochem. 7, 1 (1969).

Reproduced with permission of the copyright owner. Further reproduction prohibited without permission.

B The Bimolecular (Intermolecular) Mechanism

The second possible mechanism by which methylene may cross over from the $^1A_1$ state to the $^3B_1$ state requires an external event, a collision, to effect the crossover. This is opposed to the spontaneous crossover described above. A collision-induced intersystem crossing is typical of molecules in the "resonant limit" of radiationless transition theory.[16] A molecule is said to be in the "resonant limit" when the vibronic energy levels in the molecule are not closely spaced and when the vibronic interaction between the two states is very small.

Anderson, et al.[17] estimated the energy levels spacings for the glyoxal intersystem crossing, $^1A_u \rightarrow {}^3A_u$ (first excited singlet to lowest triplet) to be large enough to put glyoxal in the resonant limit. Since the energy level spacings are roughly inversely proportional to the size of the molecule, and since ketene and methylene are both smaller than glyoxal, it is expected that they, too, will be in the resonant limit.

In a collision-induced intersystem crossing, the function of a collision partner is to provide a coupling between the two

16. Jortner, J., Rice, S. A., and Hochstrasser, R. M., Adv. Photochem. 7, 149 (1969).

17. Anderson, L. G., Parmenter, C. S., Poland, H. M., and Rau, J. D., Chem. Phys. Letters 8, 232 (1971).

Reproduced with permission of the copyright owner. Further reproduction prohibited without permission.

states. The coupling is in the form of a perturbation which broadens the vibronic energy levels of an electronic state so that a "quasi-contimuum" of levels results during the time of the collision and a crossing can be made from one electronic state to another. This mechanism is depicted by pathways d and e in figure 5-2b, a collision-induced intersystem crossing and then a vibrational relaxation within the $^3B_1$ state of methylene. At a given energy level, the larger the coupling provided by the colliding molecule, the faster the rate of intersystem crossing.

C The Evidence Against the Intramolecular Intersystem Crossing

Bader and Generosa,[14] Eder and Carr,[8] and Cox and Preston[6] studied the $^1CH_2(^1A_1)$ reactions with trans-butene-2, propane, and ketene, respectively, in the presence of large amounts of relatively unreactive gases. Both Eder and Carr and Cox and Preston found the relative efficiencies in converting $^1CH_2$ to $^3CH_2(^3B_1)$, i.e., the relative rate of intersystem crossing of $^1CH_2$ to $^3CH_2$, to decrease in the order Xe> $CF_4 \sim N_2$> Ar> He. Bader and Generosa found the efficiency of CF_4 to be greater than that of Xe, but otherwise agreed with the order of efficiencies found by Eder and Carr. Among the monatomic gases, the efficiency of vibrational transfer from CH_2 should be greatest for He because its translational velocity should be closest to

Reproduced with permission of the copyright owner. Further reproduction prohibited without permission.

the velocity of H during a CH vibration. Thus, the order expected if the transfer of vibrational energy were the rate limiting step would be He> Ar> Xe, the opposite of what is found. Therefore, the vibrational relaxation of $^1CH_2$ must not be the limiting step and the spontaneous molecular intersystem crossing of $^1CH_2$ to $^3CH_2$ can not be the correct mechanism.

On theoretical grounds, an intramolecular or spontaneous intersystem crossing is very unlikely. As mentioned before in explaining the bimolecular mechainsm, if the density of energy levels for an intersystem crossing of the first excited singlet (^1A_u) state of glyoxal (HC(CO)C(CO)H) to the lowest triplet(^3A_u) state of glyoxal is so small that when there are no collisions this crossing is not observed, it is extremely improbable that such an intersystem crossing would occur in methylene.[17] If the vibronic coupling between the $^1A_1$ and $^3B_1$ states of methylene were very large, i.e., if the Franck-Condon factors were very large, methylene could be intermediate between the "statistical limit" (where an intramolecular crossover is possible) and the "resonant limit". However, there is no a priori reason to expect an unusually large vibrational overlap between the $^1A_1$ and $^3B_1$ states.

Reproduced with permission of the copyright owner. Further reproduction prohibited without permission.

D The Effect of the Nature of the Collision Partner in the Bimolecular Intersystem Crossing of Methylene

As demonstrated above, the order of the effects of addenda on the rate of intersystem crossing cannot be correlated with the efficiency of vibrational transfer. This leaves the question of what does correlate with the efficiency of an added gas to induce an intersystem crossing in methylene. Since this is a spin-forbidden process, a likely property to test a correlation with is the spin-orbit parameter of the colliding molecule or atom. Since the spin is not a good quantum number for systems in which there is a strong interaction between the orbital angular momentum and the spin, the larger the spin-orbit parameter, the less stringent the restrictions on spin.

The quenching of iodine by several gases was studied by Selwyn and Steinfeld.[18] The quenching process in I_2 is reported to be a collision-induced predissociation from a bound state of I_2. Selwyn and Steinfeld also apply their theory to the quenching of fluorescence in SO_2, a collision-induced internal conversion. They found a good correlation of the square of the quenching cross-section with $\mu^{\frac{1}{2}} I\alpha/R_c^3$, where $\mu^{\frac{1}{2}}$ is the reduced mass of the

18. Selwyn, J. E. and Steinfeld, J. I., Chem. Phys. Letters 4, 217 (1969).

Reproduced with permission of the copyright owner. Further reproduction prohibited without permission.

collision complex and is proportional to the duration of the collision, I is the ionization energy of the collision partner, R_c is the hard-sphere collision radius, and α is the polarizablity of the collision partner. The product $\alpha\mu^{\frac{1}{2}}$ also correlated with the square of the cross-section but not as well as $\mu^{\frac{1}{2}} I\alpha/R_c^3$.

In light of Selwyn and Steinfeld's work, Eder and Carr[8] tried to correlate the rate of the intersystem crossing of methylene with α, I, $\mu^{\frac{1}{2}}$, $\alpha I\mu^{\frac{1}{2}}/R_c^3$, and the mass of the collision partner and found the best correlation to be with α, the polarizability of the collision partner. A plot of the ratio of the rate of intersystem crossing and the rate of $^1CH_2$ reaction with propane against polarizability was linear. Eder and Carr also tried a correlation with the spin-orbit parameter of the collision partner, but this failed. The polarizability of each of the gases used in this study and to be discussed later is listed in Table 4-I. These will be of use in explaining the variations in the percent of $^3CH_2$ formed during the photolysis of ketene.

E The Effect of an Unreactive Gas in a Methylene System

Assuming that the polarizability of the colliding molecule is the major factor in determining the rate of intersystem crossing, then according to the preceding arguments, the percent of $^3CH_2$ formed will be larger when the colliding molecule has a

Reproduced with permission of the copyright owner. Further reproduction prohibited without permission.

larger polarizabilty. If the colliding molecule does not react with the $^1CH_2$ chemically, the limiting value of the percent of $^3CH_2$ is 100% (as per scheme B), but the rate at which the percent of $^3CH_2$ approaches the limit will depend on the polarizabilty of the molecule. In other words, although the addition of large amounts of Xe or Ar to the methylene system, in each case, means 100% of the $^1CH_2$ is converted to $^3CH_2$, since the polarizabilty of Ar is less than that of Xe, the pressure of Xe at which all of the $^1CH_2$ has crossed over to the $^3CH_2$ is less than the required pressure of Ar.

F The Effect of a Reactive Gas in a Methylene System

If the gas in the methylene system reacts with $^1CH_2$ to form products (e.g., isobutane reacting with $^1CH_2$ to form pentanes) and if the gas also induces an intersystem crossing, a competition for the $^1CH_2$ is set up by the two different events.

$$M + {}^3CH_2 \xleftarrow{k_{isc}} {}^1CH_2 + M \xrightarrow{k_{sprod}} \text{Products}$$

The percent of $^1CH_2$ that is converted to $^3CH_2$ is given by

$$\frac{[{}^3CH_2]}{[{}^3CH_2] + [\text{Products}]} = \frac{k_{isc}}{k_{isc} + k_{sprod}} \qquad \text{(Eq. 5)}$$

where it has been assumed that only $^1CH_2$ was originally present.

Reproduced with permission of the copyright owner. Further reproduction prohibited without permission.

TABLE 4-I

The Polarizabilities of Different Gases Used in Methylene Systems

Gas	Polarizabilty $\times 10^{-25}$ cm^3	
Ar	16.6	b
Xe	41.1	b
N_2	17.6	a
CH_2CO	159.	c
C_3H_8	63.	a
$isoC_4H_{10}$	81.4	a
$n\text{-}C_4H_{10}$	81.2	a
CO	19.5	b
O_2	16.0	a

a Landolt-Bornstein, Zahlenwerte und Funktionen, Vol.I, part 3, page 510, Springer-Verlag, Berlin (1951).

b Bridge, N. J. and Buckingham, A. D., J. Chem. Phys. 40, 2733 (1964); Proc. Roy. Soc. A295, 334 (1966).

c Hanney, H. B. and Smyth, C. P., J. Am. Chem. Soc. 68, 1357 (1946).

Reproduced with permission of the copyright owner. Further reproduction prohibited without permission.

Equation 5 indicates that the percent of $^3CH_2$ formed is independent of the pressure of the reactive gas (as long as the concentration of the reactive gas is large enough so that it is the major reactant). This agrees with our experiments at 313 nm in which the pressure of isobutane was doubled but neither the measured percent of $^3CH_2$ ($^3CH_2\%-O_2$) nor the neopentane to isopentane ratio changed.

As above, the polarizabilty of M is assumed to be the major factor determining the magnitude of k_{isc}. If k_{sprod} is the same for two different molecules, the percent of $^3CH_2$ will be determined by the polarizabilty alone. As long as there is a significant reaction of $^1CH_2$ with M, i.e., as long as k_{sprod} is not negligible, the amount of $^3CH_2$ formed from $^1CH_2$ is always limited by k_{sprod}.

Clearly, if this mechanism is operative, the reaction represented by k_{isc} must be added to the reaction scheme presented in the chapter of results, Chapter 3.

G The Percent of $^3CH_2$ Formed from $^1CH_2$ During the Photolysis of Ketene-Alkane Mixtures at Short Wavelengths

The polarizabilities of the alkanes (see Table 4-I) are at least as large as that of Xe and, therefore, must also induce the intersystem crossing of $^1CH_2$. The percent of $^3CH_2$ measured by

Reproduced with permission of the copyright owner. Further reproduction prohibited without permission.

adding O_2 ($^3CH_2$%-O_2) as described in Chapter 3, is the percent or fraction of methylene formed during the photolysis of the ketene-isobutane mixture which is $^3CH_2$, but it is not necessarily the amount of $^3CH_2$ formed directly from the photodecomposition of ketene. The fraction of $^3CH_2$ is a measure of the sum of the amount of $^3CH_2$ formed directly from the photolyzed ketene, ϕ_t, and the amount of $^3CH_2$ formed by the intersystem crossing of $^1CH_2$. This can be expressed as follows,

$$f(^3CH_2) = \phi_t + \frac{\phi_s\,(k_3[\text{IsoB}] + k_{isc}[M])}{(k_1+k_2+k_3)[\text{IsoB}] + k_{isc}[M]} \quad , \qquad \text{(Eq. 6)}$$

where k_3 refers to the collision-induced intersystem crossing by isobutane:

$$^1CH_2 + \text{IsoB} \xrightarrow{k_3} {}^3CH_2 + \text{IsoB}.$$

In the absence of any added gases in the ketene-isobutane mixtures, i.e., [M] = 0, the fraction of $^3CH_2$ formed during the photolysis is

$$f(^3CH_2) = \phi_t + \frac{\phi_s k_3}{k_1+k_2+k_3} \quad . \qquad \text{(Eq. 7)}$$

In the presence of large amounts of unreactive gas, M, Eq. 6 predicts that $f(^3CH_2)$ will approach 1.0 as expected. Since the fraction of $^3CH_2$ formed during the photolysis is known for some conditions, if ϕ_t, ϕ_s, or $k_3/(k_1+k_2+k_3)$ were known, the $f(^3CH_2)$ could be calculated for any conditions.

Reproduced with permission of the copyright owner. Further reproduction prohibited without permission.

At wavelengths shorter than 290 nm, but longer than 250 nm, the quantum yield of CO for ketene photolysis is independent of pressure.[6,9,11,19] This suggests that any excited ketene present has a very short lifetime with respect to its decomposition to methylene and carbon monoxide. The absorption of light in the 250 nm- 380 nm wavelength region has been attributed to the $^1A_2$ state $\longleftarrow$ $^1A_1$ (ground) state transition in ketene.[20,21] (An unambiguous absorption to the $^3A_2$ state has not been identified, even at long wavelengths.) $^1A_2$, the lowest excited singlet state of ketene, must be the state reached by the absorption of 290 nm and responsible for the decomposition of ketene. Since $^1A_2$ is the state of ketene which is decomposing, the products must be $^1CH_2$ and $CO(^1\Sigma)$. Thus, all of the methylene produced in this wavelength region must be $^1CH_2(^1A_1)$ and so ϕ_s=1.0.

In this wavelength region, the fraction of $^3CH_2$ is due only to the intersystem crossing reaction, i.e., ϕ_t=0, and as long as the alkane is the major reactant, equation 7 becomes

$$f(^3CH_2) = \frac{k_3}{k_1+k_2+k_3} \quad .$$

When the ketene-isobutane mixture was photolyzed at 277 nm, the

---

19. DeGraff, B. A. and Kistiakowsky, G. B., J. Phys. Chem. 71, 1553, 3984 (1967).

20. Dixon, R. N. and Kirby, G. H., Trans. Faraday Soc. 62, 1406 (1966).

21. Laufer, A. H. and Keller, R. A., J. Am. Chem. Soc. 93, 61 (1971).

Reproduced with permission of the copyright owner. Further reproduction prohibited without permission.

measured percent of $^3CH_2$ was 36% and therefore, $k_3/(k_1+k_2+k_3)=0.36$ and $k_3/(k_1+k_2)=0.56$. Thus, as long as isobutane is the major reactant, a ketene-isobutane reaction mixture always contains at least $36\pm 4\%$ of $^3CH_2$.

Bell[9] photolyzed mixtures of diazomethane and propane in the presence of several gases including argon, xenon, and nitrogen. He measured the ratio $k_{isc}/(k_1+k_2)$ for each gas. If these three ratios for argon, xenon, and nitrogen are plotted against the polarizabilty of the added gas and if the ratios from our work with isobutane and Ho and Noyes's[11] work with propane are added, the result is a straight line as shown in figure 4-3. Since Hase and Simons[22] found the rate of reaction of $^1CH_2$ with isobutane to be the same as with propane, i.e., (k_1+k_2) is the same for propane and isobutane, we can use Ho and Noyes's data to check the consistency of our method of evaluating $k_3/(k_1+k_2)$. Ho and Noyes photolyzed mixtures of ketene and propane at 270 nm, so that for propane, $k_3/(k_1+k_2+k_3)$ is 0.27 and $k_3/(k_1+k_2)$ is 0.37. The value of $k_3/(k_1+k_2)$ agrees well with the values in figure 4-3. (Note that $k_3=k_{isc}(M)$.)

As Bell mentions, these ratios do not agree with Eder and Carr.[8] One of the experimental reasons for this discrepancy may be found

---

22. Hase, W. L. and Simons, J. W., J. Chem. Phys. 54, 1277 (1971).

Reproduced with permission of the copyright owner. Further reproduction prohibited without permission.

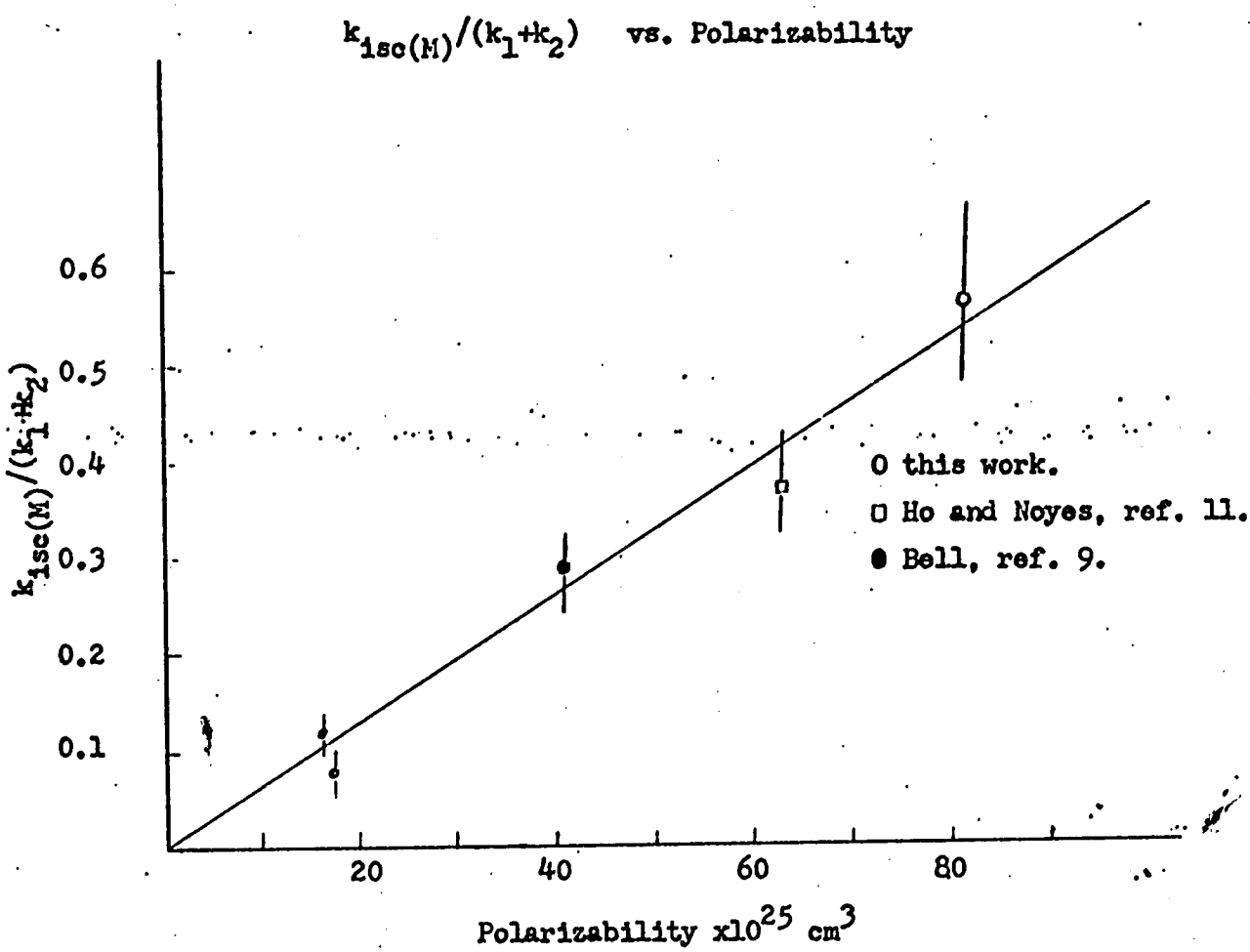

Figure 4-3

Reproduced with permission of the copyright owner. Further reproduction prohibited without permission.

in the variation of the ratio of propane to ketene in Carr's work. Carr kept the total pressure of the reactants constant and the amount of ketene constant and varied the ratio of inert gas to propane. Bell points out that the polarizability of propane is larger than the polarizability of any of the gases Carr added. This means that Carr replaced a molecule effective in inducing an intersystem crossing of $^1CH_2$ with a molecule that is less effective. Carr's method has the disadvantage of decreasing the ratio of propane to ketene when the inert gas is added. Although the larger concentration of inert gas means that more $^1CH_2$ crosses over to $^3CH_2$ (which is removed by the O_2 which is present), it also means that the ketene begins to compete with propane for the $^1CH_2$ which further complicates the system. As Bell emphasizes, however, the exact reasons for the differences between the ratios of $k_{isc}(M)/(k_1+k_2)$ are not known.

III The Reaction of Ketene with $^1CH_2$ and $^3CH_2$

In the preceding section, we have assumed that the reactions of both methylenes with ketene were negligible compared to the reactons with isobutane. If the reactions with ketene were not negligible, our measurements of the percent of $^3CH_2$ would be in error. The determination of the percent of $^3CH_2$ is based on measurements of the total quantum yield, which is defined in Chapter 3, page 76, as the sum of the yields of the products of

Reproduced with permission of the copyright owner. Further reproduction prohibited without permission.

the reactions of both methylenes with isobutane. The total quantum yield does not include reactions of both methylenes with ketene and as long as these are negligible, the total quantum yield is a perfectly valid measure of the amount of methylene produced.

A $^1CH_2$ and Ketene

Eder and Carr[8] found the rate of reaction of $^1CH_2$ with ketene was one fourth the rate of reaction of $^1CH_2$ with propane at 313 nm. Since the ratio of propane to ketene is 10 to 1, only 2.5% of the $^1CH_2$ is expected to react with ketene and this would be well within our experimental error. Indeed, when the concentration of isobutane was doubled and the ketene-isobutane mixture was photolyzed at 313 nm in the presence of O_2, the total quantum yield was no different from the total quantum yield measured when the standard mixture was photolyzed with O_2 at 313 nm. Thus, our measurements confirm that the ratio of the rate of the $^1CH_2$ reaction with ketene compared to the rate of the $^1CH_2$ reaction with isobutane is not much larger than 0.25. Dees and Setser[12] estimate that this ratio in the ketene-n-butane system is 0.5. Thus, in our system, where the ratio of isobutane to ketene is 10:1, and if isobutane and n-butane have the same relative reactivity with respect to $^1CH_2$, 5% of the $^1CH_2$ will react with ketene which is again within our experimental error. Considering these findings, it is safe to conclude that at concentrations of isobutane to ketone of at least 10:1, the reaction of $^1CH_2$ with ketene is

Reproduced with permission of the copyright owner. Further reproduction prohibited without permission.

negligible compared to the reaction with isobutane.

B $^3CH_2$ and Ketene

When the amount of isobutane in the standard mixture was doubled, the total quantum yield at 313 nm was the same as found when the standard mixture was photolyzed (see Table 3-III). Since the reaction of $^1CH_2$ with ketene is negligible, the unchanged total quantum yield in the absence of O_2 must mean that the reaction of $^3CH_2$ with ketene is also negligible in mixtures having a ratio of at least 10:1. If the $^3CH_2$ reacted to a significant extent with ketene, doubling the isobutane concentration would increase the total quantum yield, as it was defined above.

In their study of the photolysis of the ketene-n-butane system at 320 nm, Dees and Setser[12] estimate the reaction of $^3CH_2$ with ketene to be twenty times faster than the reaction with n-butane. If this were also true in the isobutane system where the ratio of isobutane to ketene is 10:1, two thirds of the $^3CH_2$ would react with ketene and one third with isobutane. Then, doubling the isobutane concentration would mean that half of the $^3CH_2$ would react with the isobutane and so the total quantum yield, the measured $^3CH_2\%-O_2$, and the neopentane to isopentane ratio would increase. This did not occur.

Reproduced with permission of the copyright owner. Further reproduction prohibited without permission.

Most workers have found hydrogen abstraction by $^3CH_2$ to be about ten times faster from a secondary C-H bond than from a primary C-H bond.[23] Thus, if a relative reactivity of 1.0 is assigned to a primary C-H bond, the "total relative reactivity" of n-butane is 6 + 4(10) = 46 and of propane is 6 + 2(10) = 26.

This work shows that the tertiary H is abstracted from isobutane about 60 times faster than the primary H of the C-H bond (see Table 3-III). Hence, the "total relative reactivity" of isobutane is 69. Simplistically assuming that no other factor is important in determining the ratio of reactivites, the isobutane is 1.4 times as reactive as n-butane towards $^3CH_2$. However, this is not enough to account for the difference between Setser's results and our findings with isobutane.

Dees and Setser's estimate of the proportion of $^3CH_2$ reacting with ketene compared to that with n-butane was based on the ratio of the products of methyl radicals to the products of the butyl radicals. However, they did not measure the disproportionation product of the sec-butyl radical. They concluded that the olefin forming reaction was negligible and cited Ring and Rabinovitch[7] who used 0.64 for the ratio of disproportionation to recombination rates for the sec-butyl radical. Kraus and Calvert [24], whom

---

23. Whitten, G. Z. and Rabinovitch, B. S., J. Phys. Chem. 69, 4358 (1965). And see also, references 7, 10 and 11.

24. Kraus, J. W. and Calvert, J. G., J. Am. Chem. Soc. 79, 5921 (1957).

Reproduced with permission of the copyright owner. Further reproduction prohibited without permission.

whom Setser did not cite, found this ratio to be 2.27. Since Dees and Setser[112] do not show the observed yields of octanes, a correction for the disproportionation product cannot be made.

Bell[9] used the results of Ho and Noyes[11] to find that the ratio of the rates of reaction of $^3CH_2$ with ketene compared to that with propane is 6 ± 2. Again being simplistic, the "total relative reactivity" of isobutane towards $^3CH_2$ is 2.7 times that of propane. Hence, the rate of reaction of $^3CH_2$ with ketene is 2.3 times as fast as that with isobutane. In this case, less than 20% of the $^3CH_2$ reacts with ketene. When $^3CH_2$ is 50% of both methylenes, less than 10% of the total amount of methylene will be reacting with ketene via reaction 14. This is within the error limits of our experiments, if Bell's estimate is correct.

As mentioned earlier, Voisey[5] found a decrease in his ether reaction yield when the ketene-ether mixture was photolyzed in the presence of an inert gas. If the $^3CH_2$ reacts much faster with ketene than with the ethyl-methyl ether, then, even at a ratio of ten parts of ethyl-methyl ether to one part ketene, the $^3CH_2$ could be reacting with ketene to a significant extent. As the pressure of the inert gas increased, the amount of $^3CH_2$ would increase and the yield of ether products would decrease because less methylene would be reacting with ethyl-methyl ether.

Reproduced with permission of the copyright owner. Further reproduction prohibited without permission.

IV The Second Source of $^3CH_2$

A Introduction and Evidence

If the only source of $CH_2(^3B_1)$ were the intersystem crossing of $CH_2(^1A_1)$, we would not expect a large change in the percent of $^3CH_2$ with a change in the photolyzing wavelength. However, there is ample evidence in many ketene photolysis studies for a large and abrupt increase in the percent of $^3CH_2$ as the photolyzing wavelength increases from 250 nm to 370 nm. This abrupt change in the $^3CH_2$ products occurs at about 320 nm and has been noted by several workers, but they have not proposed an adequate explanation for it. [5,10,11,25]

Figure 3-1 depicts the ratio of neopentane to isopentane and the $^3CH_2$-O_2 (the percent of $^3CH_2$ measured by the oxygen experiments) as a function of the photolyzing wavelength. For comparison, the variation in the ratio of the quantum yield of ethylene to the quantum yield of ethylene in the presence of O_2 when ketene alone was photolyzed is also shown. This graph was taken from DeGraff and Kistiakowsky.[19] This ratio, $\phi_{C_2H_4} / \phi_{C_2H_4(O_2)}$, represents the ratio of triplet to singlet products in the photolysis of ketene alone. The graph includes the values of the ratio found by several other workers; the value at 365 nm is from G. B. Porter[26]

---

25. Strachan, A. N. and Thornton, D. E., Can. J. Chem. 46, 2353 (1968).

Reproduced with permission of the copyright owner. Further reproduction prohibited without permission.

and the value at 270 nm is from Strachan and Noyes.[27] All three graphs show a distinct change in the percent of $^3CH_2$ or $^3CH_2$ reaction products at 320 nm. Mitschele's[10] data for the ketene-propane system photolyzed at several wavelengths between 250 nm and 366 nm shows this same abrupt change at 320 nm.

Several workers[25,27,28,29] have investigated the pressure dependence of ketene decomposition at several wavelengths. Although nothing specific can be said about $^3CH_2$ in these experiments, there is evidence that more than one process is involved in the photolytic decompositon of ketene. The quantum yield for ketene decomposition at 270 nm is independent of the pressure of ketene or of an added unreactive gas, C_4F_8 or SF_6. The quantum yield in the 330 nm to 366 nm wavelength region decreases as the pressure of ketene is increased or when an unreactive gas, C_4F_8 or SF_6, is added to increase the total pressure. In the intermediate wavelength region around 313 nm, the quantum yield is pressure independent up to a certain pressure of ketene (250 Torr, Strachan and Thornton's results[25]) and beyond that is pressure dependent, although the pressure dependence is much smaller than

---

26. Porter, G. B., J. Am. Chem. Soc. 79, 1878 (1957).

27. Strachan, A. N. and Noyes, W. A., Jr., ibid. 76, 3258 (1954).

28. Taylor, G. B. and Porter, G. B., J. Chem. Phys. 36, 1353 (1962).

29. Porter, G. B. and Connelly, B. T., ibid. 33, 81 (1960).

Reproduced with permission of the copyright owner. Further reproduction prohibited without permission.

that at the longer wavelengths. Strachan and Thornton found that C_4F_8 and SF_6 added to 50 Torr of ketene decreased the quantum yield and they attributed the increased efficiency in decreasing the quantum yield to an increase in the number of vibrational degrees of freedom compared to ketene.

The pressure dependence in ketene decomposition implies the presence of an excited state of ketene that lives long enough before decomposition to lose energy in collisions. The longer lifetime in the presence of a gas with more vibrational degrees of freedom implies that the excited state of ketene vibrationally relaxes to an energy where further relaxation successfully competes with decomposition to CH_2 and CO.

B The Absorption Spectrum of Ketene

The absorption spectrum of ketene is expected to be typical of that of carbonyl compunds. Aldehydes and ketones have a weak absorption band in the 340 nm to 230 nm region which is attributed to a forbidden $\pi^* \leftarrow$ n singlet-singlet transition. A second, much stronger absorption band begins at wavelengths shorter than 220 nm which is believed to be related to an allowed $\pi^* \leftarrow \pi$ transition. A third, very weak absorption band ($\varepsilon \approx 10^{-3}$ liters/mole-cm) occurs near 400 nm, often close to the

Reproduced with permission of the copyright owner. Further reproduction prohibited without permission.

long wavelength limit of the $\pi^* \leftarrow\!\!-$ n transition. This is attributed to the doubly forbidden (spin and symmetry forbidden) $\pi^* \leftarrow\!\!-$ n transition, the singlet ground state to first triplet state transition.[30]

The absorption spectrum of ketene[20,21,31] in the visible and near ultraviolet consists of two regions, a weak ($\epsilon \approx 10$ liters-mole^{-1}cm^{-1}) absorption with a maximum at 330 nm and a strong absorption ($\epsilon \approx 10^3$ liters-mole^{-1}cm^{-1}) below 240 nm. (See figure 2-3.) The spectrum consists of broad, diffuse vibrational bands in both regions and extends into the visible to a limit at 473.5 nm.[20] Dixon and Kirby [20] searched the absorption spectrum in the 260 nm to 480 nm region for evidence of the lowest triplet ($^3A_2$) state of ketene. They thought they had observed a distinct change in the vibrational spacings near 385 nm and attributed the absorption at longer wavelengths to the $^3A_2 \leftarrow\!\!- {}^1A_1$ transition. The absorption at wavelengths shorter than 385 nm was attributed to the $^1A_2 \leftarrow\!\!- {}^1A_1$(ground) or $\pi^* \leftarrow\!\!-$ n transition. However, the data implied an upper limit for the dissociation of ketene of 61 kcal mole^{-1}. This was much lower than the heat of dissociation calculated from the heats of formation of ketene, methylene and carbon monoxide (78 kcal mole^{-1}).

---

30. Calvert, J. G. and Pitts, J. N., Jr., Photochemistry, John Wiley and Sons, Inc., New York, 1966.

31. Sauer, K. H. and Kistiakowsky, G. B., J. Am. Chem. Soc. 80, 1066 (1958).

Reproduced with permission of the copyright owner. Further reproduction prohibited without permission.

Because of the disagreement between Dixon and Kirby's values and thermochemical data, Laufer and Keller[21] reinvestigated the absorption spectrum of ketene and concluded that the change in vibrational spacing was not distinct, but was continuous and so probably due to the anharmoncity of the vibration. They did not rule out the possibility of a direct absorption from the singlet ground state to the triplet ($^3A_2$) state, but suggested that it might be hidden under the $^1A_1$ (ground) to $^1A_2$ absorption.

This singlet to triplet absorption is doubly forbidden, so its extinction coefficient will be very small. The absorption will be even weaker if the minimum of the potential energy surface of the $^3A_2$ state is shifted with respect to the $^1A_1$ state so that the Franck-Condon transitions to the $^3A_2$ state must occur from the vibrational level of $^1A_1$ larger than v=0. (See figure 4-2.) If this is true, the strength of the singlet to triplet absorption will increase with an increase in temperature. Strachan and Thornton[25] and Taylor and Porter[28] studied ketene absorption at several temperatures and observed an increase of light absorption by ketene at the wavelengths 313 nm, 334 nm, and 366 nm as the temperature increased. The largest increase in absorption with increasing temperature was at 366 nm where the percent of $^3CH_2$ is largest. The increase in absorption parallels the increase in the quantum yield of ketene decompsition which also occurs with an increase in temperature.

Reproduced with permission of the copyright owner. Further reproduction prohibited without permission.

Although the direct absorption from the $^1A_1$ (ground) state to the $^3A_2$ state has not yet been observed, similarities between the absorption spectrum of ketene and of other carbonyls (aldehydes and ketones) suggest that it does occur. The kinetic data discussed in the previous section (and the results of the CO experiments to be discussed in a later section) indicate a process other than the intersystem crossing of methylene from the $^1A_1$ state must occur at longer wavelengths to explain the increase of methylene in the $^3B_1$ state, $^3CH_2$. The production of the $^3A_2$ state of ketene by direct absorption of light at wavelengths longer than 320 nm and its subsequent decomposition to $CH_2(^3B_1)$ and $CO(^1\Sigma)$ is the most likely process.

C The Excited States of Ketene

In the two previous sections we have discussed the arguments and evidence (the absorption spectrum of ketene and the abrupt change in the observed percentage of $^3CH_2$ at 320 nm) which necessitate the postulation of two different processes of formation of $^3CH_2$ in ketene photolyses. A summary describing how both processes occur and the conditions under which each predominates is now in order.

The absorption spectrum of ketene involves transitions from

Reproduced with permission of the copyright owner. Further reproduction prohibited without permission.

the ground, $^1A_1$, state to the three excited states, $^1A_1$, $^1A_2$, and $^3A_2$. The relative energies and qualtitative potential energy surfaces are shown in figure 4-2. The absorption of 214 nm light results in a transition from the ground state, $^1A_1$, to the second excited singlet, $^1A_1$. This is an allowed transition (a $\pi^* \leftarrow\!\!- \pi$ transition) and the oscillator strength is expected to be large; the observed extinction coefficient ($\epsilon \approx 2000$ liters-mole^{-1}cm^{-1}) reflects this. Absorption in the region 260 nm to 380 nm and beyond corresponds to transitions to both the $^1A_2$ and $^3A_2$ states. The stronger absorption corresponds to a transition from the $^1A_1$ to the $^1A_2$ state. This is a symmetry forbidden transition; its oscillator strength and therefore its extinction coefficient are expected to be much smaller (ϵ = 10 liters mole^{-1}-cm^{-1}) than for the transition from the $^1A_1$ (ground) state to the $^1A_1$ state. A transition from the $^1A_1$ state to the $^3A_2$ state is symmetry forbidden and also spin forbidden. The vibrational overlap for this transition is larger at the higher vibrational levels of the $^1A_1$ ground state (v>0). Because of the spin and symmetry forbiddeness and because of the small vibrational overlap between the ground state predominant at room temperature and the $^3A_2$ excited state, the oscillator strength and extinction coefficient are expected to be very small. This direct absorption to the $^3A_2$ state must have a maximum at a wavelength longer than 320 nm (although the exact position has not been determined) and

Reproduced with permission of the copyright owner. Further reproduction prohibited without permission.

might be hidden beneath the stronger $^1A_2 \leftarrow\!\!- {}^1A_1$ absorption.

The decomposition from the $^1A_2$ state of ketene can be described with the aid of figure 4-2. Absorption of the shorter wavelengths, e.g., 270 nm, results in a highly vibrationally excited $^1A_2$ state of ketene. Since at this wavelength, the primary quantum yield for ketene decomposition is pressure independent, the lifetime of the $^1A_2$ state of ketene must be very short prior to decomposition into $CH_2(^1A_1)$ and CO. In this region the intersystem crossing from $CH_2(^1A_1)$ is the only source of $CH_2(^3B_1)$; ϕ_s (the quantum yield of $^1CH_2$) is equal to 1.0. As the photolyzing wavelength is increased, the $^1A_2$ state of ketene is formed with less vibrational energy. At the energies reached by the intermediate wavelengths, such as 313 nm, enough vibrational energy could be lost by one or two strong collisions that the resultant energy would be close to the minimum energy required for decomposition to $^1CH_2$ and CO. At this lower energy, the decreased rate of decomposition of the $^1A_2$ state of ketene to $^1CH_2$ and CO decreases the quantum yield of ketene decomposition. This mechanism is basically the same as that proposed by Strachan and Thornton for the photolysis of ketene at 313 nm. Close to 366 nm, the $^1A_2$ state of ketene does not have enough energy to decompose to $^1CH_2$ and CO and thus, the $^1A_2$ state is expected to have a long lifetime and the quantum yield for ketene

Reproduced with permission of the copyright owner. Further reproduction prohibited without permission.

decomposition from the $^1A_2$ state will be very small and pressure dependent. At this wavelength, the observed percent of $^1CH_2$ is so small, that not only the quantum yield but also the absorption coefficient for the $^1A_2$ transition must be extremely small if not zero, and almost all of the absorption must be to the $^3A_2$ state of ketene.

At wavelengths longer than approximately 320 nm, direct absorption to the $^3A_2$ state of ketene and the subsequent decomposition of the $^3A_2$ state to $CH_2(^3B_1)$ and CO becomes the major pathway for ketene decomposition. This means that as the photolyzing wavelength increases beyond about 320 nm, ϕ_t (the quantum yield of $^3CH_2$ production) becomes larger and ϕ_s becomes smaller. At the same time, $\phi_s + \phi_t$, the total quantum yield of methylene, becomes less than 1.0 because of the reduced decomposition of both excited states. It is important to note that even at 380 nm,[11] neither the ratio of isobutane to n-butane nor the butane yield relative to the CO yield in a ketene-propane system changes when the total pressure changes from 60 Torr to 200 Torr. Thus, even at the longest wavelengths that have been studied, the intersystem crossing of $^1A_2$ ketene to $^3A_2$ ketene is not important.

The next objective is to find ways to measure the individual quantum yields of $^1CH_2$ and $^3CH_2$ produced when ketene is photolyzed.

Reproduced with permission of the copyright owner. Further reproduction prohibited without permission.

V Discussion of the CO Experiments and the Measurements of ϕ_s

A The Determination of ϕ_s from the CO Experiments

As mentioned earlier (Chapters 1 and 3) CO reacts with both $^1CH_2$ and $^3CH_2$. The reaction of $^3CH_2$ with CO is faster than its reaction with isobutane so that in the presence of only 60 Torr of CO, there is no measurable reaction of $^3CH_2$ with isobutane at 50 Torr. CO can also induce the intersystem crossing of $^1CH_2$ to $^3CH_2$ via the reaction

$$^1CH_2 + M \longrightarrow {}^3CH_2 + M , \qquad k_{isc}(M).$$

In these experiments, it is impossible to distinguish between the reaction isc(CO) and 13.

$$^1CH_2 + CO \longrightarrow CH_2CO \qquad k_{13}.$$

Reaction isc(CO) is included within reaction 13 in the equations for the rates of formation of isopentane and neopentane (Eqs. 3 and 4) which were derived assuming a steady state rate of formation for $^1CH_2$. Equations 3 and 4 apply when only $^1CH_2$ is reacting with CO. Reaction 13 and equations 3 and 4 are repeated here for the reader's convenience (see also page 84 of Chapter 3).

$$R_{IsoP} = \frac{d}{dt}[IsoP] = \frac{k_1[IsoB]\,\phi_s I_a}{(k_1+k_2)[IsoB] + k_{13}[CO]} \qquad \text{(Eq.3)}$$

$$R_{NeoP} = \frac{d}{dt}[NeoP] = \frac{k_2[IsoB]\,\phi_s I_a}{(k_1+k_2)[IsoB] + k_{13}[CO]} \qquad \text{(Eq.4)}$$

Reproduced with permission of the copyright owner. Further reproduction prohibited without permission.

Equations 3 and 4 predict that, at a given pressure of CO larger than 60 Torr, the ratio of the isopentane or neopentane yield[32] at one wavelength compared to the yield at a second wavelength is the ratio of the quantum yields of $^1CH_2$, ϕ_s, at those wavelengths. The pentane yield ratios are calculated from figures 3-3, 3-4, and 3-5 (the plots of the pentane yields versus the pressure of CO added to the standard photolysis mixture). For example,

$$\frac{R_{IsoP}(\text{at 313 nm}) \text{ for } P_{CO}}{R_{IsoP}(\text{at 277 nm}) \text{ for } P_{CO}} = \frac{\phi_s \text{ (at 313 nm)}}{\phi_s \text{ (at 277 nm)}} .$$

This method assumes that k_1, k_2, and k_{13} do not change very much with wavelength. If ϕ_s is known at one wavelength, it can be calculated at each of the other wavelengths. As mentioned above, $\phi_s = 1.0$ at 277 nm. Thus the ϕ_s at each of the other wavelengths are calculated from figures 3-3, 3-4, and 3-5 at both 120 Torr of CO and 200 Torr of CO as follows: ϕ_s(214 nm) = 1.0, ϕ_s(313 nm) = 0.75-0.80, ϕ_s(322 nm) = 0.70-0.75, and ϕ_s(330 nm) = 0.19-0.20.

B The Fraction of $^3CH_2$ Determined from ϕ_s

Earlier (page 106) the fraction or percent of $^3CH_2$ was expressed as a sum of the amount of $^3CH_2$ formed directly from the photolyzed ketene, ϕ_t, and the amount of $^3CH_2$ formed from the intersystem

---

32. The pentane yields are the rates of formation multiplied by the photolysis time which was the same in all of the CO experiments.

Reproduced with permission of the copyright owner. Further reproduction prohibited without permission.

crossing of $^1CH_2$, equation 6. For convenience, equation 6 is reproduced below. In deriving equation 6, we have assumed that k_{isc}, k_1, k_2, and k_3 (the reactions of $^1CH_2$ with the diluent gas and with isobutane) do not depend on the photolyzing wavelength and that $\phi_s + \phi_t = \phi_M = 1.0$.

$$f(^3CH_2) = \phi_t + \frac{\phi_s\,(k_3[IsoB] + k_{isc}[M])}{(k_1+k_2+k_3)\,[IsoB] + k_{isc}[M]} \qquad \text{(Eq. 6)}$$

At 277 nm, the value of the ratio $k_3/(k_1+k_2+k_3)$ was determined (page 108) to be 0.35 and can be used with equation 6 to calculate the fractions of $^3CH_2$ present under different reaction conditions if ϕ_s or ϕ_t is known for each photolyzing wavelength.

As before, when M = 0, i.e., when there is no added diluent gas equation 6 becomes equation 7,

$$f(^3CH_2) = \phi_t + \frac{\phi_s\, k_3}{k_1+k_2+k_3} \qquad \text{(Eq.7)}$$

Using 0.35 for the value of $k_3/(k_1+k_2+k_3)$ and ϕ_s as calculated from the CO experiments above, the fractions of $^3CH_2$ are 0.35, 0.48-0.51, 0.51-0.54, and 0.79-0.80 at the wavelengths 214 nm, 313 nm, 322 nm, and 330 nm, respectively. Except for 214 nm, these values are somewhat larger than the percent of $^3CH_2$ measured via the oxygen experiments. For convenience, Table 4-II, column 1, compares the calculated fraction of $^3CH_2$ with that measured by the oxygen experiments, $^3CH_2$%-O_2, for each wavelength.

Reproduced with permission of the copyright owner. Further reproduction prohibited without permission.

The use of equation 6 is also applicable for the experiments done when xenon was added to the reaction mixtures which were photolyzed at 277 nm and 313 nm. The presence of xenon in the reaction mixture is expected to increase the fraction of $^3CH_2$ that is formed the intersystem crossing of $^1CH_2$. (As discussed before, pages 85, 86, and 114, the presence of xenon did not change the quantum yield of methylene, ϕ_M, in these two experiments.) The ratio of $k_{isc}(Xe)/k_3$ is needed to apply equation 6 to the xenon experiments and is determined from the data of figure 4-3 to be 0.49. Thus, according to equation 6, the fraction of $^3CH_2$ calculated to be present in the ketene-isobutane-xenon mixtures is 0.65 with 250 Torr of Xe photolyzed at 277 nm and 0.65-0.63 with 115 Torr of Xe photolyzed at 313 nm. The calculated fraction of $^3CH_2$ in the xenon experiment at 313 nm is larger than the measured $^3CH_2$ by O_2.

Thus, the quantum yields of $^1CH_2$ and $^3CH_2$ as determined from the CO experiments together with a knowledge of the relative rates of intersystem crossing can be used to determine the percentages or fractions of $^3CH_2$ and $^1CH_2$ present in the ketene-isobutane photolysis mixtures. The fraction of $^3CH_2$ determined in this way however is only in a fair agreement with the percentage of $^3CH_2$ measured by the oxygen experiments. Possible improvements in the agreement are discussed in the following sections.

Reproduced with permission of the copyright owner. Further reproduction prohibited without permission.

TABLE 4-II

Comparison of Calculated and Measured Fractions of $^3CH_2$

Column 1 lists the fraction of $^3CH_2$ calculated from Eq. 6. In these calculations $k_3/(k_1+k_2) = 0.54$ for all wavelengths. The value of $k_3/(k_1+k_2)$ was determined from the experiments with and without O_2 at 277 nm as described in the text.

Column 2 lists the fraction of $^3CH_2$ calculated from Eq.6, but $k_3/(k_1+k_2)$ was varied with wavelength to give a better agreement with the measured amount of $^3CH_2$. The ϕ_s used for each wavelength are 0.80 for 313 nm, 0.75 for 322 nm, 0.32 for 330 nm, and 1.0 for 277 nm and 214 nm.

Column 3 lists the percent of $^3CH_2$ measured from the O_2 experiments and the last two columns list the quantum yield of $^1CH_2$ measured from the CO experiments and the total quantum yield of both methylenes measured from the total quantum yields.

Reproduced with permission of the copyright owner. Further reproduction prohibited without permission.

Reproduced with permission of the copyright owner. Further reproduction prohibited without permission.

TABLE 4-II

Comparison of Calculated and Measured Fractions of $^3CH_2$

Wavelength	Column 1 (calculated) $f(^3CH_2)$	Column 1 (calculated) $k_3/(k_1+k_2)$	Column 2 (calculated) $f(^3CH_2)$	Column 2 (calculated) $k_3/(k_1+k_2)$	Column 3 (measured) $^3CH_2$ % $-O_2$	ϕ_s/ϕ_M	ϕ_M
214 nm	0.35	0.54	.0.45	0.82	49± 6	1.0	1.0
277 nm	0.35	0.54	0.35	0.54	36± 5	1.0	1.0
313 nm	0.51-0.48	0.54	0.44	0.43	41± 5	0.75-0.80	1.0
322 nm	0.54-0.51	0.54	0.48	0.43	42± 5	0.70-0.75	1.0
330 nm	0.80-0.79	0.54	0.78	0.43	76± 3	0.30-0.32	0.62
277 nm + 250 Torr Xe	0.65	0.54	0.65	0.54	60± 6	1.0	1.0
313 nm + 115 Torr Xe	0.65-0.63	0.54	0.58	0.43	52± 6	0.75-0.80	1.0

C The Variation of the Quantum Yield of Methylene Production with Wavelength

In deriving equation 6, we made the assumption that $\phi_s + \phi_t = \phi_M = 1.0$. As already mentioned, the quantum yield for methylene production at the longer wavelengths (330 nm and 366 nm) is less than 1.0. In order to use equation 6 and also 7, we must know the quantum yield for methylene production, ϕ_M, and ϕ_s or ϕ_t. Then for ϕ_s and ϕ_t in equation 6, we substitute ϕ_s/ϕ_M and ϕ_t/ϕ_M. This was done when the fractions of $^3CH_2$ were calculated for Table 4-II.

Several workers[6,11,19] have measured the quantum yield of CO production at wavelengths shorter than 290 nm (but longer than 250 nm) in ketene-alkane systems to be 1.0 and in ketene alone to be 2.0 which both imply a ϕ_M of 1.0. At 313 nm and 322 nm, $\phi_M = 1.0$ since the total quantum yields in the isobutane system at both wavelengths are the same as at 277 nm (Table 3-I). At 330 nm, $\phi_M = 0.62$ as calculated from the ratio of the total quantum yields as given in Table 3-I, and ϕ_s as calculated from the CO experiments is 0.19-0.20 and so ϕ_s/ϕ_M is 0.32-0.30, or in other words, 30-32% of all methylene produced from the photolysis of ketene at 330 nm is $^1CH_2$. At 214 nm, Kistiakowsky and Walter estimated the quantum yield of CO produced during the

Reproduced with permission of the copyright owner. Further reproduction prohibited without permission.

photolysis of ketene to be 2 (2.2-2.5) over a range of pressures.[33] Although this was only an estimate, we have assumed that since ϕ_{CO} was approximately 2, and therefore that ϕ_M was approximately 1, and was independent of the pressure of ketene, ϕ_M in our system should also be 1. In any case, ϕ_{Total} and ϕ_{CO} in our isobutane experiments were set equal to ϕ_{Total} and ϕ_{CO} at 313 nm (where both quantum yields are 1.0) so that ϕ_s at 214 nm as calculated from the CO experiments is actually the ratio of ϕ_s/ϕ_M. The results of the CO experiments indicate that, if $\phi_M = 1.0$ at 214 nm, $\phi_s = 1.0$. However, since ϕ_s as measured by the CO experiments is actually ϕ_s/ϕ_M, the experimental result is that ϕ_s/ϕ_M is 1.0 regardless of the value of ϕ_M. Thus, the results reveal that all of the methylene produced from the photolysis of ketene at 214 nm is $^1CH_2$.

VI Changes in the Rate of Intersystem Crossing with the Energy of $^1CH_2$

The calculated fractions of $^3CH_2$ at 313 nm and 322 nm were larger than the measured percents of $^3CH_2$, $^3CH_2$%-O_2, and although they were both within 20% of the measured values, the agreement should have been better. On the other hand, the calculated

---

33. Kistiakowsky, G. B. and Walter, T. A., J. Phys. Chem. 72, 3952 (1968).

Reproduced with permission of the copyright owner. Further reproduction prohibited without permission.

fraction of $^3CH_2$ at 214 nm was much smaller than the measured $^3CH_2$%-O_2 and these, too, should have agreed better. If the intersystem crossing rate constant, k_3 or $k_{isc}(M)$, is faster when the methylene has more energy. (when it is formed by photolyses at the shorter wavelengths), the agreement between the calculated fractions of $^3CH_2$ and $^3CH_2$%-O_2, for the photolyses both at 313 nm and 322 nm and at 214 nm would improve. If we change the value of the ratio $k_3/(k_1+k_2)$ at 313 nm (and 322 nm and 330 nm) so that it is smaller than the value at 277 nm, the calculated fractions of $^3CH_2$ are smaller and agree better with the measured $^3CH_2$%-O_2 at those three wavelengths. Thus, our results can be interpreted as indicating a wavelength dependence for $k_3/(k_1+k_2)$, and since k_1 and k_2 probably do not depend on the wavelength used to produce the $^1CH_2$, the intersystem crossing rate, k_3, must depend on the wavelength. This is shown in column 2 of Table 4-II. However, both Cox and Preston[6] and Eder and Carr[8] claim that according to their results there is no energy dependence in the k_{isc}/k_{sprod} ratio (the ratio of the intersystem crossing rate in singlet methylene compared to the rate of reaction to form products, e.g., k_1+k_2 or k_{16}). As will be discussed later in more detail, it is not very surprising that neither of these workers found a measurable energy dependence of the rate of intersystem crossing; this trend is too small to have been seen in the type of data obtained from their experiments.

Reproduced with permission of the copyright owner. Further reproduction prohibited without permission.

A wavelength dependence of k_{isc}/k_{sprod} would not be unexpected. According to the mechanism described above for the intersystem crossing of $CH_2(^1A_1)$, the function of the collision partner is to provide a brief coupling of the vibronic energy levels which allow a crossing of methylene from a vibronic energy level of the $^1A_1$ state to a vibronic level in the $^3B_1$ state which is almost equal in energy; the small difference in energy is converted to translational and rotational modes in the $^3B_1$ state. Combinations of the three normal vibrations in methylene result in smaller energy spacings between the higher vibrational states than between the lower vibrational states. Thus, the more vibrational energy $CH_2(^1A_1)$ has, the closer together its vibronic energy levels will be, or in other words, the greater the density of states. Because the spacing between vibrational levels within the $CH_2(^1A_1)$ manifold of states is smaller at higher vibronic energies, there is a greater chance that the vibronic energy levels of both the $^1A_1$ and $^3B_1$ states will be closer than a specified energy difference before a collision. If the energy levels are very nearly equal, the coupling provided by the collision will be more effective, i.e., less of the energy will need to be converted to the translational and rotational modes, and so, the rate of intersystem crossing will be larger.

Reproduced with permission of the copyright owner. Further reproduction prohibited without permission.

If the ratio of $k_{isc}(M)/k_{sprod}$ depends on the internal energy of the methylene, an obvious question is: why does there appear to be such a good correlation between the $k_{isc}(M)/k_{sprod}$ ratio determined by our work with isobutane and ketene at 277 nm, and Ho and Noyes's[11] work with propane and ketene at 270 nm, and Bell's[9] work with propane and diazomethane (and various inert gases) at 405 nm and the polarizability of the gases as shown in figure 4-3? The photolysis of ketene at 277 nm results in 25 kcal/mole of energy in excess of the decomposition energy of CH_2CO which must be distributed between the CH_2 and CO as vibrational, rotational, and translational energy. The photolysis of diazomethane at 405 nm results in 48 kcal/mole of energy in excess of the decomposition energy of CH_2N_2 which must be distributed between the CH_2 and N_2. Exactly how this energy is distributed in both ketene and diazomethane is not known. However, unimolecular studies of methylcyclopropane isomerization produced by the reaction of $^1CH_2$ and propene have indicated that there is only a small difference between the lifetimes of methylcyclopropane in the diazomethane system at 436 nm and in the ketene system at 320 nm.[34]

If we assume that 70% of the energy available from the photolysis of ketene goes into the $^1CH_2$,[35] in order for the energies of

---

34. Dorer, F. H. and Rabinovitch, B. S., J. Phys. Chem. 69, 1952, 1964, 1973 (1965).

35. Based on our experiments with ketene and cyclopropane, see Chapter 5.

Reproduced with permission of the copyright owner. Further reproduction prohibited without permission.

$^1CH_2$ from diazomethane photolyzed at 436 nm and $^1CH_2$ from ketene at 320 nm to be approximately equal, we must assume that only 20% of the photolysis energy from the diazomethane goes into the $^1CH_2$. If the fraction of energy does not change with wavelength, $^1CH_2$ produced from ketene at 277 nm has almost 9 kcal/mole more energy than $^1CH_2$ produced from diazomethane produced at 405 nm. However, these calculations apply to the addition of $^1CH_2$ to the C=C double bond in propane which occurs approximately 10 times faster than the insertion of $^1CH_2$ into a C-H bond.[34] By the time $^1CH_2$ reacts with isobutane, it has undergone ten more collisions than it would have if it were reacting with a C=C double bond and so will be more vibrationally relaxed. Thus, the actual difference between $^1CH_2$ produced in a ketene-alkane system at 277 nm and $^1CH_2$ produced in a diazomethane system is less than 9 kcal/mole, and the agreement between our results with ketene at 277 nm, Ho and Noyes's[11] results with ketene at 270 nm, and Bell's[9] results with diazomethane at 405 nm does not appear to be too fortuitous.

A Experimental Results of Other Workers

Eder and Carr[8] studied the photolysis of a ketene-propane mixture in the presence of various inert gases at 260 nm, 313 nm, and 350 nm and claimed to have found no trend in the $k_{isc}(M)/k_{sprod}$ ratio with photolyzing wavelength. At the longer wavelengths, 330 nm-366 nm, a wavelength dependence is not easy to observe since

Reproduced with permission of the copyright owner. Further reproduction prohibited without permission.

most of the $^3CH_2$ is formed from the ketene via the $^3A_2$ state of ketene, and only a small fraction of the $^3CH_2$ is formed from the $^1CH_2$. There is considerable scatter in Eder and Carr's results which would have hidden a difference between the $k_{isc}(M)/k_{sprod}$ ratio at 313 nm and 260 nm if the difference were not large as expected from our data. (The value of the $k_{isc}(M)/k_{sprod}$ ratio in some of Eder and Carr's experiments varied by at least 50%.)

Cox and Preston[6] studied the photolysis of ketene in the presence of various inert gases at 249 nm and 280 nm and found no wavelength dependence in the $k_{isc}(M)/k_{sprod}$ ratio. They only looked at the change in the ratio when two gases were added, Xe and N_2. Only two experiments were done at 280 nm in which Xe was added to the ketene-oxygen misture and two in which Xe was added to the ketene-carbon monoxide mixture. The least-squares slope of a plot of the reciprocal of the quantum yield of C_2H_4 against the ratio of the concentrations of diluent gas to ketene determined the value of $k_{isc}(M)/k_{sprod}$. The error which Cox and Preston report is 40% of the value of the slope for the Xe-O_2 experiments (although it is smaller for other experiments). Thus, any dependence less than 40% could not have been seen. Furthermore, nitrogen reacts with $^1CH_2$ to form CH_2N_2[36] and since their experiments measured the total removal of $^1CH_2$ by N_2, if the

---

36. Shilov, A. E., Shteinman, A. A., and Tjabin, M. B., Tet. Letters 39, 4177 (1968).

Reproduced with permission of the copyright owner. Further reproduction prohibited without permission.

associated rate constant is comparable to that for the intersystem crossing reaction, any trend of the intersystem crossing reaction with wavelength could easily be masked by the reaction to form CH_2N_2.

Koob, et al.[37] used an entirely different source of methylene, the vacuum ultra-violet photolysis of cyclopropane and propane. They claimed to find no wavelength dependence in the rate of the intersystem crossing reaction. However, less is known about the decomposition of these molecules and a comparison between their systems and the ketene system may not be valid because the distribution of energy in these larger molecules is even less well known than in the simpler ketene or diazomethane molecules.

B Summary of Arguments for Energy Dependence in the Rate of Intersystem Crossing

Although the ratio of the intersystem crossing rate to the reaction rate has been determined in this work at only a few wavelengths, our experiments suggest that there may be an energy dependence in this ratio. The largest change in the intersystem crossing rate relative to the value at 277 nm occurs when 214 nm is

37. Dhingra, A. K. and Koob, R. D., J. Phys. Chem. 74, 4490 (1970); Dhingra, A. K., Vorachek, J. H., and Koob, R. D., Chem. Phys. Letters 9, 17 (1971); Koob, R. D., J. Chem. Phys. 73, 3068 (1969).

Reproduced with permission of the copyright owner. Further reproduction prohibited without permission.

used, but we are reluctant to give much weight to the value of the $k_3/(k_1+k_2)$ ratio at this wavelength for reasons to be discussed in the next section. Experiments by other workers have indicated that the intersystem crossing is not a function of the energy of the $^1CH_2$, however, as discussed above, their data are such that an absence of an energy dependence can not be proven. The theory of bimolecular intersystem crossing can explain an increase in the rate of crossing with an increase in the energy of the $^1CH_2$, and so, all that really can be said is that an energy dependence in the intersystem crossing rate for methylene cannot be very large if it exists, but that experiments have not shown its absence. A determination of whether or not there is such a dependence must wait for more accurate experiments, ideally in a less complicated system than ours.

VII The Photolysis of Ketene at 214 nm

The results of our experiments at 214 nm have been referred to but, so far, they have not been discussed in any detail. As shown in Table 3-III and figure 3-1, except for the experiments at 214 nm, as the photolyzing energy increases, both the measured percent of $^3CH_2$, $^3CH_2\%-O_2$, and the neopentane to isopentane ratio decrease. The $^3CH_2\%-O_2$ and the ratio of neopentane to isopentane are both larger at 214 nm than expected from the trends in both at the longer wavelengths. The quantum yield of $^1CH_2$, ϕ_s, as determined from the

Reproduced with permission of the copyright owner. Further reproduction prohibited without permission.

CO experiments (see Table 4-VI) approaches 1.0 as the photolyzing energy increases. At 214 nm, $\phi_s = 1.0$ as anticipated from this trend with photolyzing wavelength. If the experiments with O_2 have correctly measured $^3CH_2$ as 48% of the total methylene and if $\phi_s = 1.0$, this must mean that at 214 nm the ratio of $k_3/(k_1+k_2)$ is almost twice as large as at 277 nm or 313 nm (see Table 4-IV). But if the rate of intersystem crossing from $^1CH_2$ were twice as large at 214 nm, then the pentane yields in the presence of large concentrations of CO should be smaller than at 277 nm since the amount of $^1CH_2$ reacting with isobutane would be smaller. As seen in Table 3-I and figures 3-3, 3-4, and 3-5, this is not the case; the pentane yields are almost the same at 214 nm and 277 nm. Thus, since an increase in the rate of intersystem crossing cannot explain these results, an examination of the difference between the absorption spectrum of ketene in this region and at other wavelengths may give a clue to the explanation.

As described earlier (pages 117-121), the absorption of radiation at 214 nm excites ketene from the $^1A_1$ ground state to the $^1A_1$ second excited singlet state. A priori, ketene in the $^1A_1$ excited state would be expected to dissociate to either $CH_2(^1A_1)$ and $CO(^1\Sigma)$ or $CH_2(^1B_1)$ and $CO(^1\Sigma)$. At 214 nm, 56 kcal/mole of energy (the energy in excess of the amount needed to decompose the ketene) is available to the which may be distributed between the two products, CH_2 and CO, differently when the $^1A_1$

Reproduced with permission of the copyright owner. Further reproduction prohibited without permission.

state dissociates than when the $^1A_2$ (the first excited singlet) state of ketene dissociates. As can be seen from figure 4-2b, this is enough energy to reach the $^1B_1$ state (the second excited singlet state) of methylene even if CO also gets some of the energy (the vibrational frequency of CO is 2174 cm^{-1}, or 6.2 kcal/mole). The $^1B_1$ state of methylene has almost the same configuration as the $^3B_1$ state (Table 1-I). Although $CH_2(^1B_1)$ is a singlet, unlike $CH_2(^1A_1)$, its electrons are not paired. Thus, if $CH_2(^1B_1)$ is formed, some of its reactions might be similar to the reactions of $CH_2(^3B_1)$. The likely presence of $CH_2(^1B_1)$ and its reactions with O_2, CO, and C-H bonds can explain the anomalies in the results of the photolysis of ketene at 214 nm.

A The Reaction of $CH_2(^1B_1)$ with Isobutane

As we have mentioned in the introduction, Chapter 1, the reactions of $CH_2(^1B_1)$ have not been studied experimentally. Hoffmann's calculations of the reaction paths of methylenes[38] indicate that the concerted reaction of the $^1A_1$ state is based on the availability of the unfilled p orbital rather than on the singlet character of the methylene. The $^1B_1$ state does not have an unfilled p orbital and so cannot react via the same pathway as the $^1A_1$ state does. Since the spatial arrangement of the electrons seems

38. Hoffmann, R., J. Am. Chem. Soc. 90, 1475 (1968); Dobson, R. C., Hayes, D. M., and Hoffmann, R., ibid 93, 6188 (1971).

Reproduced with permission of the copyright owner. Further reproduction prohibited without permission.

to be the important factor in this type of reaction, it is more likely that the $^1B_1$ state reacts similar to the $^3B_1$ state than to the $^1A_1$ state. Thus, $CH_2(^1B_1)$ would be expected to abstract a H atom from the C-H bonds and thus must have the same relative preference for the tertiary C-H bonds as $CH_2(^3B_1)$ does. Once we have made this assumption, we must conclude from the oxygen and carbon monoxide experimental results that the $CH_2(^1B_1)$ reaction with isobutane has been eliminated or else the neopentane to isopentane ratio would not have been 0.14-0.15 in both O_2 and CO.

B The Reaction of $CH_2(^1B_1)$ with O_2

If the reaction of $CH_2(^3B_1)$ is very fast compared to the reaction of $CH_2(^1A_1)$ with O_2 because of the presence of unpaired electrons in $CH_2(^3B_1)$ and not because of its triplet nature, the reaction of O_2 with $CH_2(^1B_1)$ should also be faster than with $CH_2(^1A_1)$. This would not be unexpected since the reactions of O_2 with CH_3 and other radicals with an unpaired electron are fast.[39] If the reaction of O_2 with $CH_2(^1B_1)$ is fast, then the percent of $^3CH_2$ measured by the O_2 experiments could actually be a measure of both $CH_2(^1B_1)$ and $CH_2(^3B_1)$.[40]

---

39. See, for example, van den Bergh, H. E. and Callear, A. B., Trans. Faraday Soc. 67, 2017 (1971).

40. Of course, one must remember that in these experiments only a few percent of O_2 is present so that the $CH_2(^3B_1)$ and $CH_2(^1B_1)$ (continued)

Reproduced with permission of the copyright owner. Further reproduction prohibited without permission.

Unfortunately, neither in this work at 214 nm nor in that of Kistiakowsky and Walter[33] was the concentration of oxygen systematically varied. Thus, there is no unequivocal experimental evidence on which an estimate of the extent of the reaction of O_2 with the methylene produced at 214 nm can be made. We will come back to this point a little later in the discussion, but for now, because of the assumption already made about the reaction of $CH_2(^1B_1)$ with isobutane, we must assume that the reaction of O_2 with $CH_2(^1B_1)$ is relatively fast.

C The Reaction of $CH_2(^1B_1)$ with CO

The reaction of $CH_2(^3B_1)$ with $CO(^1\Sigma)$ is faster than with isobutane. This has been attributed to the formation of the fairly stable $^3A_2$ state of ketene thus removing $CH_2(^3B_1)$ from the reaction system.[12,19] The reaction of $CH_2(^1B_1)$ with $CO(^1\Sigma)$ is not expected to be faster than the reaction with isobutane since $CH_2(^1B_1)$ and $CO(^1\Sigma)$ undoubtedly correlates with an unbound state of ketene as $CH_2(^1A_1)$ does. (The bands in the 180 nm-200 nm region are diffuse which suggests strong predissociation of the excited $^1A_1$ state.) If the $CH_2(^1B_1)$ does not react faster with CO than with isobutane,

---

40.(cont'd,) react with O_2 much faster than with isobutane and the $CH_2(^1A_1)$ reacts with isobutane faster than with O_2. Thus, O_2 removes $CH_2(^3B_1)$ and $CH_2(^1B_1)$ but only a very small percent of $CH_2(^1A_1)$. See, also, page 110.

Reproduced with permission of the copyright owner. Further reproduction prohibited without permission.

the ϕ_s measured by the CO experiments might be larger than that expected from the measured $^3CH_2$%-O_2, (if k_1, k_2, and k_{13} are not very different with $CH_2(^1B_1)$ than with $CH_2(^1A_1)$) because the ϕ_s would be a measure of both $CH_2(^1A_1)$ and $CH_2(^1B_1)$, i.e., of all the methylene present after the $^3B_1$ state has been removed by reaction with CO. However, if the $CH_2(^1B_1)$ were not removed by reaction with CO, the neopentane to isopentane ratio in the presence of more than 60 Torr of CO would be larger than 0.14-0.15 because the $CH_2(^1B_1)$ is expected to react with C-H bonds as $CH_2(^3B_1)$ does. This was not found to be true experimentally.

The addition of at least 60 Torr of CO more than doubles the total pressure of the reaction mixture compared to the standard mixture of 50 Torr of isobutane, 5 Torr of ketene, and 0.5 Torr of propane. This increase in pressure compared to the experiments without CO may cause methylene in the $^1B_1$ state to relax to the $^1A_1$ state because of the increase in the number of collisions $CH_2(^1B_1)$ experiences before it can react with isobutane. An internal conversion from $CH_2(^1B_1)$ to $CH_2(^1A_1)$ is expected to be quite fast since there is no change in multiplicity. Thus, the addition of enough CO to remove any $CH_2(^3B_1)$ probably also converts most of the $CH_2(^1B_1)$ to the lower energy $CH_2(^1A_1)$. Only $CH_2(^1A_1)$ would then be present to react with the isobutane. If ϕ_s is 1.0 under these conditions, the most likely explanation is that only CH_2 in the $^1B_1$ state is formed by the photodecomposition

Reproduced with permission of the copyright owner. Further reproduction prohibited without permission.

TABLE 4-III

A Summary of CH_2 Reactions

Rate of Reaction Compared to the Rate of CH_2 + alkane	State of CH_2 $^1A_1$	$^3B_1$	$^1B_1$
$CH_2 + O_2$	slow	fast	fast
CH_2 + ketene	slow	fast	slow[a]
CH_2 + CO	slow	fast	slow
$^1B_1 \longrightarrow {}^1A_1$, internal conversion by collisions with alkane	----	----	same

a) Based on the data of Kistiakowsky and Walter, reference 33.

Reproduced with permission of the copyright owner. Further reproduction prohibited without permission.

of ketene at 214 nm and it has been converted by collisions with CO and isobutane to $CH_2(^1A_1)$.

Thus, starting with the assumption that $CH_2(^1B_1)$ reacts with isobutane to abstract H from C-H bonds, in the same way that $CH_2(^3B_1)$ does, our experimental results are consistent with the following description of the photolysis of ketene at 214 nm. The photodecomposition of ketene at 214 nm produces only $CH_2(^1B_1)$ and $CO(^1\Sigma)$. The $CH_2(^1B_1)$, with the aid of collisons, can be converted into $CH_2(^1A_1)$ and $CH_2(^3B_1)$. The internal conversion (via collisions) is undoubtedly the faster reaction since there is no change in multiplicity and since a $A_1 \longleftrightarrow B_1$ transition is allowed by the C_{2v} symmetry of methylene. In the presence of more than 60 Torr of CO (a total pressure of more than 115 Torr), the reaction of $CH_2(^1B_1)$ with isobutane has been eliminated because the $CH_2(^1B_1)$ has been converted to $CH_2(^1A_1)$. In the presence of O_2, the reactions of $CH_2(^1B_1)$, and of any $CH_2(^3B_1)$ that has been formed from the intersystem crossings of CH_2 either in the $^1A_1$ state or the $^1B_1$ states with isobutane have been supressed because of the relatively fast reaction of $CH_2(^1B_1)$, and $CH_2(^3B_1)$, with O_2.

D Other Possibilities

Suppose the reaction of $CH_2(^1B_1)$ with isobutane did not involve the abstraction of H from C-H bonds, but that $CH_2(^1B_1)$ reacted

Reproduced with permission of the copyright owner. Further reproduction prohibited without permission.

somewhat like $CH_2(^1A_1)$, i.e., concertedly and with no preference for either type of C-H bond. In this case, the reaction of O_2 with $CH_2(^1B_1)$ must be slower than the reaction with isobutane. If it were faster, the neopentane to isopentane ratio would not agree with the percent of $^3CH_2$ measured by the oxygen experiments. (See figure 3-2.) The oxygen experiments would then imply that the rate of intersystem crossing from methylene in the $^1B_1$ state to the $^3B_1$ state must be about twice as fast as from the $^1A_1$ state. (See Table 4-II.) The $^1B_1 \longrightarrow {}^3B_1$ crossing is expected to be faster than that of $^1A_1 \longrightarrow {}^3B_1$ because of the vibrational spacing arguments described previously(page 132). The reaction of CO with both $CH_2(^1B_1)$ and $CH_2(^1A_1)$ must again be slower than that with isobutane. Since the pentane yields in the CO experiments are almost equal at 214 nm and 277 nm, if ϕ_s is still equal to 1.0, then the rate of reaction of $CH_2(^1B_1)$ with CO must be even slower than the reaction of $CH_2(^1A_1)$ with CO. (See equations 3-3 and 3-4.) However, if the intersystem crossing rate from the $^1B_1$ state is relatively fast, it is unlikely that the internal conversion, via collisions, to the $^1A_1$ is not even faster. Thus, it would be hard to believe that in the concentrations of CO used any significant amounts of $CH_2(^1B_1)$ remain. The presence of $CH_2(^1A_1)$ that is highly vibrationally excited cannot be completely ruled out as contributing to a larger yield of pentanes in the CO experiments, but in the presence of large concentrations of CO, this does not seem that likely. (The

Reproduced with permission of the copyright owner. Further reproduction prohibited without permission.

point here being that the efficiency of the reaction of $CH_2(^1A_1)$ with CO is small enough so that collisions with CO will either take away most of the vibrational energy of the $CH_2(^1A_1)$ or else convert it to $CH_2(^3B_1)$.)

A third possibility is that $CH_2(^1A_1)$ as well as $CH_2(^1B_1)$ is produced at 214 nm. This is not impossible since the unbound states correlating to $CH_2(^1B_1)$ and $CH_2(^1A_1)$ probably both cross the $^1A_1$ bound state (see figure 4-2a). However, the experimental evidence to date does not warrant this more sophisticated picture.

It is apparent that further experiments with O_2 and also with different gases, such as Xe, Ar, and CF_4, would be very useful in describing the ketene photolysis at 214 nm.

Reproduced with permission of the copyright owner. Further reproduction prohibited without permission.

VIII Summary of Conclusions

The results of our experiments with the photolysis of a ketene-isobutane mixture at several wavelengths can only be explained by assuming that there are three different electronic species of methylene which can be formed. At wavelengths longer than 320 nm, most of the ground state of methylene, $CH_2(^3B_1)$, results from the decomposition of the $^3A_2$ state of ketene. The $^3A_2$ state of ketene is formed from the absorption, by the $^1A_1$ ground state, of radiation longer than 320 nm. At wavelengths shorter than 320 nm, most of the $CH_2(^3B_1)$ is formed by the collision-induced intersystem crossing of methylene in the first excited singlet state, $CH_2(^1A_1)$. This intersystem crossing rate may depend on the energy of the $CH_2(^1A_1)$. In the region around 277 nm (250 nm-290 nm), only $CH_2(^1A_1)$ is formed from the photodecomposition of ketene; any $CH_2(^3B_1)$ present is a result of the intersystem crossing from $CH_2(^1A_1)$. At the shortest wavelength studied, 214 nm, the photolysis of ketene produces methylene in the second excited state, $CH_2(^1B_1)$. The $CH_2(^1B_1)$ behaves as the $CH_2(^3B_1)$ does in its reactions with O_2 and alkanes. Presumably this is because the spatial distribution of the electrons is the same in both B_1 states.

The technique of using CO to remove the $CH_2(^3B_1)$ can be used to measure the quantum yield of $CH_2(^1A_1)$, ϕ_s, at wavelengths longer than about 250 nm, but it cannot be used to measure ϕ_s in the 214 nm

Reproduced with permission of the copyright owner. Further reproduction prohibited without permission.

region where $CH_2(^1B_1)$ is produced because $CH_2(^1B_1)$ does not react as $CH_2(^3B_1)$ does with CO. The collision-induced internal conversion of $CH_2(^1B_1)$ to $CH_2(^1A_1)$ is faster than the collision-induced intersystem to $CH_2(^3B_1)$.

Reproduced with permission of the copyright owner. Further reproduction prohibited without permission.

5

Results and Discussion of the Cyclopropane Experiments

Results

$^1CH_2$ inserts into the C-H bonds of cyclopropane to form energy-rich methylcyclopropane. The fate of the excited methylcyclopropane is decided according to the following scheme.[1,2,3,4]

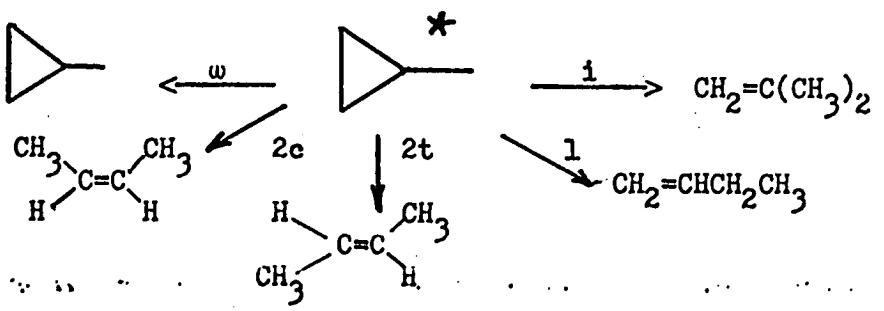

The overall rate of the decomposition of methylcyclopropane, k_a, is equal to the collision frequency, ω, multiplied by the ratio of the products from decomposition, D, to the products from collisional stabilization, S,

$$k_a = \omega \left(\frac{D}{S} \right) .$$

---

1. Butler, J. N. and Kistiakowsky, G. B., J. Am. Chem. Soc. 82, 759 (1960).

2. Setser, D. W. and Rabinovitch, B. S., ibid 86, 564 (1964).

3. Dorer, F. H. and Rabinovitch, B. S., J. Phys. Chem. 69, 1952, 1964, 1973 (1965).

4. Chesick, J. P., J. Am. Chem. Soc. 82, 3277 (1960).

Reproduced with permission of the copyright owner. Further reproduction prohibited without permission.

The sum of the decomposition products is the sum isobutene + butene-1 + cis-butene-2 + trans-butene-2 and, of course, methylcyclopropane is the product of collisional stabilization. The reciprocal of k_a is the lifetime of the excited methylcyclopropane. The rate constant for the decomposition of excited methylcyclopropane is the slope of the plot of D/S versus ω^{-1} or 1/(total pressure) since the frequency of the gas kinetic collisions is proportional to the total pressure of the gas.

The insertion of $^1CH_2$ into cyclopropane was studied at four wavelengths, 214 nm, 277 nm, 313 nm, and 330 nm. Oxygen (5% of the total pressure) was added to the photolysis mixture to ensure that both $CH_2(^3B_1)$ and $CH_2(^1B_1)$, $^3CH_2$, were substantially eliminated from the reaction system. Plots of D/S versus 1/total pressure were made for each wavelength and are shown in figure 5-1. The k_a's calculated from these plots for the cyclopropane-ketene mixtures are presented in Table 5-V along with the k_a determined by Dorer and Rabinovitch[3] from their propylene-ketene system at 320 nm. As expected, the k_a's increase as the photolyzing energy increases. The inversion Butler and Kistiakowsky observed in their experiments, in which $^3CH_2$ was not eliminated, is not present in this series of experiments.

Reproduced with permission of the copyright owner. Further reproduction prohibited without permission.

The butene-1 and isobutene were not resolved on the chromatograph and thus a detailed study of the isomer distribution could not be made. The problems in resolution have already been described in the chapter on apparatus and techniques. Other workers have not shown any startling trends in the isomer distribution with changes in the energy of the excited methylcyclopropane over the pressure region we studied, and so none were expected here. The ratio of the yields of trans-butene-2 to cis-butene-2 and the ratio of the sum of the yields of the butenes-2 to the sum of the yields of the isobutene and butene-1 yields were measured. These ratios are included among the results listed in Table 5-I. As a general trend, both ratios decrease slightly as the total pressure of the system increases. Butler and Kistiakowsky[1] observed a similar trend.

When the total pressure was large, the methylcyclopropane was the major product and the methylcyclopropane peak was the dominant peak. Cis- and trans-butene-2 were the last of the products to be eluted from the column and thus had the broadest peaks. When the pressure was large, all of the butene peaks were small, but the butenes-2 peaks were the broadest and therefore the hardest to measure accurately. The smaller value of the ratio of butenes-2 to the sum of isobutene and butene-1 at larger pressures is proabably due to the increase in the error of the butene-2 peak area measurements.

Reproduced with permission of the copyright owner. Further reproduction prohibited without permission.

Figure 5-1

$$\frac{\text{Butenes}}{\triangleright\text{-CH}_3} \text{ vs. } \frac{100}{\text{P(mm of Hg)}}$$

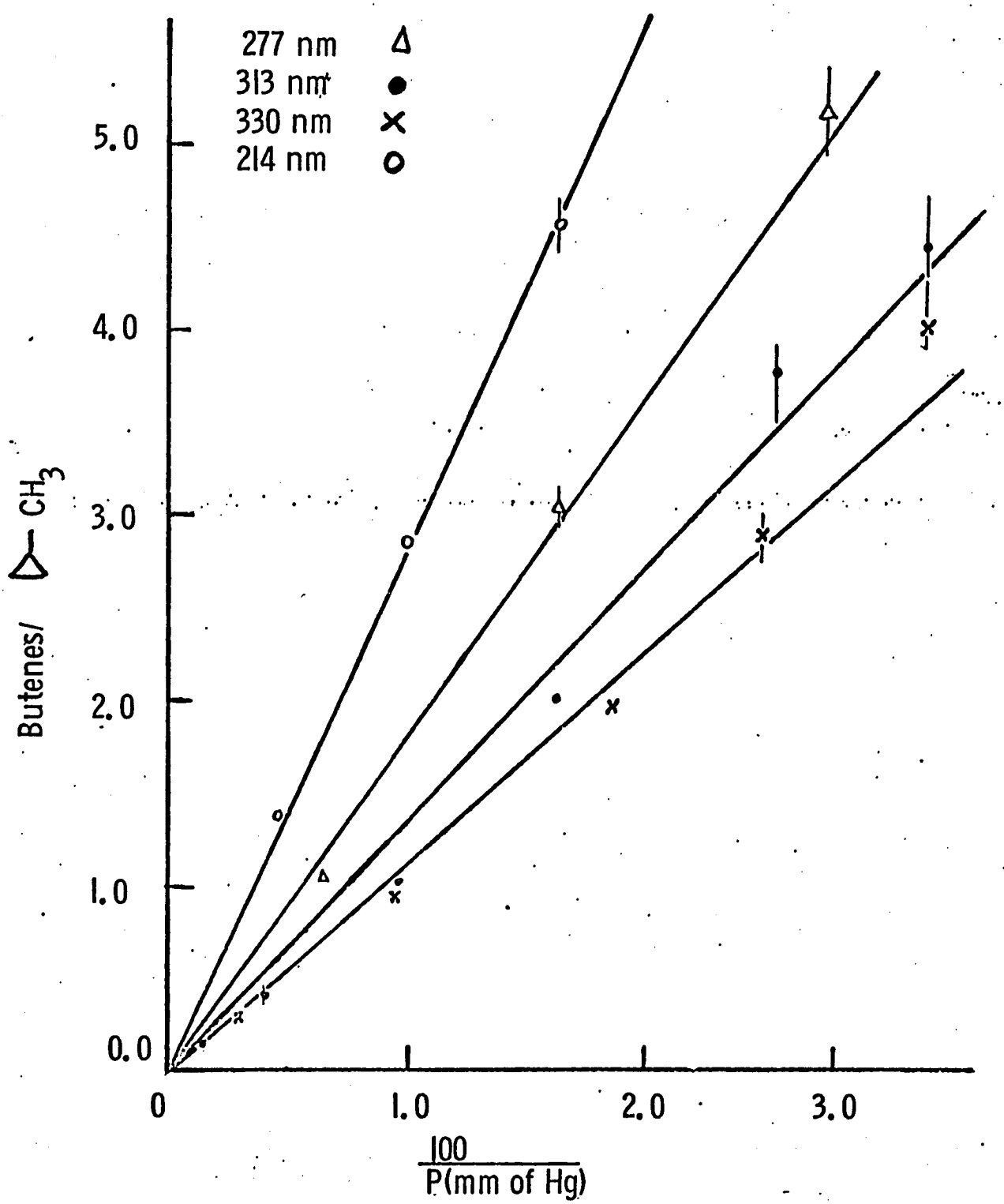

Reproduced with permission of the copyright owner. Further reproduction prohibited without permission.

TABLE 5-I

Results of the Ketene-Cyclopropane Photolyses

Wavelength	$\frac{\Sigma \text{ Butenes}}{\text{MCP}}$*	$\frac{100}{\text{Pressure (Torr)}}$	$\frac{\text{Butenes-2}}{\text{Isobutene + butene-1}}$	$\frac{\text{trans}}{\text{cis}}$**
214 nm	2.84	1.00	1.19	1.13
	4.52	1.65	1.20	1.15
	1.38	0.44_5	1.04	0.89
277 nm	3.03	1.65	1.09	0.96
	1.04	0.64_0	1.00	0.95
	5.15	2.78	1.23	1.03
313 nm	4.38	3.19	1.19	1.10
	3.75	2.57	1.09	1.12
	2.00	1.63	0.97	1.03
	1.02	0.95_7	0.84	0.95
	0.39_4	0.40_1	0.75	0.88
	0.13_4	0.14_5	0.75	0.58
330 nm	3.96	3.19	1.09	1.05
	1.92	1.87	0.89	1.06
	0.92_7	0.94_1	0.87	0.76
	0.27_6	0.30_3	0.79	0.75

* MCP is methylcyclopropane. ** the ratio of trans-butene-2 to cis-butene-2.

Reproduced with permission of the copyright owner. Further reproduction prohibited without permission.

The decrease in the ratio of trans-butene-2 to cis-butene-2 as the pressure increases results from a small amount of the cis-butene-2 isomerizing to trans-butene-2 at low pressures. This is discussed in greater detail in a later section.

An Introduction to Previous Work on the Decomposition of Methylcyclopropane

Dorer and Rabinovitch[3] have studied the isomerization of several cyclopropanes including methylcyclopropane. They formed the methylcyclopropane by reacting propylene with methylene which was produced by the photolysis of ketene at 320 nm or the photolysis of diazomthane at 435 nm. They were unable to resolve the iso-butene products, and so estimated the yield from Butler and Kistiakowsky's[1] data. Dorer and Rabinovitch[3](DR) constructed a set of models for the isomerization of methylcyclopropane which they claim fit Setser and Rabinovitch's data for the thermal isomerization of 1,2-dideutero-3-methylcyclopropane.[2] DR used these models to fit the overall isomerization rate of methylcyclopropane, k_a, for the addition of $^1CH_2$ to propylene. These models were used for $^1CH_2$ produced from diazomethane and from ketene. The construction of these models was based on the results of Setser and Rabinovitch's (SR) work with CH_2 additions to ethylene and butene-2.[5]

---

5. Setser, D. W. and Rabinovitch, B. S., Can. J. Chem. 40, 1425 (1962).

Reproduced with permission of the copyright owner. Further reproduction prohibited without permission.

Setser and Rabinovitch[5] studied the addition of methylene to ethylene. The methylene was generated by the thermal decomposition of diazomethane in the range from 225°C to 450°C and the photolyses of diazomethane at 456 nm and ketene at 320 nm. They constructed their cyclopropane models to fit the thermal isomerization results of cyclopropane[6] and then used these models to determine an average energy, $< E >$, for the excited complexes produced from each methylene source. The $< E >$'s obtained by this method fit the thermochemical values, but several of the heats of formation they used are now known to be wrong. DR used the $< E >$ calculated by SR for cyclopropane, i. e., an $< E >$ of about 110 kcal/mole, but corrected this $< E >$ to account for the extra methyl group in methylcyclopropane. DR constructed their models so that their experimental rate constants for CH_2 generated from diazomethane corresponded to an $< E >$ of 108 kcal/mole and also gave a "good fit" to the thermal isomerization results of Setser and Rabinovitch[2].

The rate constants, k_a, which we determined for the ketene and cyclopropane system are all larger than the rate constants determined by DR for diazomethane and cyclopropane ($k_a = 9.7 \times 10^8 sec^{-1}$).

---

6. Falconer, W. E., Hunter, T. E., and Trotman-Dickenson, A. F., J. Chem. Soc. 1962, 609; Pritchard, H. O., Sowden, R. G., and Trotman-Dickenson, A. F., Proc. Roy. Soc. A217, 563 (1953); Schlag, E. W. and Rabinovitch, B. S., J. Am. Chem. Soc. 81, 5996 (1960).

Reproduced with permission of the copyright owner. Further reproduction prohibited without permission.

Therefore, the average energies, $< E >$'s, of our methylcyclopropane are expected to be larger than 108 kcal/mole. At this point, it is important to check the thermochemistry of our ketene-cyclopropane system to be sure that the $< E >$'s can be larger than 108 kcal/mole.

The insertion of CH_2 into the C-H bonds of cyclopropane to form methylcyclopropane is 99.2 kcal/mole exothermic when both reactants have no energy in excess of their thermal energy. The photolysis of ketene at 330 nm has 10.2 kcal/mole more energy than required to decompose ketene (76.4 kcal/mole). If all of this energy went into the methylene and if the methylene did not lose energy before reacting with cyclopropane, the $< E >$ for methylcyclopropane would be 109.4 kcal/mole; this is referred to as the $< E >_{max}$ at 330 nm. Thus for our smallest rate constant, $< E >$ cannot be larger than 109 kcal/mole. This is just larger than the 108 kcal/mole DR find for the $< E >$ of methylcyclopropane produced in their diazomethane-propylene system at 436 nm. The $< E >_{max}$ for each wavelength we have studied with our ketene-cyclopropane system is listed in Table 5-V along with the k_a measured at that wavelength. Also included in Table 5-V is the $< E >_{max}$ for the ketene-propylene system at 320 nm studied by DR, their experimental rate constant, k_a, and the k_a found by Chesick[4] at large pressures, k_∞, in his studies of the thermal isomerization of methylcyclopropane.

Reproduced with permission of the copyright owner. Further reproduction prohibited without permission.

When we first started these experiments, the newest heat of formation of ketene, -11.4± 0.4 kcal/mole, had not appeared in the literature,[7] and the $< E >_{max}$ for each wavelength was 4 kcal/mole smaller than listed in Table 5-IV. This meant that at the longest wavelength we used, 330 nm, and also for DR's photolysis of ketene and propylene at 320 nm, the $< E >$'s calculated with DR's published model were larger than $< E >_{max}$. In order to resolve this difficulty, we constructed a number of different models which were modifications of DR's models, and we also tried several new models. These models are described in Table 5-III. The results of the calculations for each model are presented in Table 5-IV. Table 5-II describes the frequencies in the methylcyclopropane molecule.

The model DR published, ignoring the methyl torsion of the methyl group attached to the ring, complex 3 in Table 5-II but with E_o= 61.4 kcal/mole, gives the following parameters:

1) at T = 298°K, log A = 14.34 and E_a= 62.1 kcal/mole,
   at T = 720.1°K, log A = 14.92, E_a= 63.4 kcal/mole and
   k_∞= 0.472 x 10^{-4} sec^{-1},
   at T = 763.8°K, log A = 14.97, E_a= 63.6 kcal/mole and
   k_∞= 5.98 x 10^{-4} sec^{-1},

---

7. Nuttal, R. L., Laufer, A. H., and Kilday, M. V., J. Chem. Thermodynamics 3, 167 (1971).

Reproduced with permission of the copyright owner. Further reproduction prohibited without permission.

and

2) the $< E >$'s for the ketene systems are 102.5 kcal/mole for propylene at 320 nm (DR's results) and 107.1, 108.0, 109.7, and 112.5 kcal/mole for cyclopropane at 330 nm, 313 nm, 277 nm, and 214 nm, respectively.

The Applicability of the Strong Collision Assumption

The RRKM theory (and most other unimolecular theories) assumes that each gas kinetic collison of the excited complex is strong enough to deactivate it. Any decomposition of the complex must occur, therefore, before the first collision. This strong collision assumption was used to calculate the lifetimes of the methylcyclopropane from the plot of the ratio of the yields, butenes/methylcyclopropane, versus the reciprocal of the pressure of the system. The decomposition rate constants are about 2×10^9 sec^{-1}. At 100 Torr, the collision frequency, ω, of methylcyclopropane in cyclopropane is 1.4×10^9 collisions/sec, which is of the same order of magnituded as k_a. DR's value of k_a is 0.72×10^9 sec^{-1} for their ketene-propylene system at 320 nm, which implies, in the most simplistic view, that at about 100 Torr, the methylcyclopropane will be hit twice before it decomposes.

Reproduced with permission of the copyright owner. Further reproduction prohibited without permission.

Other workers[8] have shown that in similar systems, i.e., where $< E >$ is about 100 kcal/mole, each collision deactivates the excited molecule or complex by at least 30 kcal/mole. The critical energy for methylcyclopropane isomerization is about 60 kcal/mole. Thus, it is possible that one collision will be sufficient to take away enough energy so that the resulting energy of the methylcyclopropane is less than 60 kcal/mole.[9] As the pressure increases to the point where there are one or more collisions during the lifetime of the excited complex, the average energy of the complex will decrease, and so, k_a will become smaller. Evidence for this effect is seen in the upward curvature in figure 5-1; the ratio of the yields of the butenes/methylcyclopropane is larger at small pressures.

An Estimate of the Rate of Reaction of $^1CH_2$ with Cyclopropane

There is a decided difference between the lifetimes of the methylcyclopropane produced at the different wavelengths used which must reflect the difference in energies carried into the methyl-

---

8. Kohlmaier, G. H. and Rabinovitch, B. S., J. Chem. Phys. 38, 1692, 1709 (1963); Setser, D. W., Rabinovitch, B. S., and Simons, J. W., ibid 40, 1751 (1964); Rynbrandt, J. D. and Rabinovitch, B. S., ibid 74, 1679 (1970); Rabinovitch, B. S. and Flowers, M. C., Quart. Rev. 18, 122 (1964).

9. Using model 7 of Tables 5-III and 5-IV, if 30 kcal/mole is subtracted from $< E >$ for 313 nm, the k_ε will decrease from 0.185×10^{10} sec^{-1} to 0.117×10^{7} sec^{-1}. Thus, after the complex loses 30 kcal/mole of energy, the k_ε of the complex will be so much smaller that it is even more likely to be hit again before decomposing. This is effectively a strong collision situation.

Reproduced with permission of the copyright owner. Further reproduction prohibited without permission.

TABLE 5-II

Frequency Assignments for Methylcyclopropane Ring Vibrations [a]

Frequency	Description	Representation for Cyclopropane (D_{3h})
ν_3, 1202 cm^{-1}	"breathing", ring	A_1'
ν_{10}, 1047 }	CH_2 bending deformations	E'
ν_{10}, 889 }	via C-C stretch	E'
ν_{11}, 804	ring deformation	E'
ν_4, 1111	CH_2 twisting	A_1''
ν_4, 911	CH_2 rocking	A_2''
ν_5, 983	CH_2 bending	A_2'
ν_{13}, 1016	CH_2 rocking	E''
ν_{14}, 810	CH_2 twisting	E''
ν_{14}, 756	CH_2 twisting	E''

The remaining vibrations were averaged and are

3015 (8)	CH stretches
1436 (6)	3 HCH methyl bends, 2 HCH ring bends, and 1 $HC(CH_3)$ bend
320 (2)	skeletal binding
0	methyl-ring torsion
1046 (2)	CCH methyl bends.

a. See Appendix II.

Reproduced with permission of the copyright owner. Further reproduction prohibited without permission.

Tables 5 - III and 5 - IV describe some of the models tried and the experimental parameters obtained using these models in the RRKM teory. Table 5-III lists the molecular frequencies,.the frequencies changed in the complex, and the E_o (the critical energy for isomerization). Table 5-IV is the result of the calculations and lists the average energy, $< E >$, of the complex produced at each wavelength, and the thermal rates predicted by these models. As described in the text, model 7 is the best fit.

Reproduced with permission of the copyright owner. Further reproduction prohibited without permission.

Reproduced with permission of the copyright owner. Further reproduction prohibited without permission.

TABLE 5-III MODELS

Model	Molecule	1	2	3	4	5
CH stretch	3015(8)	3015(7)	3015(7)	3015(7)	3015(5)*	3015(7)
ν_3	1202			1300	1300	1020
ν_{10}	1047	900	930	930	930	884
ν_{10}	889	500	575	640	640	747
ν_4	1111					790
ν_7	911					648
ν_5	983					700
ν_{13}	1016					723
ν_{14}	810					545
ν_{14}	756	600	600	670	670	538
E_o		62.5	62.5	62.5	62.5	62.5

*The molecule used in the calculations had 3015(6).

Reproduced with permission of the copyright owner. Further reproduction prohibited without permission.

TABLE 5-III MODELS (continued)

Model	6	7	8	9	10	11
CH stretch	3015(7)	3015(7)	3015(7)	3015(5)*	3015(3)**	3015(3)**
ν_3	868	1082	1082	1082	1082	1020
ν_{10}	755	884	884	884	884	884
ν_{10}	641	747	747	747	747	747
ν_{11}	418	570	570	570	570	570
ν_4	578	890	890	1000	1000	790
ν_7	475	730	730	820	820	648
ν_5	512	790	790	885	885	700
ν_{13}	530	815	815	914	914	723
ν_{14}	421	421	421	421	421	575
ν_{14}	393	393	393	393	393	538
E_o	62.5	62.5	61.2	62.5	62.5	62.5

** The molecule used in the calculations had 3015(4).

Reproduced with permission of the copyright owner. Further reproduction prohibited without permission.

TABLE 5-IV

Results of RRKM Calculations

Model		1	2	3	4	5	
	Photolysis* System						$\langle E \rangle_{max}$
	A	108.0	110.1	103.7	92.5	108	104.5
	B	113.4	116.1	108.0	100.0	115	109.3
$\langle E \rangle$	C	115.0	117.5	108.9	100.8	116	114.2
kcal/mole	D	117.8	120.0	110.6	102.8	120	126.0
	E	121.3	124.1	113.0	105.4	124	156.8
T= 298°K	$\log_{10} A$	14.49	14.41	14.33	14.34	14.53	
	$E_a - E_o$	0.8	0.8	0.7	0.7	0.9	
T= 720.1°K	$\log_{10} A$	15.12	14.98	14.92	14.91	15.00	
	$E_a - E_o$	2.2	2.0	2.0	2.0	1.8	
	$10^4 k_\infty$	0.314	0.259	0.230	0.229	0.312	
T= 763.8°K	$\log_{10} A$	15.15	15.01	14.95	14.95	15.00	
	$E_a - E_o$	2.3	2.1	2.1	2.1	1.8	
	$10^4 k_\infty$	4.17	3.43	3.01	3.01	4.08	

* Photolysis system, see Table 5-V.

Reproduced with permission of the copyright owner. Further reproduction prohibited without permission.

TABLE 5-IV (continued)

Results of RRKM Calculations

Model		6	7	8	9	10	11	
< E > kcal/mole	Photolysis System A	88.9	99.6		102.8	80.5	84.4	
	B	91.8	104.2		108.0	85.6	90.9	
	C	93.4	105.1		108.9	86.6	92.0	
	D	95.1	107.2		114.2	88.5	94.9	
	E	97.4	110.5		115.0	91.6	98.9	
T= 298°K	$\text{Log}_{10}A$	15.23	14.75	14.75	14.66	14.66	14.53	
	$E_a - E_o$	1.5	1.1	1.1	1.0	1.0	0.9	
T= 720.1°K	$\text{Log}_{10}A$	16.60	15.68	15.68	15.54	15.45	15.00	
	$E_a - E_o$	4.4	3.1	3.1	2.7	2.6	1.8	
	$10^4\ k_\infty$	2.00	0.621	1.53	0.479	0.434	0.313	0.535**
T= 763.8°K	$\text{Log}_{10}A$	16.66	15.73	15.73	15.49	15.49	15.01	
	$E_a - E_o$	4.6	3.2	3.2	2.8	2.8	1.8	
	$10^4\ k_\infty$	29.1	8.56	20.	6.45	5.91	4.08	6.79**

**Chesick's data, reference 4.

N.B. The thermal activation calculations assumed a collision diameter of 5.9Å.

Reproduced with permission of the copyright owner. Further reproduction prohibited without permission.

TABLE 5-V

Ketene Photolysis System	$\langle E \rangle_{max}$	$\langle E \rangle$ from Model 7 (Tables 5-III and 5-IV)	k_a*
A 320 nm and propylene	104.5 kcal/mole	99.6 ± 1.4 kcal/mole	0.72×10^9 sec^{-1}**
B 330 nm and cyclopropane	109.4	104.2 ± 0.7	$1.59 \times 10^9 \pm 12\%$
C 313 nm and cyclopropane	114.2	105.1 ± 0.8	$1.85 \times 10^9 \pm 12\%$
D 277 nm and cyclopropane	126.0	107.2 ± 0.1	$2.55 \times 10^9 \pm 3\%$
E 214 nm and cyclopropane	156.8	110.5 ± 0.6	$3.92 \times 10^9 \pm 8\%$

Chesick's data: $E_a = 65.0$ kcal/mole

$k_\infty = 0.535 \times 10^{-4}$ at 720.1°K

$k_\infty = 6.79 \times 10^{-4}$ at 763.8°K

*k_a was determined from $\omega(\frac{D}{S}) = k_a$. $\sigma = 5.4$Å was used in calculating ω.

**k_a was determined by Dorer and Rabinovitch. Although the error bounds are not given for the overall decomposition rate constant, the error for the decomposition to the individual isomers is given as ±25%.

cyclopropane by the $^1CH_2$. At lower pressures (pressures less than 100 Torr), there is still a difference in the lifetimes even when the difference in photolyzing energy is only 5 kcal/mole and the excess energy available to the CH_2 is 5 and 10 kcal/mole, at 330 nm and 313 nm. If $^1CH_2$ collided with the cyclopropane without reacting, at least some of its energy would be carried off by the cyclopropane which is relatively efficient in transferring vibrational energy. CH_2 has fewer vibrational degrees of freedom than methylcyclopropane and so collisions between CH_2 and cyclopropane are likely to be less efficient in transferring vibrational energy than collisions between methylcyclopropane and cyclopropane. Even though the collisions of methylene will be less efficient than those of methylcyclopropane, if the collisions of methylcyclopropane transfer 30 kcal/mole to the cyclopropane, it is hard to imagine that the collisions of methylene will transfer less than a few kcal/mole. The difference in lifetimes at 313 nm and 330 nm means that the CH_2 must not have lost much energy by collisions before it reacts and, therefore, it must react within one or two collisions.

Modifications of Dorer and Rabinovitch's Models

If DR's models are modified by assuming there are fewer oscillators actively involved in the methylcyclopropane complex, or more specifically, that some of the CH stretches of the CH_2 groups in the ring do not contribute to breaking the cyclopro-

Reproduced with permission of the copyright owner. Further reproduction prohibited without permission.

pane ring and, thus, do not contribute to the distribution of the total energy of the complex or molecule, the $< E >$'s calculated for the k_a's are significantly reduced. Only one model with such a modification is shown in Tables 5-III and 5-IV, model 4, although several others were also tried.

Reducing the degrees of freedom in the model will also change the shape of the"thermal fall-off"curve. The isomerization rate constant, k, is calculated for thermal isomerization at several temperatures and several pressures. The high pressure limit of k is k_∞. At each temperature, the log of k/k_∞ is plotted against the log of the pressure, and this plot is referred to as the"thermal fall-off" curve. This curve is a convenient way to help judge the applicability of the models constructed. Reducing the number of oscillators by ignoring the CH ring stretches results in a sharper "fall-off", i.e., a faster decrease in the ratio of k/k_∞ with decreasing pressure. This comparison was used in discarding some of the models, but the plots are not shown since describing too many models would have obscured the more significant ones. Figures 5-2 and 5-3 depict some of the "thermal fall-off" curves for some of the models tried.

Despite these improvements, reducing the degrees of freedom in the complex is not really a satisfactory approach for several reasons. The RRKM theory should be able to predict the correct

Reproduced with permission of the copyright owner. Further reproduction prohibited without permission.

behavior without assuming that certain vibrations are not involved. The isomerization of cyclopropane has been sucessfully described by the RRKM theory with a model which includes all of the vibrations of the molecule.[10] Of course, the cyclopropane studies were thermal isomerizations, and the methylcyclopropane lifetimes in our chemical activation system are much shorter (10^{-10} to 10^{-9} sec) than in the thermal system (8×10^{-7} sec, Chesick[4]), so it is possible that the energy has not had a chance to be distributed among all the modes. However, the distributions of butene isomers were as anticipated from the pre-exponential factors which implies that the energy has been fairly well distributed among most of the modes. Butler and Kistiakowsky[1] found no difference in the distribution of the isomers between their cyclopropane and propylene system which meant that the energy flow in the excited methylcyclopropane in their systems was fast enough to completely distribute the energy among all the vibrational modes of the complex. Thus, since the thermal system can be described by a model which involves all of the vibrations, the chemical activation system must also be described with the same model. According to the RRKM theory, even those vibrations which are not directly involved in the reaction coordinate will contribute to the energy density of both the molecule and the complex.

---

10. Wieder, G. M. and Marcus, R. A., J. Chem. Phys. 37, 1835 (1962); Lin, M. C. and Laidler, K. J., Trans. Faraday Soc. 64, 927 (1968).

Reproduced with permission of the copyright owner. Further reproduction prohibited without permission.

The sometimes used argument[11] that vibrations of a symmetry different from that of the reaction coordinate are not involved in the free flow of energy between modes and, therefore, are not involved in the distribution of the total energy of the molecule seems to be especially weak in cyclopropane isomerizations. The isomerization of methylcyclopropane to any of the butenes involves motions of the atoms which destroy the only symmetry element, the σ_v, of methylcyclopropane. Therefore, both the A' and A" vibrations should be equally effective in distributing energy in the transition state.

A second type of modification was tried for DR's model. We "tightened" and "loosened" (increased and decreased the frequencies of) the vibrations DR assumed to be changing during the transition of the methylcyclopropane molecule to the complex. Of DR's models (Tables 5-III and 5-IV, comlexes 1, 2, 3, and 4), the looser models fit the thermal fall-off curves better (see figures 5-2 and 5-3) and also, using our experimental rate constants, predict smaller $< E >$'s for the excited methylcyclopropane than the tighter models.

The tighter models, in addition to not fitting the thermal data as well as the loose models and predicting larger $< E >$'s for

---

11. The symmetry argument is described by Gill, E. K. and Laidler, K. J., Proc. Roy. Soc. A250, 121 (1959).

Reproduced with permission of the copyright owner. Further reproduction prohibited without permission.

methylcyclopropane than the thermochemical maximum, $< E >_{max}$, also predict difference in $< E >$ between the ketene-cyclopropane (313 nm) system and the ketene-propylene (320 nm) system which are smaller than expected. The difference in photon energies of the photolyzing wavelengths is 2.1 kcal/mole and the difference in heats of reaction is 7.8 kcal/mole.[12] Thus, the difference in $< E >$'s between these two systems should be 9.9 kcal/mole if all the extra photolysis energy is carried by the $^1CH_2$ to the methylcyclopropane. Since the addition of $^1CH_2$ to C=C double bonds is faster than the insertion of $^1CH_2$ into C-H bonds,[13] it is possible that in the ketene-propylene system, the $^1CH_2$ suffers no collisions before reacting with propylene. If this is the case, and if the $^1CH_2$ reaction with cyclopropane occurs after one non-reacting collision which, however, causes the $^1CH_2$ to lose some energy, the difference in $< E >$'s between the ketene-propylene system at 320 nm and the ketene-cyclopropane system at 313 nm may be somewhat less than 9.9 kcal/mole.

Eliminating two of the ring CH stretches (cf. complexes 3 and 4) results in lower $< E >$'s but, also, in smaller differences between the $< E >$ in the ketene-propylene system at 320 nm and the

---

12. ΔH_f^o at 298°K is given in Benson, S. W., Thermochmical Kinetics, John Wiley and Sons, Inc., New York. (1968) for most of these molecules. See Table 5-VIII.

13. See the review articles, e. g., Bell, J. A., Prog. Phys. Org. Chem. 2, 1 (1964) and also refernce 3.

Reproduced with permission of the copyright owner. Further reproduction prohibited without permission.

Figures 5-2 and 5-3 are the "thermal fall-off" curves at two of Chesick's temperatures. The pressures are in cm of Hg. The figures include Chesick's data at those temperatures and the constants calculated from the RRKM theory using several different models including Dorer and Rabinovitch's published model.

Reproduced with permission of the copyright owner. Further reproduction prohibited without permission.

Figure 5-2

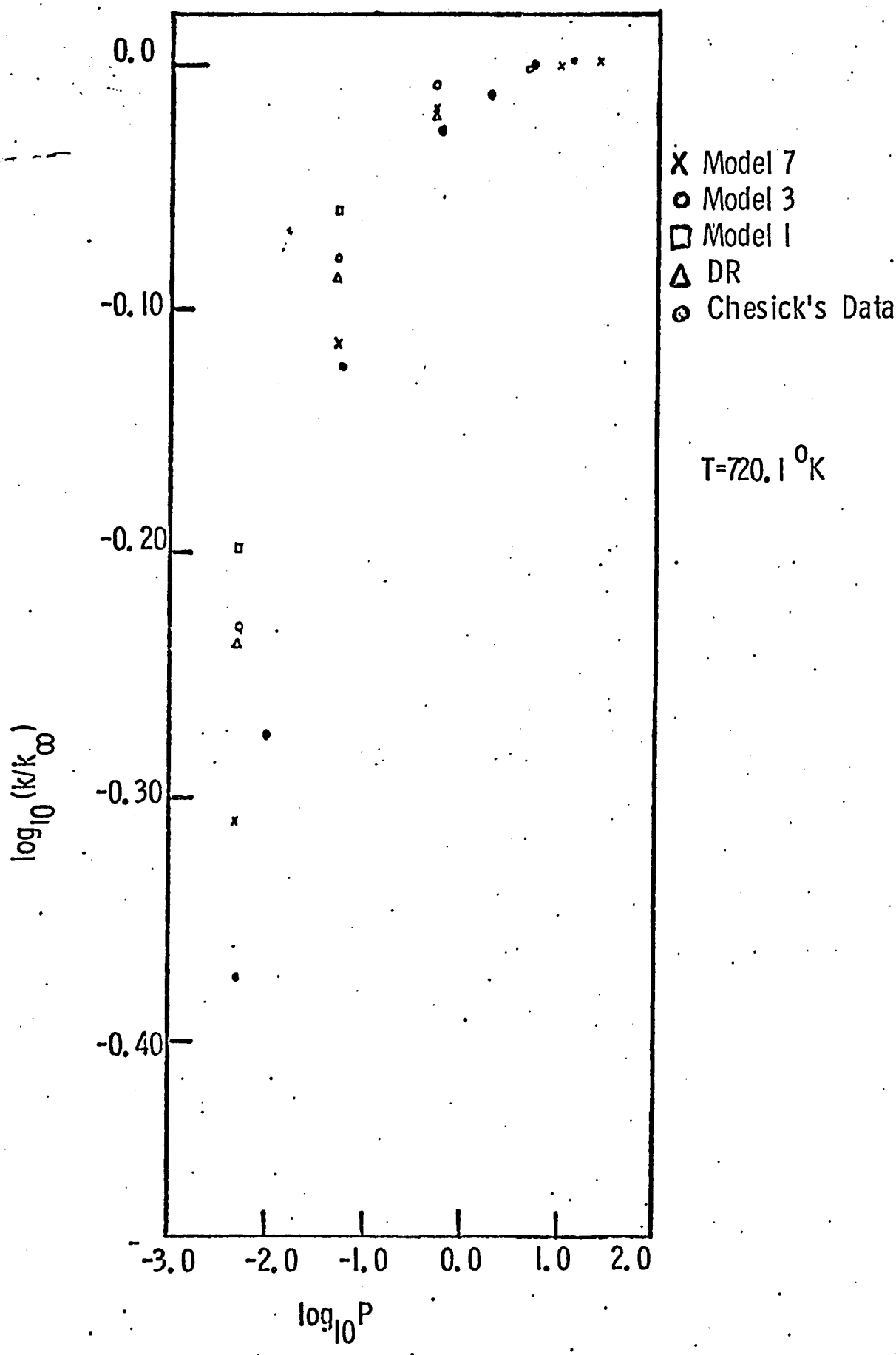

Reproduced with permission of the copyright owner. Further reproduction prohibited without permission.

Figure 5-3

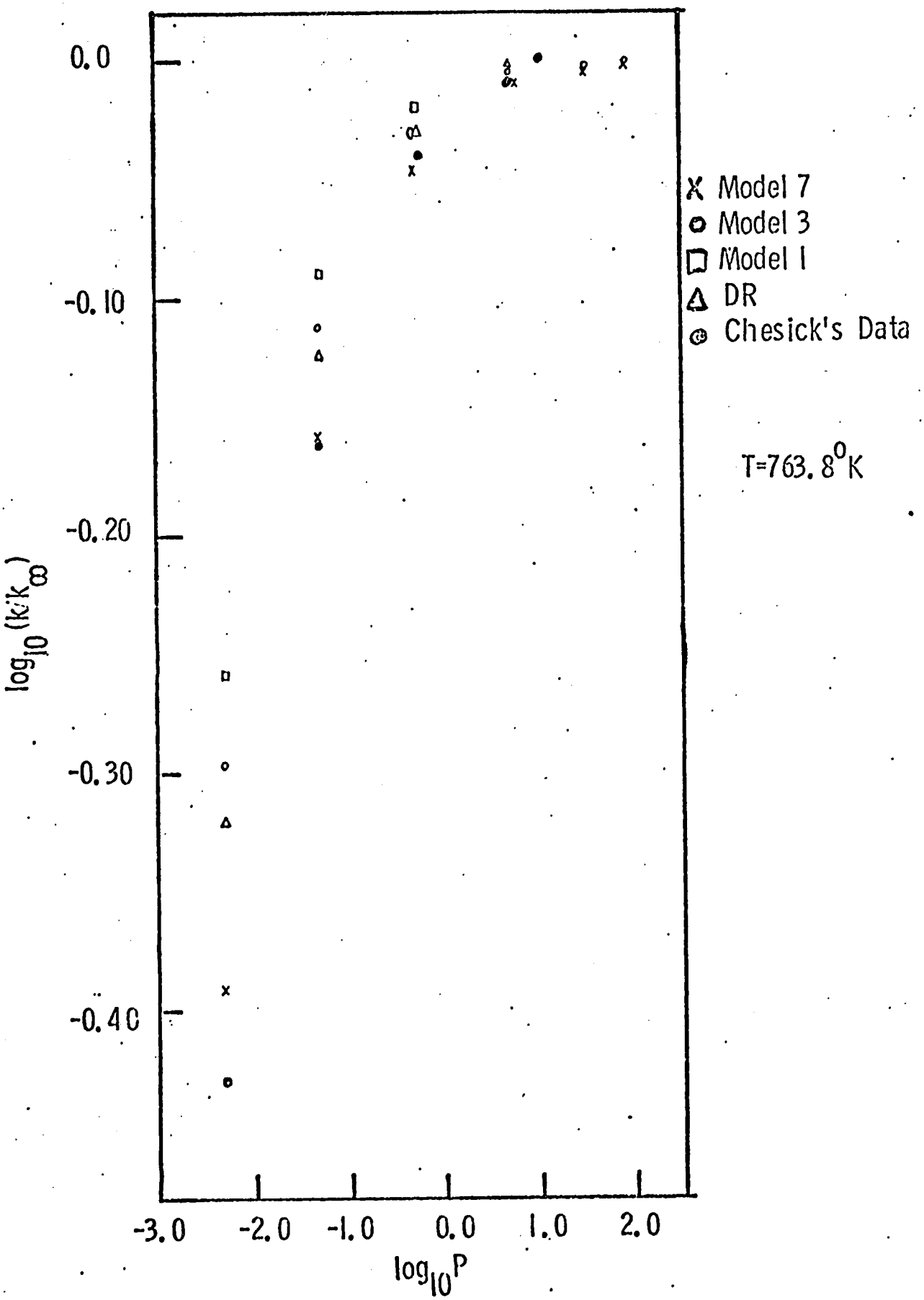

Reproduced with permission of the copyright owner. Further reproduction prohibited without permission.

$< E >$ in the ketene-cyclopropane system at 313 nm. Thus, a new model, looser than DR's model, which fits the characersitics of the thermal isomerization and which is consistent with the thermochemistry of the chemical activation systems is needed.

New Models

There are four different products of methylcyclopropane isomerization and a total,overall reaction path degeneracy of 10. Each of the butene products is the result of the breaking of one C-C single bond in the cyclopropane ring, the formation of a C=C double bond, the breaking of one C-H bond, the transferring of the H to a different carbon atom, and the formation of a new C-H bond. In constructing the models, the details of the breaking and the forming of the different bonds was ignored.

The ideal approach would have been to construct a complex for each of the four pathways and then take a weighted average of the rates of decompositions from the four different complexes to describe the overall decomposition of the methylcyclopropane. However, since the isobutene and butene-1 are not well resolved from each other, it did not seem worthwhile to take this detailed approach. Instead, we constructed four models by estimating the increase in bond lengths necessary for each separate product and

Reproduced with permission of the copyright owner. Further reproduction prohibited without permission.

took an average of the bonds in these models which we weighted by the degeneracy of each pathway. The bond lengths of the resulting complex were used as a guide for adjusting the frequencies of the vibrations in the complex. This complex should be adequate for an overall description of the rate of isomerization of methylcyclopropane. The construction of this model and the adjustment of the frequencies are described in Appendix II.

The Best Model

The vibrations which were changed in the various models are listed in Table 5-III. Table 5-III also includes some of the models DR tried (models 1-4). The various parameters, $< E >$, $\log_{10}A$, k_∞, (E_o-E_a), etc., which were calculated from each model using the RRKM theory and each model are listed in Table 5-IV. Some of these models can be eliminated as being unrealistic by looking at Table 5-IV and comparing the calculated parameters with the experimental results. From Table 5-IV, it is obvious that complexes 6 and 8 result in a k_∞ at 763.8°K (and also at 720.1°K) that is much larger than experimentally observed. Models 1, 2, and 5 result in $< E >$'s which are larger than $< E >_{max}$ for systems A, B, and C, and so can be discounted. Models 3 and 9 predict $< E >$'s which are very close to the $< E >_{max}$ (only one kcal/mole less than $< E >_{max}$) for systems A and B. It is unlikely that all

Reproduced with permission of the copyright owner. Further reproduction prohibited without permission.

of the excess energy of the ketene photolysis will go into the $^1CH_2$ and that, furthermore, $^1CH_2$ will carry all of that energy into the resulting methylcyclopropane and so models 3 and 9 are also unrealistic. Thus, only models 4, 7, 10, and 11 are left in the running and of these four, only model 7 involves all of the vibrations. As mentioned before, there is no good, a priori reason to assume that all of the vibrations are not involved in distributing the energy of the complex. Of course, all of these models assume the vibrations are harmonic, and especially if the complex has a lot of vibrational energy, which it does, the vibrations are more likely to be anharmonic. If the vibrations are anharmonic, it is even more probable that all of the vibrations are involved in distributing the energy.

Part of the empiricism of the RRKM treatment is that with enough small refinements, it would be possible to construct a model that fits the thermal data well, that results in $< E >$'s within the allowed thermochemistry for the experimental rate constants, and that results in a difference in $< E >$'s between the cyclopropane and propylene systems which is closer to that required by the heats of formation.[14] Of course, as discussed above, the difference in $< E >$'s in the cyclopropane and propylene systems may be smaller

---

14. Butler and Kistiakowsky used Kassel's classical limit for k_a (which is the same as Slater's) to find $< E >$ and, although their systems were complicated by the presence of $^3CH_2$, the difference in $< E >$'s was also much smaller than expected.

Reproduced with permission of the copyright owner. Further reproduction prohibited without permission.

than the heats of formation predict because the reaction of $^1CH_2$ with propylene is faster than that with cyclopropane.

A Comparison of the Results of the RRKM Theory with Those of Other Theories

It is interesting to compare the results calculated from the RRKM treatment with those from the RRK theory (Rice, Ramsperger, and Kassel's[15] theory, often referred to as Kassel's theory) and Slater's theory,[16] even though they are less realistic than the RRKM theory. Since the energy of the complex in both the ketene-cyclopropane and the ketene-propylene systems is approximately 40 kcal/mole more than the critical energy, E_o, required for isomerization, both theories approach the classical limit for k_a, i.e.,

$$k_a = A \left[\frac{< E > - E_a}{< E >}\right]^{s-1} ,$$

where A corresponds to the pre-exponential for the high pressure limit of the thermal isomerization, k_∞, and s is the adjustable parameter referred to as the number of effective oscillators.

Chesick found that with s=18, the statistical expression for

---

15. Rice, O. K. and Ramsperger, H. C., J. Am. Chem. Soc. 49, 1616 (1927); Kassel, L. S., J. Phys. Chem. 32, 225 (1928).

16. Slater, N. B., Theory of Unimolecular Reactions, Cornell University Press, Ithaca, N. Y., 1959.

Reproduced with permission of the copyright owner. Further reproduction prohibited without permission.

k/k_∞ in the RRK theory gave a good fit to his thermal data as expressed by a plot of the log of k/k_∞ against the log of the total pressure. As shown in Table 5-VI, however, the $< E >$'s corresponding to our experimental rates in the ketene photolysis system are larger than the thermochemical data allow. Using a smaller s results in smaller $< E >$'s, however, as mentioned before, there is no reason to assume that the number of vibrations (or the number of oscillators) involved in a chemical activation system is smaller than in a thermal system. In those calculations where s is less than 18, although the $< E >$'s decrease, the difference between the $< E >$'s in systems A and C and also between the other systems also decreases. Placzek and Rabinovitch[17] recalculated A and E_a from Chesick's[4] data using only those experiments in which the pressure of methylcyclopropane was greater than 100 Torr. This was done in order to minimize any contribution of the decomposition of the olefins which occurs at lower pressures. The results presented in Table 5-VI were calculated using Placzek and Rabinovitch's values for A and E_a.

If the difference between the $< E >$'s for the methylcyclopropane complex in the ketene-propylene system at 320 nm (system A) and the ketene-cyclopropane system at 313 nm (system C) is only the difference between the heats of formation and the small

---

17. Placzek, D. W. and Rabinovitch, B. S., J. Chem. Phys. 69, 2141 (1965).

Reproduced with permission of the copyright owner. Further reproduction prohibited without permission.

TABLE 5-VI

The Results of the Theories of Kassel and Slater

Ketene System	< E > kcal/mole	s	< E > kcal/mole	s
A	111.1	18	98.9	15
B	115.0	18	102.1	15
C	115.9	18	102.8	15
D	117.6	18	104.2	15
E	120.0	18	106.3	15

Placzek and Rabinovitch's values for the thermal system: log A= 15.25 and E_a= 64.3 kcal/mole.

Reproduced with permission of the copyright owner. Further reproduction prohibited without permission.

difference in photolyzing wavelengths, the classical limit of k_a can be solved for $< E >$ for both systems. The number of oscillators, s, is not involved in this calculation. Using Placzek and Rabinovitch's values for A and E_a, this calculation results in an $< E >$ of about 111 kcal/mole for the methylcyclopropane complex produced in system A and 119 kcal/mole in system C. Both of these values for $< E >$ are unacceptably high by more than 10 kcal/mole.

The Partitioning of Energy During the Photolysis of Ketene

Once the average energy of the complex is known, some of the details of the energy partitioning during the decomposition of ketene can be estimated. $< E >_t$ is the average energy of the methylcyclopropane complex if none of the photolysis energy in excess of that required to decompose the ketene is carried by the $^1CH_2$ to the methylcyclopropane. $< E >_{max}$ is the other extreme case, namely that in which all of the excess photolysis energy has been transferred to the $^1CH_2$ which does not lose any of this energy by collision before reacting to form methylcyclopropane, and in which the methylcyclopropane has received it all as vibrational energy. The fraction of the total energy available from the photolysis (the excess photolysis energy) that the methylcyclopropane has received as vibrational energy should be approximately the fraction of energy that the $^1CH_2$ has carried off from the photolytic

Reproduced with permission of the copyright owner. Further reproduction prohibited without permission.

decomposition of ketene (plus or minus about 5 kcal/mole) and can be expressed as

$$f_E = \frac{< E > - < E >_t}{< E >_{max} - < E >_t} .$$

$< E >_t$ is 99.2 kcal/mole for the reaction of methylene and cyclopropane and 91.4 kcal/mole for the reaction of methylene and propylene. (See Table 5-VIII for a list of the heats of formation.) Table 5-VII lists the fraction of energy, f_E, the $^1CH_2$ carries off from the decomposition of ketene in each of the five systems studied. The $< E >$'s used in the calculations are those predicted by our best model, model 7. Table 5-VII summarizes these results. The fraction of energy distributed to the $^1CH_2$ decreases as the photolyzing energy increases. This is not unexpected since the vibrational frequency of CO is 2174 cm^{-1} and the bending frequency in $^1CH_2$ is about 750 cm^{-1} [18] which means that when there is less energy available, it is more likely to go into the $^1CH_2$ than into the CO. Rabinovitch and his co-workers[5,8] have estimated that 60 to 80 % of the available energy in the photolysis of ketene at 320 nm goes into the methylene.

---

18. Herzberg, G., Proc. Roy. Soc. A262, 291 (1961); Herzberg, G., Molecular Spectra and Molecular Structure, Volume I. Spectra of Diatomic Molecules (D. Van Nostrand Co., Inc., Princeton, New Jersey, 1950).

Reproduced with permission of the copyright owner. Further reproduction prohibited without permission.

TABLE 5-VII

An Estimate of the Partitioning of Energy During the Photolysis of Ketene

System	f_E, the fraction of photolysis energy distributed to $^1CH_2$
A(320 nm)	0.7
A(330 nm)	0.7
C(313 nm)	0.6
D(277 nm)	0.5
E(214 nm)	0.3

Reproduced with permission of the copyright owner. Further reproduction prohibited without permission.

Distribution of Isomers

Even though the isobutene and butene-1 were not competely resolved, some comments may be made about the distribution of the various butene isomers. When the methylcyclopropane is formed in our experiments, it has roughly 40 kcal/mole of energy in excess of the critical energy it needs to isomerize to any of the butenes. The distribution of the isomers will parallel the pre-exponential factors since the energy available is so much greater than the activation energies. (Table 5-IX is taken from Kinetic Data on Gas Phase Unimolecular Reactions by S. W. Benson and H. E. O'Neal (1970) NRSDS-NBS 21 and lists the thermochemical data for the methylcyclopropane isomerization.) Since the ratios of cis- to trans-butene-2 yields and the ratios of cis- and trans-butene-2 yields to the sum of the isobutene and butene-1 yields in our system are the same as found by Butler and Kistiakowsky[1], we can assume that the isomer distribution is approximately the same as in their experiments.

The rate constant for the isomerization of cis-butene-2 to trans-butene-2 is log k= 13.78-62.8/(2.303 RT).[19] At lower pressures, some of the cis-butene-2 will isomerize to trans-butene-2 since the cis isomer still has an excess of energy (as do the other isomers). At higher pressures, where the cis isomer has a

19. Rabinovitch, B. S. and Michel, K. W., J. Am. Chem. Soc. 81, 5065 (1959).

Reproduced with permission of the copyright owner. Further reproduction prohibited without permission.

greater chance to be stabilized by collisons before isomerizing, the ratio of trans-/cis- butene-2 isomers should be smaller than that at lower pressures. This trend can be seen in the ratios in Table 5-I and is consistent with the results of Butler and Kistiakowsky,[1] Chesick,[4] and Jakubowski, Sandhu, and Strausz.[20]

---

20. Jakubowski, E., Sandhu, H. S., and Strausz, O. P., J. Am. Chem. Soc. 93, 2610 (1971).

Reproduced with permission of the copyright owner. Further reproduction prohibited without permission.

TABLE 5-VIII

Heats of Formation

ΔH_f^o at 298°K kcal/mole	Substance
92.2[a]	CH_2
12.7	cyclopropane
5.7	methylcyclopropane
-11.4[b]	ketene
-27.2[c]	CO
4.9	propylene
-3.7	isobutene
0	butene-1
-1.7	cis-butene-2
-2.7	trans-butene-2

a) Chupka, W. A. and Livshitz, C., J. Chem. Phys. 48, 1109 (1968).

b) Nuttal, R. L., Laufer, A. H., and Kilday, M. V., J. Chem. Thermo. 3, 167 (1971).

c) Wagman, D. D., Evans, W. H., Parker, V. B., Halow, I., Bailey, S. M., and Schumm, R. H., NBS Tech. Note 270-3 (1968).

All other values are taken from reference 12.

Reproduced with permission of the copyright owner. Further reproduction prohibited without permission.

TABLE 5-IX

A Summary of the Thermochemical Data for the Methylcyclopropane System[a]

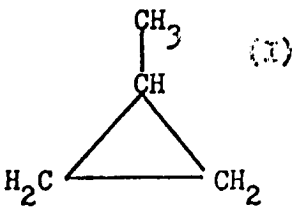

(I)

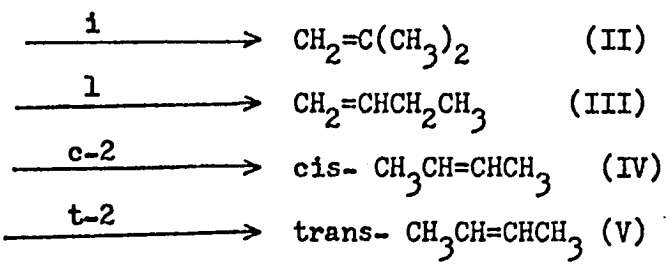

	I	II	III	IV	V
$\Delta H_f^o(298)$ kcal/mole	5.7	-3.7	0	-.17	-2.7
$\Delta S^o(298)$ cal/mole/deg	67.1	70.4	73.6	72.1	70.9
C_p^o (298) cal/mole/deg	18.5	21.3	20.5	18.9	21.0

Pathway	$\log_{10}A$	E_a
i	14.06	64.3
l	14.14	62.0
c-2	13.87	61.9
t-2	14.32	64.4

[a] Taken from Kinetic Data on Gas Phase Unimolecular Reactions by S. W. Benson and H. E. O'Neal (1970) NSRDS-NBS 21.

Reproduced with permission of the copyright owner. Further reproduction prohibited without permission.

Appendix I

Estimates of Radical Concentrations in the Ketene-Isobutane Experiments

It is useful to have an estimate of the concentrations of the radicals in the ketene-isbutane system. Estimates were made for the steady-state concentrations of the radicals, CH_3, $^1CH_2$, $^3CH_2$, and butyl radicals, in a typical photolysis of ketene and isobutane at 313 nm. The rate constants which were used were measured by other workers or were estimated using hard-sphere collision theory. It should be emphasized that the rate constants for the CH_2 reactions are not well known.

The mechanism outlined here is operative when no O_2 or CO has been added and when isobutane is the major component in the reaction system. The rate constants refer to the following reactions:

CH_2CO	$\xrightarrow{h\nu}$	$^1CH_2 + CO$, $\phi_s I_a$	1s
CH_2CO	$\xrightarrow{h\nu}$	$^3CH_2 + CO$, $\phi_t I_a$	1t
$^1CH_2$ + IsoB	$\longrightarrow$	$^3CH_2$ + IsoB	2
$^1CH_2$ + IsoB	$\longrightarrow$	NeoP	3s
$^1CH_2$ + IsoB	$\longrightarrow$	IsoP	4s
$^1CH_2$ + CH_2CO	$\longrightarrow$	C_2H_4 + CO	5s
$^3CH_2$ + IsoB	$\longrightarrow$	$(CH_3)_3C^\cdot$ + $CH_3^\cdot$	3t
$^3CH_2$ + IsoB	$\longrightarrow$	$(CH_3)_2CHCH_2^\cdot$ + $CH_3^\cdot$	4t
$^3CH_2$ + CH_2CO	$\longrightarrow$	C_2H_4 + CO	5t
$(CH_3)_3C^\cdot$ + $CH_3^\cdot$	$\longrightarrow$	NeoP	6
$(CH_3)_2CHCH_2^\cdot$ + $CH_3^\cdot$	$\longrightarrow$	IsoP	7

Reproduced with permission of the copyright owner. Further reproduction prohibited without permission.

$2\ CH_3^{\bullet}$	⟶	C_2H_6	8
$2\ (CH_3)_3C^{\bullet}$	⟶	octane B	9
$(CH_3)_3C^{\bullet} + (CH_3)_2CHCH_2^{\bullet}$	⟶	octane A	10
$2\ (CH_3)_3CHCH_2^{\bullet}$	⟶	octane C	11
$2\ (CH_3)_3C^{\bullet}$	⟶	isobutene + IsoB	12
$CH_3^{\bullet} + (CH_3)_3C^{\bullet}$	⟶	isobutene + CH_4	13

The values of the rate constants used were:

$k_2 = 3 \times 10^{-12}$ cm^3/molecule-sec	1
$k_{5s} = 3 \times 10^{-12}$	1, 2, and 3
$k_{4s} = 7 \times 10^{-12}$	1 and 9
$k_{3s} = 10^{-12}$	1 and 9
$k_{3t} = 2 \times 10^{-12}$	1 and 9
$k_{4t} = 0.03 \times 10^{-12}$	1 and 9
$k_{5t} = 4.6 \times 10^{-12}$	1 and 4
$k_8 = 4 \times 10^{-11}$	5
$k_9 = 0.5 \times 10^{-11}$	6
$k_{10} = 10^{-11}$	10 and values for k_9 and k_{11}
$k_{11} = 0.5 \times 10^{-11}$	estimate based on the value of k_9
$k_6 = 2.8 \times 10^{-11}$	10 and the values of k_8, k_9 and k_{10}
$k_7 = 2.8 \times 10^{-11}$	
$k_{12} = 1.4 \times 10^{-11}$	7 and 9
$k_{13} = 0.35 \times 10^{-11}$	k_9, k_8 and 8

(If the reactions analoguous to k_{12} and k_{13} were included for $(CH_3)_2CHCH_2^{\bullet}$, they would be negligible since their rate constants would be 0.1×10^{-11} and 0.04×10^{-11}, respectively. These numbers are estimated from hard sphere collision theory.)

Reproduced with permission of the copyright owner. Further reproduction prohibited without permission.

A steady state treatment of the radicals for the mechanism on page I-1 results in the following equations:

$$\left[{}^1CH_2\right]_{ss} = \frac{\phi_s I_a}{(k_2+k_{3s}+k_{4s})\,[IsoB] + k_{5s}\,[CH_2CO]}$$

$$\left[{}^3CH_2\right]_{ss} = \frac{\phi_t I_a + k_2\,[{}^1CH_2\cdot]_{ss}\,[IsoB]}{(k_{3t}+k_{4t})\,[IsoB] + k_{5t}\,[CH_2CO]}$$

$$R_{NeoP} = k_{3s}\left[{}^1CH_2\right]_{ss}[IsoB] + k_6\left[(CH_3)_3C\cdot\right][CH_3\cdot]$$

$$R_{IsoP} = k_{4s}\left[{}^1CH_2\right]_{ss}[IsoB] + k_7\left[(CH_3)_2CHCH_2\cdot\right][CH_3\cdot]$$

$$R_{Ethane} = k_8\left[CH_3\cdot\right]^2$$

$$R_{OctB} = k_9\left[(CH_3)_3C\cdot\right]^2$$

$$R_{OctA} = k_{10}\left[(CH_3)_3C\cdot\right]\left[(CH_3)_2CHCH_2\cdot\right]$$

$$R_{OctC} = k_{11}\left[(CH_3)_2CHCH_2\cdot\right]^2$$

Reproduced with permission of the copyright owner. Further reproduction prohibited without permission.

The observable parameters for a typical experiment at 313 nm are:

I_a = 40 x 10^{10} photons/sec-cm^3

IsoB = 1.3 x 10^{18} molecules/cm^3

CH_2CO = 1.3 x 10^{17} molecules/cm^3

ϕ_s=0.80 and ϕ_t=0.20

R_{IsoP}= 29 x 10^{10} molecules/cm^3-sec

R_{NeoP}= 8 x 10^{10} molecules/cm^3-sec

R_{OctA}= 0.25 x 10^{10} molecules/cm^3-sec

R_{OctB}= 1.2 x 10^{10} molecules/cm^3-sec

R_{Ethane}= 4 x 10^{10} molecules/cm^3-sec

Using the above equations and rate constants and the observed rates of formation, etc., the calculated steady-state concentrations and rates of formation are: (The rates of formation of neopentane and isopentane were calculated to serve as a check for the steady-state concentrations we calculated.)

$[CH_3]_{ss}$= 3.2 x 10^{10} molecules/cm^3

$[(CH_3)_3C\cdot]_{ss}$ = 4.8 x 10^{10} molecules/cm^3

$[(CH_3)_3CHCH_2\cdot]_{ss}$= 1.3 x 10^{10} molecules/cm^3

$[{}^1CH_2]_{ss}$ = 2.3 x 10^4 molecules/cm^3

$[{}^3CH_2]_{ss}$ = 5.1 x 10^4 molecules/cm^3

R_{IsoP} = 21.1 x 10^{10} molecules/cm^3-sec

R_{NeoP} = 7.2 x 10^{10} molecules/cm^3-sec

R_{OctC} = 8.2 x 10^6 molecules/cm^3-sec

Reproduced with permission of the copyright owner. Further reproduction prohibited without permission.

The agreement between the observed and calculated rates of formation of the pentanes is amazing considering all of the approximations and estimates involved. Assuming the calculations are correct, the fact that octane C was not observed among the products is not at all surprising, since it is calculated to be one-tenth the rate of formation of octane A, which itself was very small. The reaction of methyl and butyl radicals to form methane and isobutene, k_{13}, is negligible in this reaction system since, according to the values of the rate constants, this reaction would be one-eighth that of the recombination reaction to form neopentane.

References for the rate constants on page I-2.

1. Braun, W., Bass, A. M., and Pilling, M., J. Chem. Phys. 52, 5131 (1970).

2. DeGraff, B. A. and Kistiakowsky, G. B., J. Phys. Chem. 71, 3984 (1967).

3. Herzog, B. M. and Carr, R. W., Jr., J. Phys. Chem 71, 2688 (1967).

4. Bell, J. A., J. Phys. Chem. 75, 1537 (1971).

5. Kistiakowsky, G. B. and Roberts, E. K., J. Chem. Phys. 21, 1637 (1953).

6. Metcalf, E. L., J. Chem. Soc. 1963, 3560.

7. Kraus, J. W. and Calvert, J. G., J. Am. Chem. Soc. 79, 5921 (1957).

8. Kerr, J. A. and Trotman-Dickenson, A. F., Prog. React. Kinetics 1, 107 (1961).

9. From experimental values in Chapters 3 and 4.

10. Calculated using hard sphere collision theory.

Reproduced with permission of the copyright owner. Further reproduction prohibited without permission.

Appendix II

Construction of the Model for Methylcyclopropane Decomposition

An illustration of the method used to construct the complex is given for butene-1.

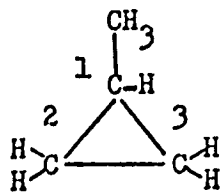

(a)

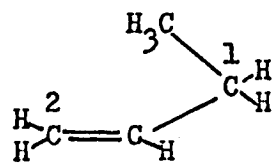

(b)

The bond length for C-C bonds in the ring of methylcyclopropane is 1.53 Å.[1] The C-C bond lengths in butene-1 are 1.54 Å for the alkane C-C bonds and 1.34 Å for the C-C double bonds. The bond angle between the carbons is 60° in the cyclopropane ring and the angle C_1-C_2-C_3 in butene-1 is 120°. We constructed a complex to describe the C_1-C_2 bond breaking. The C_1-C_2-C_3 angle was assumed to be 90°, the C_2-C_3 bond length 1.44 Å, and the C_3-C_1 bond length 1.54 Å. By simple geometry, the C_1-C_2 bond length must be 2.16 Å. A similar model describes the C_1-C_3 bond breaking and is degenerate with the C_2-C_1 bond breaking. The superposition of the two complexes results in a triangular molecule with C_1-C_3 and C_1-C_2 bond lengths equal to 1.84 Å and a C_2-C_3 bond length of 1.44 Å.. This complex has a weight of two when averaged with the other complexes because two hydrogens can migrate to form the same product. (The carbons, C_3 and C_2 were made equivalent when the two complexes were superimposed.)

Reproduced with permission of the copyright owner. Further reproduction prohibited without permission.

A similar procedure was used in constructing the complexes for the other products. The final complex has bond lengths of 1.75 Å for the C_1-C_3 and C_1-C_2 bonds and a bond length of 1.62 Å for the C_2-C_3 bond. Since these bond lengths are to be used as a guide for adjusting the vibrational frequencies, an average bond length of 1.7 Å is an adequate estimate.

Frequency Assignments and Adjustments

Table 5-II (page 159) lists the frequency assignments for the cyclopropane ring according to Sverdlov and Krainov[2] and Herzberg.[1]

Some of the rationale behind the frequency assignments made for the best model, complex 7 of Tables 5-III and 5-IV, is as follows. ν_3 is the completely symmetrical C-C stretch and was reduced by only 10% (corresponding to the 10% increase in the C-C bond lengths) since it cannot contribute significantly to the actual breaking of the ring. ν_4, ν_5, and ν_7 are symmetric in the sense that for each mode, the same motion occurs to all the carbons in the ring, and thus, neither of these modes can be particularly effective towards breaking the ring. These are bending modes and therefore, even though they are not very effective, they will be more effective than a symmetrical stretching mode. Consequently, we reduced the frequencies of these modes by 20%. ν_{10} and ν_{11}

Reproduced with permission of the copyright owner. Further reproduction prohibited without permission.

were reduced by 30% because these are asymmetrical ring deformations which can contribute even more towards breaking the C-C bonds of the ring than any symmetrical motions.

According to Pauling's Rule for bond lengths and bond orders, a C-C bond length of 1.7 Å corresponds to a bond order of 0.52. The two twisting of ν_{14} are most effective towards breaking the C-C bonds in the ring. These are bending motions and by a crude and simple-minded analogy to Badger's Rule which relates the force constants of a vibration to the bond orders of the bonds involved, the frequencies of this twisting motion were reduced to 52% of the original frequencies.

The rocking motion of ν_{13} is probably not really effective towards breaking the C-C bonds in the ring, however, it can bring the H atoms closer to the other C atoms in the ring as the C-H bond is "rocked" towards the plane of the ring. For this reason, the frequency of the ν_{13} mode was reduced by 20%.

The other modes in methylcyclopropane do not directly contribute to the breaking of the cyclopropane ring and so were left unchanged.

---

1. Herzberg, G., Infrared and Raman Spectroscopy of Polyatomic Molecules. (Van Nostrand Co., nc. Princeton, New Jersey, 1949).

2. Sverdlov, L. M. and Krainov, E. P., Opt. i. Spekt. 7, 296 (1959).

Reproduced with permission of the copyright owner. Further reproduction prohibited without permission.